Quantification of Metal Loading by Tracer Injection and Synoptic Sampling, 1996–2000

By Briant A. Kimball, Katherine Walton-Day, and Robert L. Runkel

Chapter E9 of
Integrated Investigations of Environmental Effects of Historical Mining in the Animas River Watershed, San Juan County, Colorado
Edited by Stanley E. Church, Paul von Guerard, and Susan E. Finger

Professional Paper 1651

U.S. Department of the Interior
U.S. Geological Survey

Contents

Figures

Tables

Conversion Factors and Abbreviated Water-Quality Units

Multiply	By	To obtain
meter (m)	0.30481	foot (ft)
liter per second (L/s)	28.317	cubic foot per second (ft^3/s)
kilometer (km)	.62137	mile (mi)
square kilometer (km^2)	.3861	square mile (mi^2)
kilogram per day (kg/day)	2.205	pounds per day (lb/day)

Temperature in degrees Celsius (°C) may be converted to temperature in degrees Fahrenheit (°F) by using the following equation:

$$°F=9/5°C+32$$

The following terms and abbreviations also are used in this report:

milligram per liter (mg/L)
microgram per liter (µg/L)
millimoles per liter (mmol/L)
milliliters per minute (mL/min)
milligram per second (mg/s)

Chapter E9
Quantification of Metal Loading by Tracer Injection and Synoptic Sampling, 1996–2000

By Briant A. Kimball, Katherine Walton-Day, and Robert L. Runkel

Abstract

Prioritizing mine site remediation efforts at the watershed scale requires an understanding of all trace- and major-element sources in the watershed. We established a hydrologic framework to study metal loading in the Animas River watershed study area in Colorado by conducting a series of tracer-injection studies. Each study used the tracer-dilution method to quantify stream discharge in conjunction with synoptic sampling to provide downstream profiles of pH and solute concentration. Discharge and concentration data were then used to develop mass-loading profiles for the various solutes of interest. The discharge and load profiles (1) identify the principal sources of solute load to the streams; (2) demonstrate the scale of unsampled, dispersed subsurface inflows; and (3) estimate the amount of solute attenuation resulting from physical, chemical, and biological processes.

Weathering of extensive alteration zones in basins near Mineral and Cement Creeks contributes to metal loading in these areas. In contrast, alteration in the upper Animas River basin is focused along discrete veins, and metal loading corresponds closely with these features. Mass-loading analysis indicates that at base flow, Mineral Creek basin dominates the contribution of total copper load. Mineral Creek basin contributes 60 percent, Cement Creek contributes 30 percent, and the upper Animas River basin contributes 4 percent of the cumulative instream copper load in the watershed. The remaining 6 percent is from sources downstream from these three basins. Cement Creek had the greatest contribution of total zinc load: 40 percent of the cumulative instream load at the A72 gauging station, downstream from Silverton, was from Cement Creek, 31 percent was from the upper Animas River basin, and 24 percent was from Mineral Creek. The contribution of aluminum and iron loads from Cement Creek and Mineral Creek was more substantial than for copper and zinc. Mass-loading results indicate that 9 percent of the aluminum load was from the upper Animas River basin, 43 percent from Cement Creek, and 42 percent from Mineral Creek. The contribution of iron from the upper Animas River basin was 4 percent, from Cement Creek 49 percent, and from Mineral Creek 43 percent. Manganese loading differed from the other metals because the greatest percentage, 49 percent, came from the upper Animas River basin, while 31 percent came from Cement Creek, and 15 percent came from Mineral Creek. A substantial part of the manganese load from the upper Animas River basin could result from the accumulation of large tailings piles from many different sources. Otherwise, the greater loads from Cement and Mineral Creeks correspond to geologic patterns of alteration. Within these basins, 24 locations have been identified that account for from 73 to 87 percent of the total mass loading of these selected metals. These locations include both mined and unmined areas. This detailed snapshot of mass loading can be used to support remediation decisions, and to quantify processes affecting metal transport.

Introduction

The Animas River Stakeholders Group, which includes State and Federal land-management agencies, is charged with the task of improving water quality in the Animas River watershed. Hundreds of inactive mines are scattered throughout the mountainous terrain that makes up San Juan County, Colo. (Church, Mast, and others, this volume, Chapter E5; Jones, this volume, Chapter C). The challenge facing the stakeholders group is to understand the complex variety of inflows and to determine which sources of loading have the greatest influence on water quality. These issues are of paramount importance to land managers who must implement remedial actions.

A great diversity among inflow chemistry provides a unique opportunity (1) to examine how the tracer-injection and synoptic-sampling methods, applied on a watershed scale, help to define the contributions to metal loads from many sources and (2) to understand the effects of instream processes on the transport of metals. Both mined and unmined areas contribute substantial loads of constituents to the streams that drain the Animas River watershed because of the widespread extensively altered and mineralized rocks in the area. Contributions to the stream from these sources range from well-defined tributary inflows to dispersed, ground-water inflows.

Mass-loading studies are useful to identify and compare the complex sources of loads in a watershed. These studies are based on two well-established techniques: the tracer-dilution method and synoptic sampling. The tracer-dilution method provides estimates of stream discharge that are in turn used to quantify the amount of water entering the stream, both tributary and ground-water inflow, in a given stream segment (Bencala and others, 1990). Synoptic sampling of instream and inflow chemistry provides a detailed longitudinal snapshot of stream-water quality and of the chemistry of inflows that influence changes in the stream. When used together, these techniques provide discharge and concentration data that are used to determine the mass loading associated with various sources of water.

For this chapter, the Animas River watershed study area has been divided into four basins (fig. 1). The upper Animas River basin extends from Silverton, Colo., to the headwaters of California Gulch and is detailed by the Howardsville (1997), Eureka (1998), and California Gulch (2000) mass-loading studies. The Cement Creek basin also extends upstream from Silverton to Ross Basin and is detailed by the lower Cement Creek (1996), upper Cement Creek (1999), and May Day (2000; Wright, Kimball, and Runkel, this volume, Chapter E23). The Mineral Creek basin was detailed by three mass-loading studies in 1999. The Elk Park basin was included to evaluate loading and transport in the Animas River downstream from Silverton and is detailed by the Silverton (1997) and Elk Park (1998) mass-loading studies.

The diversity among inflows results from the complex geologic history in the area of the Silverton caldera. Five distinct alteration mineral assemblages have been identified, including an acid-sulfate (AS) zone, a quartz-sericite-pyrite (QSP) zone, a vein-related quartz-sericite-pyrite (V-QSP) zone, a weak sericite-pyrite (WSP) zone, and a regional propylitic zone (Bove and others, this volume, Chapter E3; Yager and Bove, this volume, Chapter E1). In general, the rocks on both sides of the upper Animas River have propylitic alteration, but areas of QSP and V-QSP alteration also exist (Bove and others, this volume). Among the four basins discussed in this chapter, the upper Animas River basin only has one small area of AS alteration in the upper reaches of California Gulch. It mostly contains regional propylitic alteration with many locations of V-QSP alteration. Both Cement Creek and Mineral Creek basins are within the core of alteration in the Silverton caldera and contain substantial areas of AS and QSP alteration (Bove and others, this volume). There is little alteration in the Elk Park basin.

Purpose and Scope

The purpose of this chapter is to describe the application of the mass-loading studies to several stream reaches within the Animas River watershed study area. Application of the method results in mass-loading profiles that are used to answer three basic questions. First, where do the greatest loadings of metals and acidity occur? These locations will likely have the greatest effect on stream-water quality and may be the subject of further study and candidates for remedial action. Second, is the mass loading at these locations primarily composed of dispersed, ground-water inflow? Loading that is dominated by ground-water inflow may not be amenable to remediation because of more complex pathways from the source to the stream. Third, does substantial instream attenuation of metal loads take place? Attenuation of metal loads by geochemical processes should be considered as part of the remedial design, but also may change the nature of the toxic effect in the stream, and may lead to seasonal flushing of toxic metals. The analyses presented within this chapter are limited to the information that comes from mass-loading profiles; results of solute-transport simulations based on data described herein are discussed by Walton-Day and others (this volume, Chapter E24).

Acknowledgments

This work was done in cooperation with the Bureau of Land Management, which provided funding. Support was also provided by the U.S. Geological Survey Toxic Substances Hydrology Program. Many individuals helped with the synoptic sampling for the mass-loading studies, including Douglas Burkhardt, Melissa Cox, Jonathan Evans, Robert Jenkins, Kenneth Leib, Alisa Mast, Ed Vaill, Lawrence Schemel, Patricia Solberg, Paul von Guerard, Winfield Wright, and Tracy Yager, U.S. Geological Survey; Bill Carey, Cathleen Zillich, Stephanie O'Dell, and Loren Wickstrom, Bureau of Land Management; Carol Russell, U.S. Environmental Protection Agency; Paul Krabacher, James Herron, and Bruce Stover, Colorado Division of Minerals and Geology; Steve Ferron and William Simon from the Animas River Stakeholders Group; and volunteers including Anna Day, Andy Gleason, Adam Kimball, Daniel Kimball, Bryn Kimball, Aaron Packman, Francis ReMillard, Michael ReMillard, Brad Smith, and Joy von Guerard. The studies also benefited from the support of members of the Animas River Stakeholders Group.

Methods

Application of mass-loading methods to abandoned mine lands has been developed as part of the U.S. Geological Survey's (USGS) Toxic Substances Hydrology Program (Bencala and McKnight, 1987; Kimball and others, 1994; Kimball and others, 1995; Kimball and others, 2002). As described in Appendix 1, the approach includes tracer injections to quantify discharge by tracer-dilution (Kilpatrick and Cobb, 1985) and synoptic sampling to provide spatial concentration profiles of pH and inorganic constituents. Discharge and concentration data are then combined to develop mass-loading

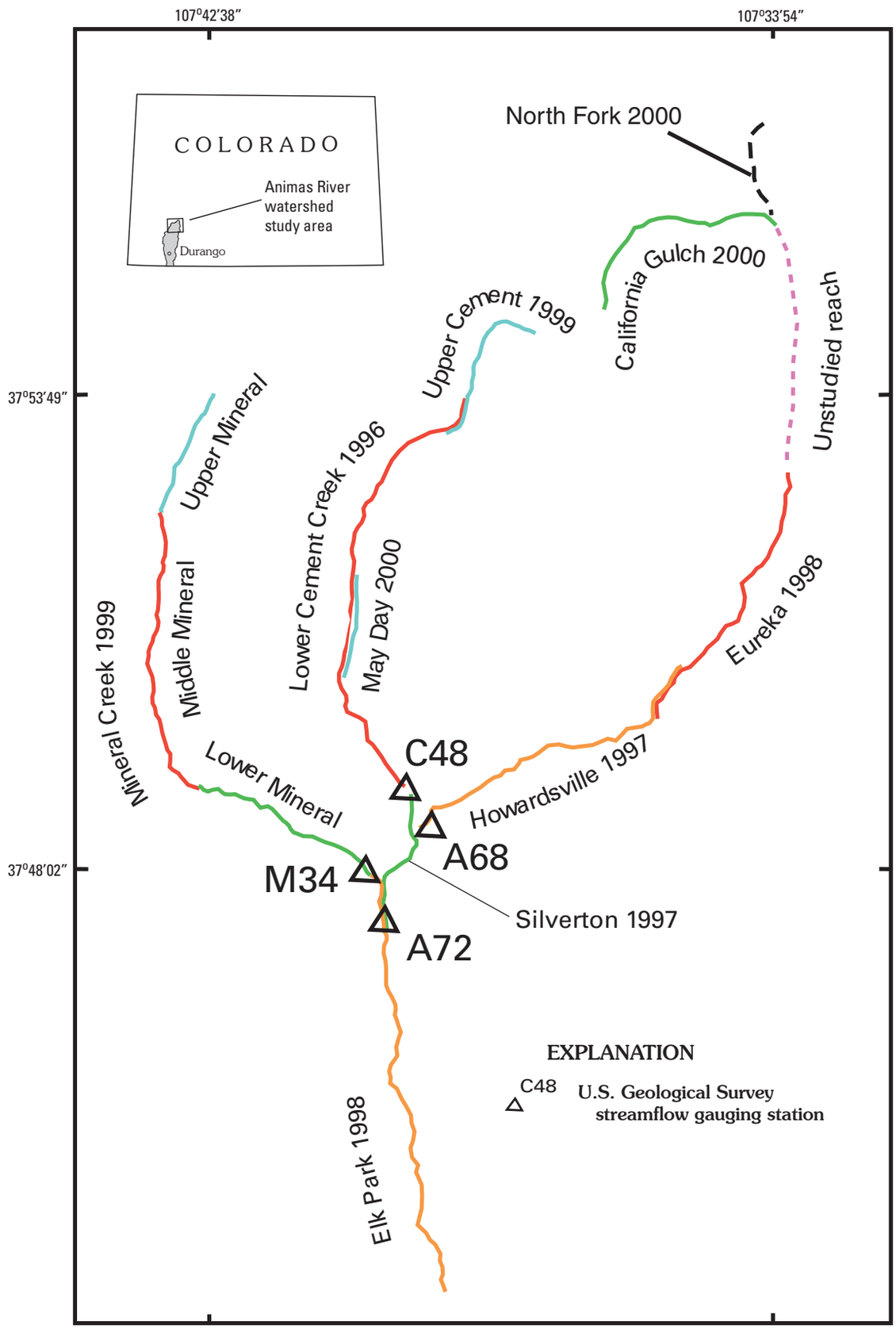

Figure 1. Location of mass-loading study reaches, Animas River watershed study area, Colorado, 1996–2000.

profiles. The appendix also includes a discussion of tracer-injection methods, equations for calculating discharge, methods for synoptic sampling, and analytical methods.

The studies described herein were undertaken during base-flow conditions (generally occurring from August to March when ground-water discharge predominates in the streamflow). Application of the method to base-flow conditions is appropriate for two reasons. First, the pattern of a mass-loading profile, expressed at base flow, reflects the importance of metal sources that enter the stream on a continuous basis. Remedial actions that address the sources identified at base flow will therefore improve water quality during the entire year; such actions will address chronic concerns. Second, the pattern of mass loading at base flow indicates those sources that contribute to high instream concentrations during the winter months, when the most toxic conditions likely occur (Besser and Leib, 1999). During the base-flow winter months, dilution of mine drainage by other sources of water is minimal, and toxicity standards are more likely to be exceeded (Besser and Leib, 1999). Although dissolved metal loads are greater during snowmelt runoff, truly dissolved metal concentrations generally are lower and pose less risk to aquatic life. Even with the focus on the base-flow period, we could identify differences in the flow regimes due to year-to-year variability in timing and quantity of snow and rain. As such, comparison of mass-loading profiles from the individual studies may be limited, but generalizations are possible.

To outline the chemical characteristics of water from each basin, downstream profiles are presented for pH and concentrations of iron, copper, and zinc. Many changes in stream chemistry arise from variations in pH, particularly the partitioning of iron between dissolved and colloidal phases. The fate and transport of many metals like copper and zinc in mine drainage are tied to the transport of the iron colloidal material (Kimball and others, 1995). Copper and zinc are two metals of particular concern because of their toxicity to aquatic life (Colorado Department of Public Health and Environment, 2000). Acute and chronic toxicity standards, which are based on the hardness of the water, are presented in graphs of copper and zinc. Values of these standards are unique to each sample because the hardness of each sample varies. During base flow, hardness generally is higher than during runoff. This means that toxicity standards are higher, because the standards are directly proportional to the hardness.

Details of sampling, chemical analysis, and tracer-injection methods are in Appendix 1. These methods were used for each of the study basins.

Mass-Loading Analysis

To quantify load requires accurate measurements of both discharge and chemistry. Profiles of mass load along the study reach use three different views of load. Sampled instream load at individual sampling sites is calculated as:

$$M_a = C_a Q_a (2.4451) \quad (1)$$

where

M_a is the constituent load at location a, in kg/day,
C_a is the concentration of the selected constituent at location a, in mg/L,
Q_a is the discharge at location a, in ft^3/s,

and

2.4451 is the conversion factor to obtain load in kg/day.

Sampled instream load is calculated from the total-recoverable concentration of the constituent, but this value for load can be divided between the dissolved and the colloidal load if both filtered and total-recoverable samples are collected. The longitudinal profile of sampled instream load presents the basic data from the mass-loading study.

The change in load between a pair of stream sites, or for a stream segment, accounts for the gain or loss of constituent load for that segment. For the change in load for the segment starting at location a and ending at location b, we calculate:

$$\Delta M_s = M_b - M_a \quad (2)$$

where

ΔM_s is the change in sampled instream load for the segment from a to b, in kg/day,
M_b and M_a are calculated for sites a and b from (1).

Gains in constituent load (ΔM_s is greater than zero) imply the presence of a source that contributes to the stream between the two stream sites. Instream load also can decrease within a stream segment (ΔM_s is less than zero), meaning that a net loss of the constituent occurred as a result of physical, chemical, or biological processes. Summing only the increases in load between sampling sites along the study reach (positive values of ΔM_s) leads to the ***cumulative instream load***. At the end of the study reach, the cumulative instream load is the best estimate of the total load added to the stream—but it is likely a minimum estimate, because it only measures the net loading between sites and does not account for loss resulting from reaction. The cumulative instream load will be greater than the sampled instream load at the end of the study reach if any loss of a constituent to the streambed has occurred.

For those segments that include a sampled inflow, calculation of a second value for load is possible based upon the change in discharge between stream sites. This change, multiplied by constituent concentration in an inflow sample, produces an estimate of the inflow load for a stream segment. If stream sites a and b surround an inflow sample, location i:

$$\Delta M_i = C_i (Q_b - Q_a)(2.4451) \quad (3)$$

where

ΔM_i is the change in sampled inflow load from location *a* to *b*, in kg/day,

C_i is the concentration of the selected constituent at inflow location *i*, in mg/L,

Q_a and Q_b are defined as in (1),

and

2.4451 is the conversion factor to obtain load in kg/day.

Summing the inflow loads along the study reach produces a longitudinal profile of the ***cumulative inflow load***. This sum can be compared to the cumulative instream load to indicate how well the sampled inflows account for the load measured in the stream. For a given stream segment, the cumulative instream and cumulative inflow loads would be equal if the sampled inflow was perfectly representative of the constituent concentration for all the water entering the stream in that segment, but that is rarely the case. It is common in streams affected by mine drainage that dispersed, subsurface inflow can have higher concentrations of metals than the surface-water inflows in the same stream segment. This causes the profile of cumulative instream load to be greater than the profile of cumulative inflow load, and can indicate important areas of unsampled inflow defined as:

$$\text{Unsampled inflow} = \Delta M_s - \Delta M_i \qquad (4)$$

This can be calculated for individual stream segments if the segment included a sampled inflow, or for the entire study reach. If the value is negative for the entire study reach, however, it can still be positive for some individual stream segments.

In considering estimates of stream discharge and metal concentration at each stream site, we find it possible to predict an error for the change in load along a stream segment. The error is determined by the precision of both discharge and chemical measurements (Taylor, 1997), according to an equation from McKinnon (2002):

$$\text{Load error} = \left(\sqrt{Q_a^2 \Delta C_a^2 + C_a^2 \Delta Q_a^2}\right)(2.4451) \qquad (5)$$

where

Q_a is the discharge at the upstream site, in ft^3/s,

ΔC_a is the concentration error at the upstream site, in mg/L,

C_a is the concentration at the upstream site, in mg/L,

ΔQ_a is the discharge error at the upstream site, in ft^3/s,

and

2.4451 is the conversion factor to obtain load in kg/day.

Load error can be calculated for each stream site and compared to the change in load from that site to the next site downstream, ΔM_s. If ΔM_s is greater than the calculated load error, then load has changed significantly, and ΔM_s is added to the sampled instream load. In developing the cumulative instream load profile, only the changes that are deemed significant according to this criterion are used. Otherwise, the cumulative instream load remains constant until there is the next significant change downstream.

In this accounting of mass loading to the stream, a contribution to the load of a particular stream segment can be missed if the net change in constituent load for the segment is negative. For example, a definite contribution to load could take place within a stream segment, but through chemical reaction, a greater amount of the constituent is removed within the segment than was added. Yet, a value for ΔM_i in that stream segment could have a measurable value in that stream segment.

Multivariate Classification of Samples

Synoptic sampling results in a large number of stream and inflow samples. Because water-rock reactions with altered and unaltered mineral assemblages may lead to particular chemical signatures among inflows to the stream, classification of samples into groups of similar chemical characteristics helps to highlight their similarities and differences, distinguish different sources, and recognize geochemical processes.

Patterns in the chemistry and pH of stream and inflow samples can be evaluated by using Principal Component Analysis (PCA), a multivariate analysis technique (Daultry, 1976). Principal components represent a set of new, transformed reference axes that are linear combinations of the original variables. A principal components transformation orients the data points so that the first of the new axes, principal component 1 (PC1), is oriented along the direction of the greatest variance in the data. The second principal component (PC2) is orthogonal to PC1, and is oriented to show the next greatest amount of variance in the data. This is easy to picture in two dimensions. One can imagine drawing a line that would go through the two most distant points in a bivariate plot of data; that line would show the direction of PC1 for those data. It would be at some angle to the original *x* and *y* axes, but any point along the line could be described by a linear combination of the original variables. PC2 would be drawn perpendicular to PC1 and it would have its own linear equation. In multidimensional space, each subsequent principal component is orthogonal to the other principal components and represents a decreasing amount of the total variance.

Typically, the first two or three principal components show enough of the variance in the data set to enable the recognition of groups among samples; this is the advantage of using the method for multivariate data. Using the scores for PC1 and PC2, which are the coordinates of the original

samples on the new axes, groups were established by using a method of partitioning around medoids (a medoid is a multivariate median of a group of samples (Kaufman and Rousseeuw, 1990)). The appropriate number of groups was based on the ability to find chemical and geologic explanations for the differences among all the groups. To carry out this multivariate analysis, the chemical data were converted to millimoles per liter and then transformed to logarithmic values, a procedure that maximized the linear relations among solutes that result from stoichiometric chemical reactions. Calculations were done using the S-Plus 2000 software package (Mathsoft, Inc., 1999).

Mass-Loading Studies

Results of 10 mass-loading studies in the Animas River watershed study area are combined here to give summaries of the upper Animas River, Cement Creek, and Mineral Creek basins. An additional study reach, called the Elk Park basin herein, serves to summarize constituent loads for the whole watershed. This study reach starts at the south end of the upper Animas River basin, at U.S. Geological Survey gauging station 09358700 (A68), and continues past the mouths of Cement Creek and Mineral Creek all the way downstream to Elk Park (fig. 1). All the chemical determinations upon which these summaries are based, along with detailed site information, are presented in Sole and others (this volume, Chapter G). Designation of inflows as right or left bank is from a downstream view, which is the typical designation in hydrology.

Upper Animas River Basin, 1997, 1998, and 2000

The upper Animas River basin extends about 26 km upstream from the U.S. Geological Survey stream gauging station at A68 (figs. 1, 2). Five mass-loading studies have been completed in the upper Animas River basin, three of which are reported here. The most upstream study reach, along California Gulch to Animas Forks (fig. 2) was studied in August 2000. The North Fork of the Animas River also was studied in August 2000, but results of that study are not included here; however, the load of metals from the North Fork is included as part of the California Gulch study reach. The section from upstream of Eureka Gulch (fig. 2, A4) to downstream of Cunningham Creek was studied in August 1998. This corresponds with a relatively low gradient reach of the upper Animas River, and includes sections where the river is braided (Blair and others, 2002; Vincent and Elliott, this volume, Chapter E22). The section from upstream of Cunningham Creek to A68 was studied in August 1997. There were overlapping sites between these two downstream studies. In August 2002, the section of the Animas River from upstream of Arrastra Creek (fig. 2, A8) to A68 was studied again. Only results for zinc are available for this report. Distances used in this report add 17,611 m to those used in the 1997 study and 12,128 m to those used in the 1998 study to reflect the total distance in the upper Animas River basin for all three studies.

Certain factors complicate the combination of these data sets into one long view of the upper Animas River basin. First, discharge at individual sites where injection reaches overlapped varied between 1997 and 1998 (fig. 3), but the difference was not too great to reasonably make an adjustment to make them equal. Second, a segment approximately 6,000 m long between the California Gulch and Eureka study reaches was not studied. A difference in pH and in several constituent concentrations appeared between the California Gulch and Eureka data sets, and as we worked on combining the two, we have assumed that the differences are a result of instream processes along the 6,000-m reach that was not studied.

Inactive mines and prospects exist along the study reach; the discharge from tailings near the Pride of the West Mill area near Howardsville (fig. 2, A6) was one of the most visually significant for its iron staining in the stream (see Church, Mast, and others, this volume, Chapter E5 for AMLI mine inventory). Along California Gulch inflows from Mountain Queen adit (CGS-350)[1], Vermillion mine (CGS-3081), and Frisco tunnel (CGS-4794) were all sampled. Individual samples of mine drainage along North Fork are not reported in this study, but combined drainage from these mines was accounted for as water from North Fork Animas River joined California Gulch near Animas Forks (fig. 2, A3). Remnants of the Sunnyside Eureka Mill occur just upstream from Eureka Gulch (fig. 2, A4). Drainage from Forest Queen mine (UAEH-2090) enters the Animas River near the end of the braided reach (A5). The Kittimack tailings are near the river, just upstream from Maggie Gulch (UAEH-3435). Downstream from Arrastra Creek (fig. 2, A8) are several large tailings repositories (sites # 507–510) stored along the stream (Nash, 2000). This is also the location of the Mayflower Mill, and the site of large tailings piles that recently (since 1995) have received tailings from several locations in the Animas River watershed, particularly from Cement Creek.

A main objective of the mass-loading study from Eureka to Howardsville was to quantify the flow and metal loading through the braided reach between Eureka Gulch (fig. 2, A4) and the site UAEH-2240 (fig. 2, A5). This braided reach could act as a source or a sink for metals in the upper Animas River. Details of the mass-loading study for this reach have been published by Paschke and others (2005).

Discharge

Sodium chloride was used as the tracer for the Eureka and Howardsville studies, and sodium bromide was used for California Gulch. Discharge increased by about 80 ft^3/s along the study reach (fig. 3). Discharge consistently increased all along the California Gulch study reach, but the two greatest

[1]Labels after sites, in the form such as CGS-350, refer to identifications in Sole and others (this volume, Chapter G).

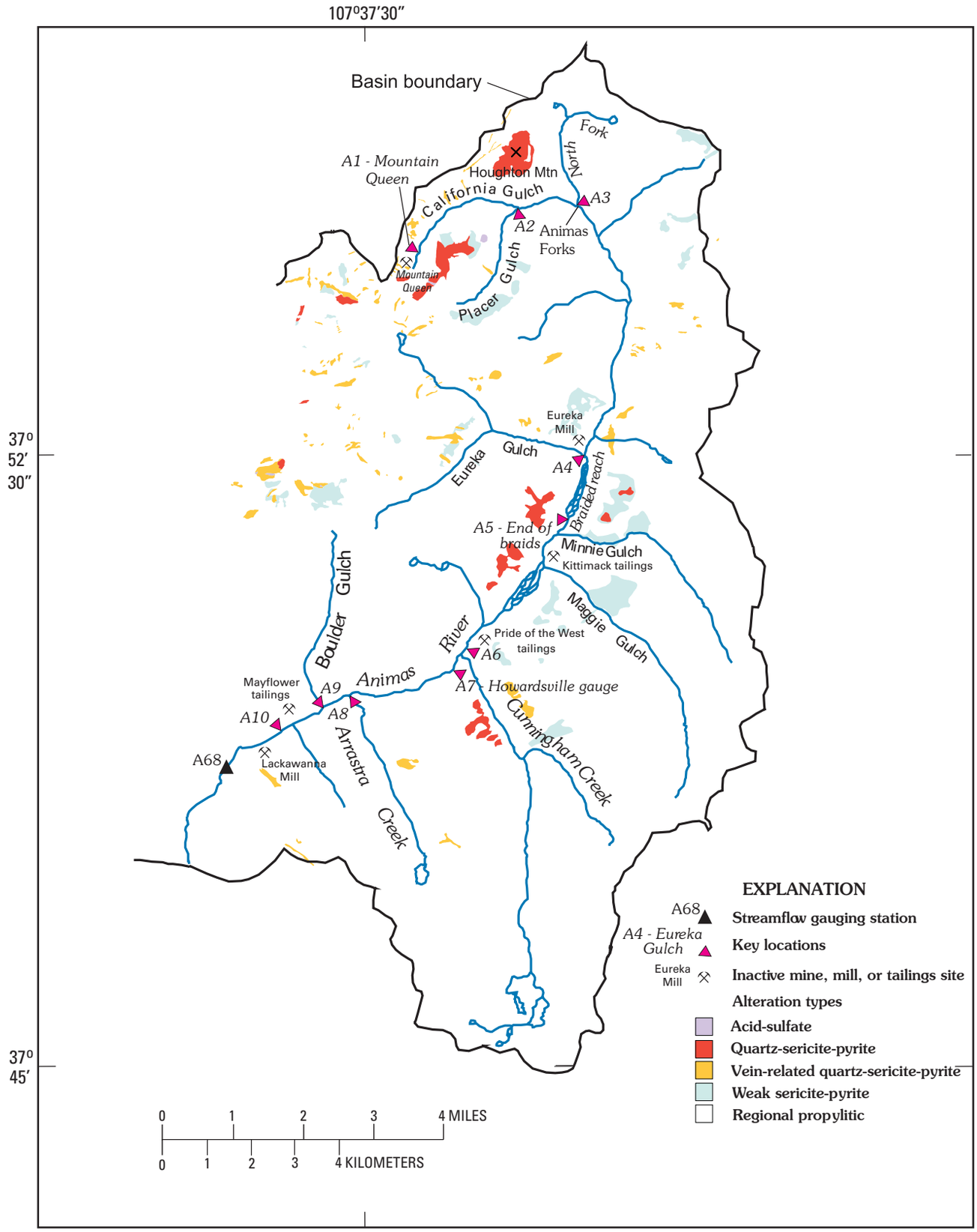

Figure 2. Location of study reaches, alteration zones, key locations, and principal sites of inactive mines, upper Animas River basin, 1997, 1998, and 2000.

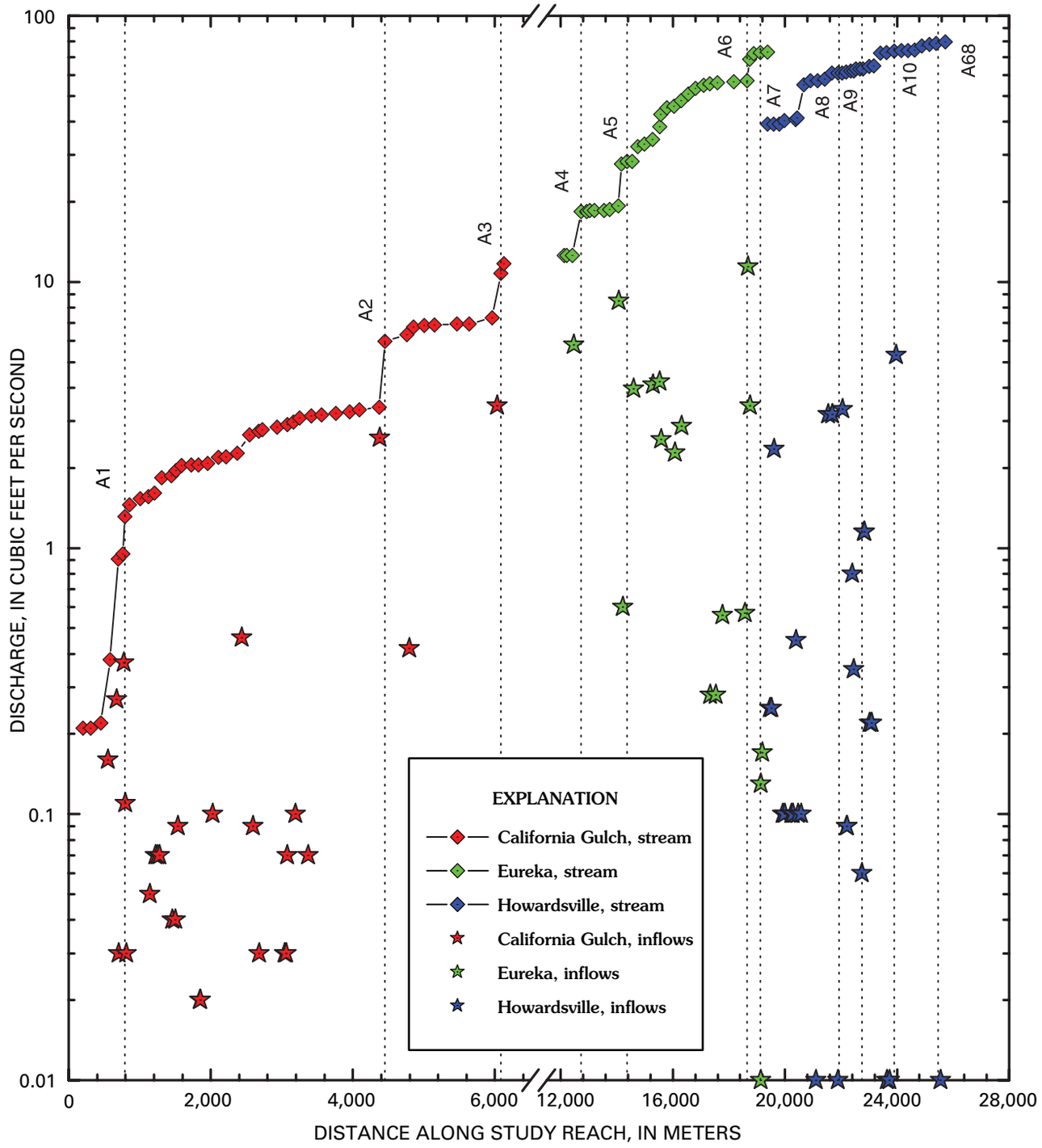

Figure 3. Variation of discharge with distance for three mass-loading studies, upper Animas River basin, 1997, 1998, and 2000. Note break of 6,000 meters between California Gulch and Eureka study reaches. Vertical lines with letters refer to locations of significant change along the study reach in figure 2.

increases occurred downstream from Placer Gulch (fig. 2, A2) and the North Fork Animas River (A3). Along the Eureka study reach, the greatest increases were at Eureka Gulch (A4), Minnie Gulch (UAEH-2620), and Cunningham Creek (UAEH-6618). Along the Howardsville study reach, discharge increased the most at Arrastra Creek (A8). At several locations between A9 and A10 (fig. 3), increases in discharge also occurred, but large, visible inflows were not observed. These increases were most likely a result of ground-water inflows, particularly upstream from 23,906 m (AMIN-6038). Note that in figure 3 and in subsequent figures that depict contributions of water or mass load to study reaches, vertical lines that

indicate inflows are drawn at the location of the stream site downstream from the inflow, not at the inflow itself. This is because the accounting for any load from the inflow is done at the downstream site.

Chemical Characterization of Synoptic Samples

Concentrations of constituents and values of pH varied substantially along the 26,000 m study reach (fig. 4). Unless noted otherwise, dissolved concentrations are from ultrafiltration and colloidal concentrations are from the subtraction of ultrafiltrate concentration from the total-recoverable concentration (Appendix 1). Chemical changes in the stream were systematic in response to groups of inflows. Differences in chemical composition resulted in the classification of five groups of inflow samples and five groups of stream samples by PCA (table 1). Among the five inflow groups, the California Gulch study reach yielded samples classified in groups 1 and 2; the Eureka and Howardsville study reaches yielded samples in groups 4 and 5; and each of the study reaches yielded group 3 samples. Values of pH were greater than 6.0 at the beginning of the California Gulch study reach (stream group 1, table 1): at the head of the basin, the stream drained propylitically altered rocks (fig. 2). As a result of several acidic inflows, pH decreased to less than 5.5 (fig. 4*A*). These acidic inflows (inflow group 1, table 1) drain areas of QSP alteration to the south of California Gulch and V-QSP altered rocks that crop out near the stream (Bruce Stover, Colorado Division of Minerals and Geology, written commun., 2000). Some of these veins have high base-metal sulfide content (Bove and others, this volume). A distinct increase in the pH of inflows (inflow group 2, table 1) occurred downstream from 1,954 m (fig. 4*A*), and these inflows caused the stream pH to increase progressively to Placer Gulch (A2, fig. 4*A*; stream group 3, table 1). Some of these inflows were from wetland ponds and had much lower concentrations of major ions (inflow group 2, table 1). They were not free of manganese and zinc, but the metal concentrations were substantially lower than in group 1, and they likely drained the propylitic alteration assemblage. Downstream from Placer Gulch (A2) and the North Fork (A3), pH increased almost to 6.0 (stream group 2, table 1).

In the Eureka and Howardsville study reaches, pH generally was greater than 7.0 (fig. 4*A*). Many inflows from the end of the braided reach (A5) to Arrastra Creek (A8) had substantially higher pH (inflow group 4, table 1). Most of these inflows, like Minnie Gulch (UAEH-2465), drained only rocks of propylitic alteration to the southeast of the Animas River. Downstream from Arrastra Creek (A8), there were more acidic inflows (inflow group 5, table 1). Although the pH of these inflows was not as low as that of group 1, their sulfate and metal concentrations were higher.

Distinct changes occurred in the concentration of iron (fig. 4*B*) along the study reach, and particularly in the dissolved versus colloidal concentrations (table 1). Colloidal iron concentrations were greater than dissolved at the beginning of the study reach (stream group 1, table 1). Inflows along the California Gulch study reach (inflow groups 1, 2, and 3, table 1) initially caused instream iron concentrations to decrease, but then to increase toward Placer Gulch (A2) and North Fork (A3). At the beginning of the Eureka study reach (near A4), the instream iron concentration was 0.085 mg/L, a decrease from 0.2 mg/L measured downstream from the North Fork (A3, fig. 4*B*). Along most of the Eureka study reach, iron concentration decreased in response to low inflow concentrations (inflow group 4, table 1). The greatest increase of instream iron concentration was downstream from the tailings discharge (A6). The higher iron concentration was mostly colloidal for the inflow (inflow group 3, table 1), and for the stream (stream group 5, table 1).

Inflows near the beginning of California Gulch (inflow group 1, table 1) caused substantial increases in concentrations of copper (fig. 4*C*) and zinc (fig. 4*D*). Inflow concentrations of copper and zinc around 2,200 m were lower (inflow groups 2 and 3, table 1), and instream concentrations decreased in response to these inflows. Concentrations of copper decreased from the end of the California Gulch study reach to the beginning of the Eureka study reach (fig. 4*C*). Copper concentration decreased substantially downstream from the braided reach (A5, fig. 4*C*). Downstream from Arrastra Creek (A8), copper concentrations increased in response to high inflow concentrations. Along the California Gulch study reach, and at the beginning of the Eureka study reach, copper concentrations exceeded chronic toxicity standards, but downstream from the braided reach (A5) instream concentrations were below the standards (fig. 4*C*).

The highest instream zinc concentrations occurred along the California Gulch study reach (stream groups 2 and 3, table 1; fig. 4*D*). Zinc weathers from sphalerite, which is prevalent in veins near the Eureka graben (Bove and others, this volume; Yager and Bove, this volume). There were differences in the zinc to manganese mole ratio among the acidic inflows in the upper part of the study reach, even though they all were classified as inflow group 1 (table 1). Manganese gangue minerals provide high manganese concentrations to inflows draining QSP and V-QSP alteration. Differences in the ratios likely reflect different amounts of sphalerite and manganese gangue minerals associated with individual occurrences because no clear spatial pattern exists. Chemical distinctions among these inflow samples, however, indicate variations in alteration mineralogy. Zinc concentration decreased substantially—from 1.73 mg/L to 0.468 mg/L—between the California Gulch and Eureka study reaches (stream groups 2 and 4, table 1).

Like concentrations of copper, zinc concentration increased downstream from Arrastra Creek. Results of a more detailed sampling for zinc during extreme base flow in August 2002 indicate four locations where zinc increased downstream from Arrastra Creek. The first was just downstream from Arrastra Creek (site I, fig. 5) where very high concentrations of zinc were found in samples of inflows along the right bank. Downstream from Boulder Gulch (site II, fig. 5), a second increase was noted where acidic inflows from an alteration zone and a draining mine occurred along the left bank. Capped tailings repositories (sites # 507–510) along the right bank also occurred in that reach. The inflow concentrations were higher

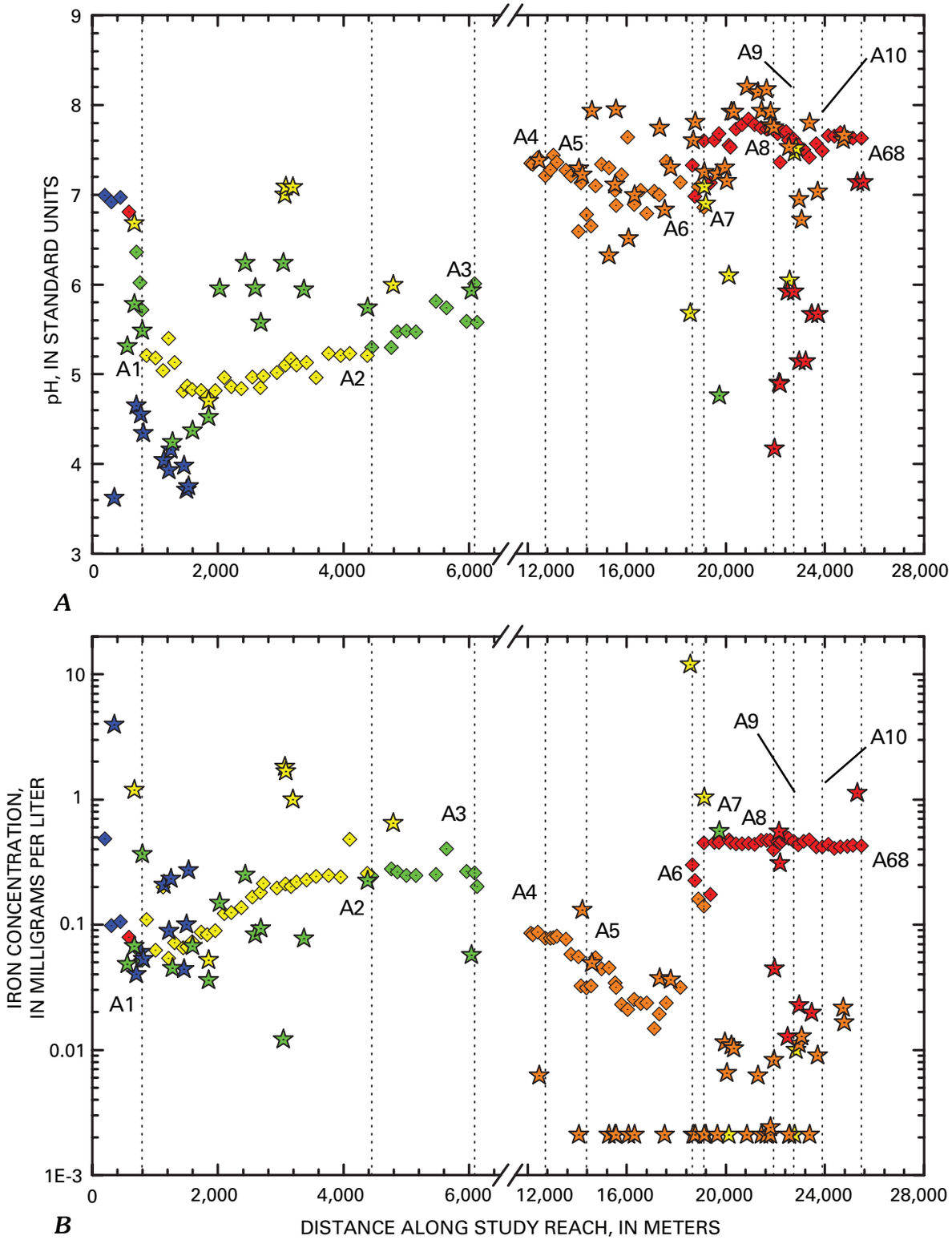

Figure 4. Variation of *A*, pH, and total-recoverable concentrations of *B*, iron, *C*, copper, and *D*, zinc with distance, upper Animas River basin, 1997, 1998, and 2000. Groups of stream samples (diamonds) and inflows (stars) are indicated by colors: 1, blue; 2, green; 3, yellow; 4, orange; 5, red. Groups were determined by principal component analysis, and their chemistry is summarized in table 1. Letters by vertical dashed lines refer to site descriptions in table 2. In *C* and *D*, blue line, acute toxicity standard; red line, chronic toxicity standard.

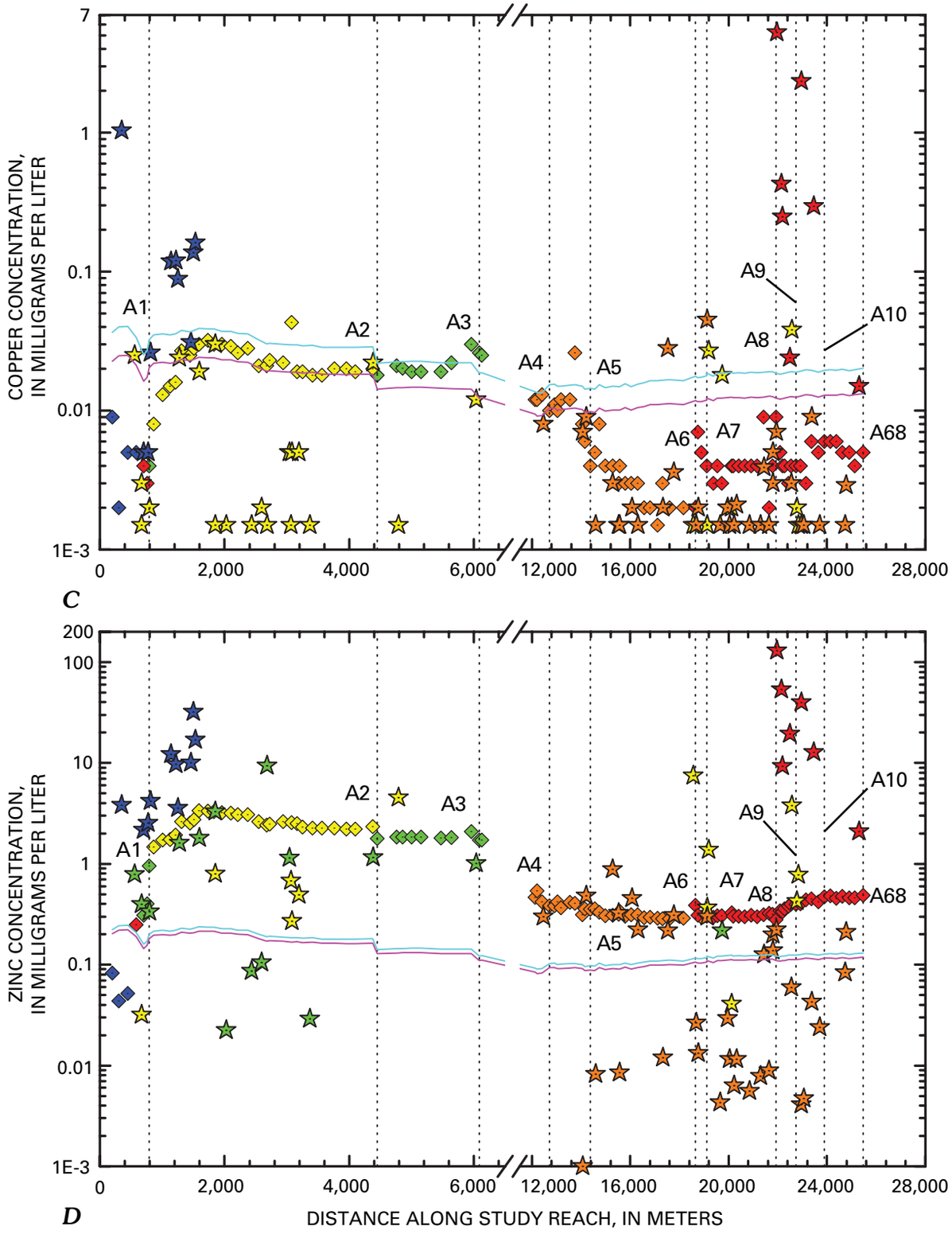

Figure 4—Continued. Variation of *C*, copper, and *D*, zinc with distance, upper Animas River basin, 1997, 1998, and 2000. Groups of stream samples (diamonds) and inflows (stars) are indicated by colors: 1, blue; 2, green; 3, yellow; 4, orange; 5, red. Groups were determined by principal component analysis, and their chemistry is summarized in table 1. Letters by vertical dashed lines refer to site descriptions in table 2. Blue line, acute toxicity standard; red line, chronic toxicity standard.

Table 1. Chemical composition of selected samples representing groups defined by principal component analysis, upper Animas River basin, 1997, 1998, and 2000.

[Values are in milligrams per liter, except pH; Phase: Diss, dissolved; coll, colloidal; <, less than]

		Inflows					Stream				
Group		1	2	3	4	5	1	2	3	4	5
SampleID		CGS-1459	CGS-4382	CGS-3081	UAEH-2465	AMIN-5858	CGS-450	CGS-5466	CGS-2725	UAEH-3400	AMIN-2515
Distance (m)		1,459	4,382	3,081	14,593	23,726	450	5,466	2,725	15,528	20,383
SiteName		Seep down slope from mine	Placer Gulch at mouth	Drains area down from Vermillion mine	Minnie Gulch	Seep along grassy bank	Stream down from Mtn Queen	Up from Columbus mine	Bracket for inflows upstream	Downstream from braids near Kittimack	Stream
pH, in standard units		3.98	5.74	7.09	7.93	5.67	6.97	5.81	4.98	7.05	7.55
Calcium		32.0	21.1	73.0	36.8	229	81.7	32.4	34.8	29.2	37.8
Magnesium		13.0	2.13	4.10	2.94	13.0	8.20	4.07	5.84	2.10	2.56
Sodium		2.30	.69	4.40	2.71	5.38	21.3	1.94	3.23	3.01	2.20
Alkalinity, as calcium carbonate		<1	<1	<1	47.6	8.85	<1	<1	<1	36.6	<1
Sulfate		262	59.6	151	61.0	861	192	112	157	64.0	77.6
Chloride		.30	.15	.39	.21	1.74	.140	.190	.110	3.33	1.61
Fluoride		1.21	.25	.47	<0.1	<0.1	.260	1.89	2.98	<0.1	<0.1
Silica		13.0	.96	6.20	6.65	24.6	5.14	8.92	12.1	5.31	6.63
Aluminum	Diss	12.9	.187	.080	.057	1.74	.083	2.26	6.41	.035	.024
	Coll	<.020	.372	.121	<.020	<.020	.053	.868	.218	.062	.065
Cadmium	Diss	.021	.004	<.001	<.001	.056	.003	.007	.011	.002	<.001
	Coll	.002	<.001	.002	<.001	<.001	<.001	<.001	<.001	<.001	<.001
Copper	Diss	.028	.017	.003	<.002	.248	<.002	.018	.023	.004	<.002
	Coll	.003	.005	<.002	<.002	<.002	.003	<.002	<.002	<.002	<.002
Iron	Diss	.044	.168	.052	.049	.020	.016	.144	.121	<.002	.017
	Coll	<.002	.056	1.62	<.002	<.002	.090	.107	.094	.032	.460
Lead	Diss	<.023	<.023	<.023	<.023	<.023	<.023	<.023	<.023	<.023	<.023
	Coll	<.023	<.023	<.023	<.023	<.023	<.023	<.023	<.023	<.023	<.023
Manganese	Diss	29.0	.912	.110	.021	34.4	.037	7.24	15.0	.242	.459
	Coll	.557	.005	.282	<.001	<.001	.002	<.001	.068	.008	.016
Nickel	Diss	.021	.004	<.003	<.003	.045	<.003	.006	.008	<.003	<.003
	Coll	<.003	<.003	<.003	<.003	<.003	<.003	<.003	<.003	<.003	<.003
Strontium	Diss	.068	.121	.860	.504	2.13	.715	.173	.164	.261	.381
	Coll	.005	.002	.029	.504	2.13	<.001	<.001	.002	.008	.006
Zinc	Diss	10.0	1.15	.082	.008	12.7	.051	1.80	2.44	.305	.273
	Coll	<.001	<.001	.186	<.001	<.001	<.001	.006	.030	.013	.056

along the right bank. Downstream from an area with substantial iron staining (site III, 23,876 m) was the third increase. Finally, there was an increase at 24,917 m, which was downstream from the Lackawanna Mill (site IV, fig. 5). Field observation indicated that tailings deposits along the right bank were a more likely source of this zinc increase, however.

Mass-Load Profiles

Constructing profiles of mass loading for the 26 km study reach required assumptions about the effects of inflows along the study reach. Loading profiles from the California Gulch study reach were used to the point downstream from the North Fork (A3). After that point, the change in load for stream segments of the Eureka study reach were applied to the new load just upstream from Eureka (A4). Downstream from the Howardsville gauge (A7), the changes in load for stream segments from the Howardsville study reach were applied. This method assumes that areas of loss and gain would be the same in all three years. Because the analysis uses the normalized load, it compares patterns rather than absolute values, and should be comparable among the different years.

Changes in concentrations of constituents need to be evaluated within the context of catchment hydrology, and this is accomplished by load calculations. Normalization of loads with respect to the cumulative instream load allows the comparison of patterns along the study reach (fig. 6). Constituents that are relatively conservative during transport have normalized values near 1 at the end of the study reach. The conservative constituents include aluminum, manganese, strontium, sulfate, and zinc. Cadmium, copper, and iron were reactive constituents, and lost mass load along the study reach.

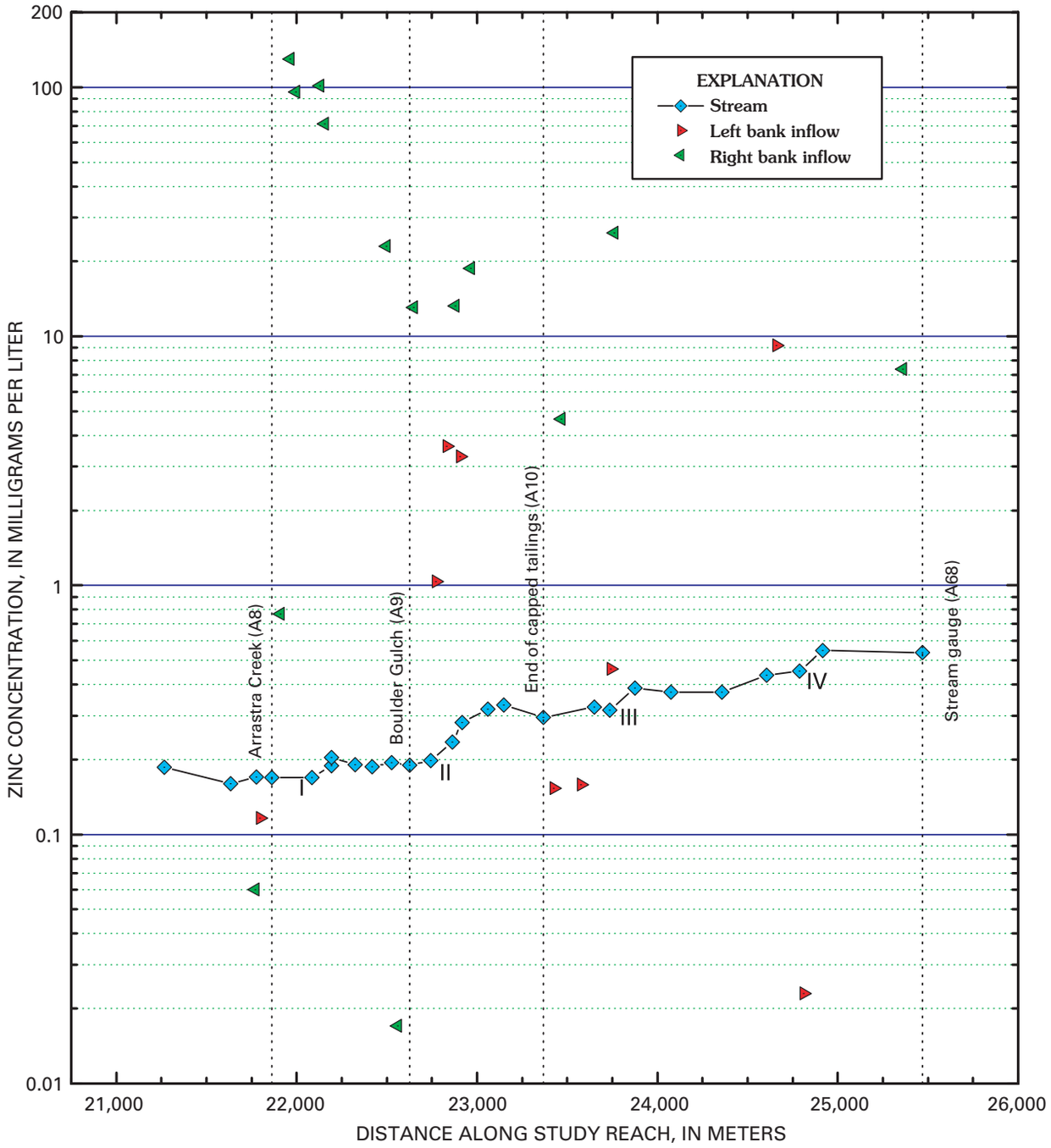

Figure 5. Variation of dissolved zinc concentration with distance, upper Animas River basin, from Arrastra Creek to Silverton, August 2002. Sites I–IV, locations of zinc increase discussed in text.

Three patterns of load profiles existed among the solutes (fig. 6). Aluminum, manganese, and zinc increased substantially in the study reach upstream from Placer Gulch (A2) and North Fork (A3; fig. 6*A*, *B*). Cadmium, copper, and iron did not increase greatly in the California Gulch study reach, but did increase greatly in the Howardsville study reach (fig. 6*A*, *B*). Strontium and sulfate had similar patterns: Their greatest increases were at Placer Gulch (A2), the tailings discharge (A6), and the reach of capped tailings (sites # 507–509; A10, fig. 6*C*).

The summary of the mass-load calculations indicates a great variation in the magnitude of cumulative instream load among the selected constituents (table 2). Sulfate load comes from both mine and non-mine related sources, and was very large in comparison to the other constituents. Manganese load was large, reflecting the importance of manganese gangue minerals in QSP deposits near the headwaters of California Gulch (fig. 2). Aluminum, iron, strontium, and zinc loads also were sizable, much greater than the loading of cadmium and copper.

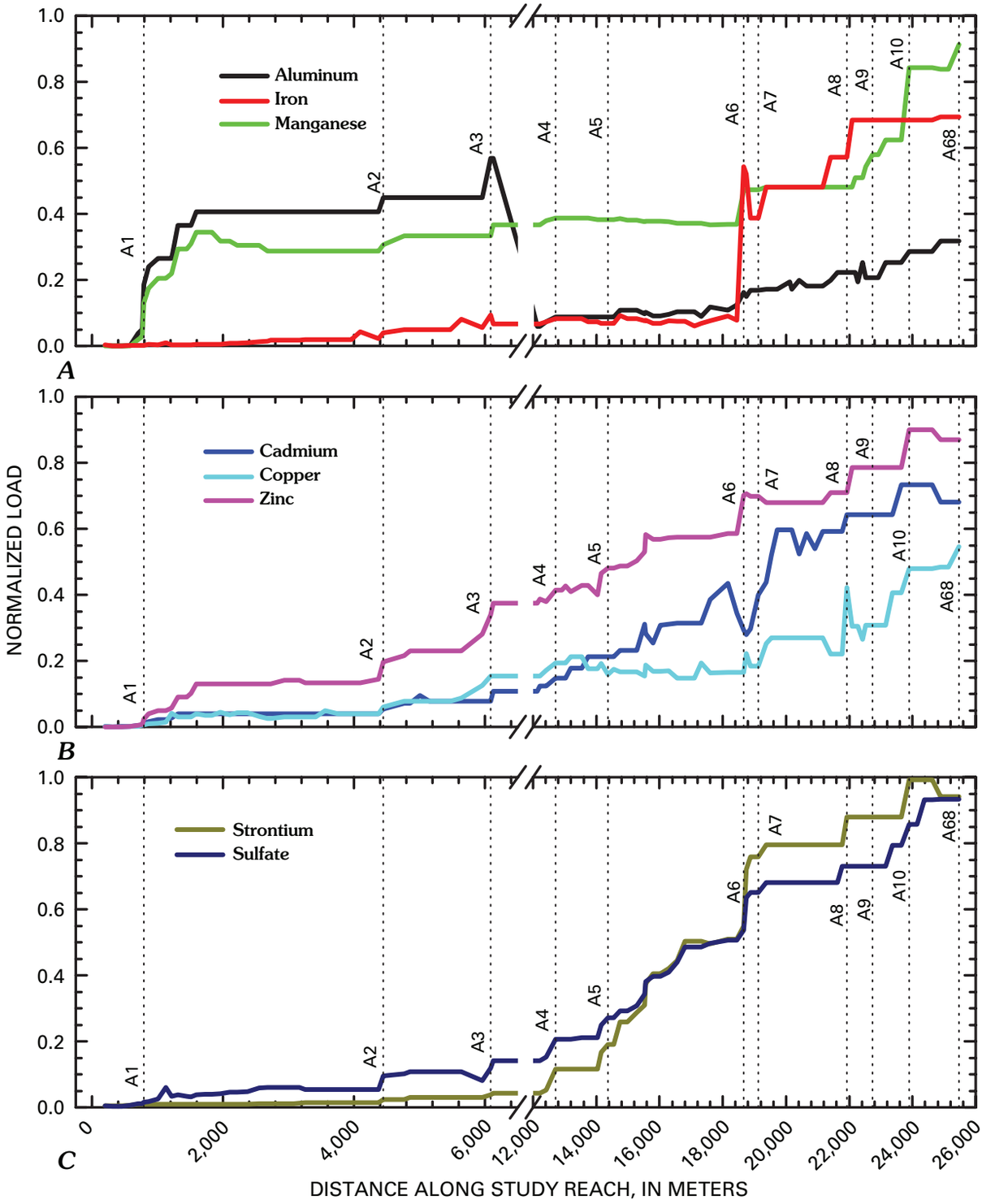

Figure 6. Variation of normalized instream loads for *A*, aluminum, iron, and manganese; *B*, cadmium, copper, and zinc; *C*, strontium and sulfate with distance, upper Animas River basin, 1997, 1998, and 2000. Labels on vertical lines refer to locations of substantial change along the study reach in figure 2 and table 2.

Principal Locations of Loading

Aluminum and manganese profiles mostly increased at similar locations (fig. 6*A*). Their basic pattern consisted of many considerable inflows between 701 m and 1,586 m and a moderate loading from Placer Gulch (A2). Aluminum loading was substantially greater from the North Fork Animas River (A3) because the North Fork drains the large QSP alteration of Houghton Mountain (fig. 2). Note that a loss of 68.5 percent of the aluminum load to the streambed occurred along the study reach (table 2; fig. 6*A*). Much of this loss occurred between A3 and A4 (fig. 6*A*), but started between A2 and A3 where the pH of the stream water exceeded 5.0. Between A2 and A3, there was not a net loss (fig. 6*A*), so the precipitate on the cobbles represents only a small mass of the colloidal aluminum, less than the error in the load calculation, that is integrated on the cobbles over time. The relatively high pH between A3 and A4 (fig. 4*A*) was sufficiently high for the substantial loss of aluminum load to the streambed cobbles in that reach.

Downstream from a rhyolite outcrop (1,586 m), where the load of manganese and other metals increased substantially, there was a loss of manganese to the streambed (fig. 6*A*). Manganese loss did not result in a visible coating on the streambed; however, gravels along the stream bank between 1,142 m and 1,310 m were coated with manganese precipitates. Visible cementing of streambed gravels with manganese forms a manganocrete that helps account for the loss of manganese load in the stream. Far downstream, along the Howardsville study reach, manganese loading from the capped tailings repositories (A10) was substantial, and manganocrete also occurred there, along the right stream bank.

The greatest increase of iron load was from the tailings discharge (A6, fig. 6*A*). Two other substantial loads occurred at 21,413 m and 22,084 m. Both increases occurred near old milling sites (site # 234) on the left and right banks. The second increase was downstream from a very acidic spring that discharged at stream level, and had very high iron concentrations. Downstream from each of these inflows, the iron load was transported mostly in the colloidal phase that made the iron transport relatively conservative despite some loss downstream from the tailings discharge inflow (A6, stream group 5, table 1).

Cadmium, copper, and zinc loading had similarities, yet each metal differed in principal locations of loading (fig. 6*B*). The greatest increase in cadmium load occurred near the Howardsville gauge (A7); an old mill site lies nearby (Nash, 2000). Loading of copper was important from acidic inflows along the California Gulch study reach (downstream from A1, fig. 6*B*) and from North Fork (A3). Arrastra Creek (A8) was the location of the greatest increase in copper load (fig. 6*B*). The historical mines at Silver Lake (sites # 343, 345, 348) are located near Arrastra Creek headwaters, and Silver Lake Mill # 2 is on the left bank near mouth of Arrastra Creek. These features, along with mineralized veins of the South Silverton mining area, could be sources for copper load along this reach. Downstream from each of these locations of copper

Table 2. Summary of load calculations and cumulative instream load for selected subreaches, upper Animas River basin, 1997, 1998, and 2000.

[Dist, distance along study reach, in meters; Al, aluminum; Cd, cadmium; Cu, copper; Fe, iron; Mn, manganese; Sr, strontium; Zn, zinc; SO_4, sulfate; all values in kilograms per day, except percentages; numbers in parentheses indicate rank of five greatest loadings for each constituent (1, greatest)]

	Al	Cd	Cu	Fe	Mn	Sr	Zn	SO_4
Cumulative instream load	116	1.51	4.60	82.9	333	84.5	129	22,500
Cumulative inflow load	72.7	0.53	2.28	24.6	185	62.4	87.9	12,200
Percent inflow load	62. 6	34.8	49.6	29.7	55.5	73.9	68.0	54.2
Unsampled inflow	43.5	.99	2.32	58.3	148	22.1	41.4	10,300
Percent unsampled inflow	37.4	65.2	50.4	70.3	44.5	26.1	32.0	45.8
Attenuation	79.5	0.46	2.53	29.1	133	8.50	54.7	3,440
Percent attenuation	68.5	30.6	55.0	35.1	40.1	10.1	42.3	15.3

Site description	Dist	Al	Cd	Cu	Fe	Mn	Sr	Zn	SO_4
Down from Placer Gulch (A2)	4,448	52.2 (1)	0.084	0.516 (3)	5.95 (5)	121 (1)	1.99	26.3 (2)	3,050 (2)
Second site down from North Fork (A3)	6,128	13.9 (2)	0.110	0.430	6.67 (4)	20.2	1.62	23.1 (3)	1,630
Downstream from Eureka Gulch (A4)	12,714	1.51	0.072	0.463 (4)	0.798	2.07	5.68	6.67	1,280
Downstream from braided reach (A5)	14,368	0.484	0.146 (4)	0.182	0.000	1.22	5.77 (5)	13.9 (5)	1,200
Downstream from tailings drainage (A6)	18,656	12.0 (3)	0.438 (1)	0.432 (5)	42.6 (1)	35.5 (3)	23.1 (1)	27.8 (1)	5,260 (1)
At State gauge at Howardsville (A7)	19,121	2.31	0.173 (3)	0.224	0.000	1.25	15.5 (2)	0.095	2,060 (4)
Downstream from Arrastra Creek (A8)	21,921	10.4 (4)	0.408 (2)	1.27 (1)	13.4 (2)	0.672	7.66 (4)	3.87	1,230
Downstream from Boulder Gulch (A9)	22,742	6.80	0.000	0.196	9.39 (3)	32.6 (4)	0.000	9.84	0
Downstream from capped tailings (A10)	23,899	9.22 (5)	0.139 (5)	0.792 (2)	0.000	87.9 (2)	9.44 (3)	14.9 (4)	2,850 (3)
Animas River at Silverton (A68)	25,469	3.68	0.000	0.304	0.728	25.2 (5)	0.000	0.000	1,720 (5)

loading, the load was attenuated. Loading of zinc also was important from the acidic inflows near the beginning of the study reach, but its pattern differed from those of aluminum and manganese (fig. 6*A*, *B*). Zinc load entered the stream at many more locations, including Placer Gulch (A2), Frisco tunnel (4,856 m), North Fork (A3), the braided reach (A5), the tailings discharge (A6), and the capped tailings repositories (A10).

The mass-loading profile of strontium and sulfate represents a final pattern that differs from that of the other constituents (fig. 6*C*). These loads resulted from weathering of both altered and unaltered rocks in the watershed. Because strontium was not associated with ore or gangue minerals, no loading came from the acidic springs between 859 m and 1,586 m that contributed large loads of aluminum and manganese. Sulfate load, on the other hand, was contributed by the acidic inflows between 859 m and 1,586 m. Both strontium and sulfate loads increased substantially downstream from the braided reach (A5), and remained elevated to the tailings discharge (A6), where both loads increased from the tailings discharge (A6). They both increased from the inflow of Cunningham Creek (18,746 m, downstream from A6). Cunningham Creek drains an area of propylitically altered rocks, which would be consistent with the loading of strontium. Several large sulfate loads entered the stream in the area of the capped tailings (A10).

Unsampled Inflow

Unsampled inflow mostly indicates loading from dispersed, subsurface inflow in most stream segments; however, it also can result from skipping some surface inflows along the study reach, either intentionally or unintentionally. To sample every inflow is not possible. Unsampled inflow was responsible for 66 percent of the loading of cadmium and 70 percent of the loading of iron (table 2). Unsampled inflow was less important for aluminum, copper, manganese, strontium, zinc, and sulfate, but it did occur for each of the selected constituents. A very noticeable change occurred from sampled to unsampled inflow along the study reach. Two main locations of unsampled inflow loading occurred. First, the tailings drainage near Howardsville (A6) was important for unsampled inflow of iron. Second, downstream from Arrastra Creek (A8) to 23,899 m, a great increase was measured in the unsampled inflow load of all the metals, except iron and sulfate. The source of metals in this reach of the stream has not been determined, but mine wastes and old mill sites lie along on both sides of the stream. Sampling in 2002, however, indicated higher concentrations of zinc along the right bank than along the left bank (B.A. Kimball, unpub. data, 2002). Seeps along the right bank had iron and aluminum precipitates, and a substantial amount of manganocrete was observed in the area of the capped tailings repositories (A10). Most of this unsampled inflow occurred in the stream segments from 23,147 m to 23,899 m. In 1997, these inflows were not visible, but in 2002 during extreme base-flow conditions, some of these inflows were sampled; they are indicated by the plot of zinc concentration (fig. 5). Considering the relatively high flow of the upper Animas River compared to other streams in this study, the small increases in concentration (fig. 4) represent a substantial increase in metal load.

Attenuation of Load

Attenuation of cadmium and copper exceeded 30 percent along the study reach, but relatively little attenuation occurred for the other constituents, particularly strontium and sulfate (table 2). Much of the copper attenuation was in the braided reach of the stream (A5). Otherwise, no spatial pattern for the loss of constituent loads was observed. Between 15,528 m and 15,793 m most constituent loads decreased. Downstream from Cunningham Creek (18,746 m) and Hematite Gulch (18,881 m) iron load decreased, as did the loads of aluminum, cadmium, and manganese. Downstream from the tailings discharge (A6) and past Cunningham Creek (18,746 m), the stream bank along the left side was heavily stained with iron precipitate. Most of the attenuation of aluminum was at 22,265 m and 22,527 m. The greatest attenuation of copper was downstream from the greatest loading of copper, at 22,084 m (fig. 6*B*). For both aluminum and copper, this attenuation was downstream from substantial unsampled inflow.

Summary

Mass loading of constituents along a study reach of almost 26 km in the upper Animas River basin was detailed by three different studies. Loading in the headwaters was dominated by drainage from zones of QSP alteration. A substantial change in the character of the water with respect to aluminum and copper occurred in the braided reach downstream from Eureka Gulch. Loading along the remainder of the study reach was dominated by inflows in the areas of tailings near Howardsville (tailings discharge, A6, site # 234) and a lower reach of capped tailings repositories (A10).

Cement Creek Basin, 1996, 1999, and 2000

Cement Creek originates above 3,000 m elevation and has a drainage area of about 52 square kilometers (Crowfoot and others, 1997). A stream gauge near the mouth of Cement Creek indicates that most of the streamflow occurs during snowmelt runoff during May and June. The best opportunity to quantify dispersed subsurface inflow to the stream is during late summer base flow. Both acidic and non-acidic inflows enter along Cement Creek, and they have a wide range of chemical composition. Among the acidic inflows, some are acidic from weathering of altered bedrock and others are acidic due to acceleration of weathering by mining activities. The most recent mining activity in the area was at Gladstone (fig. 7, C4).

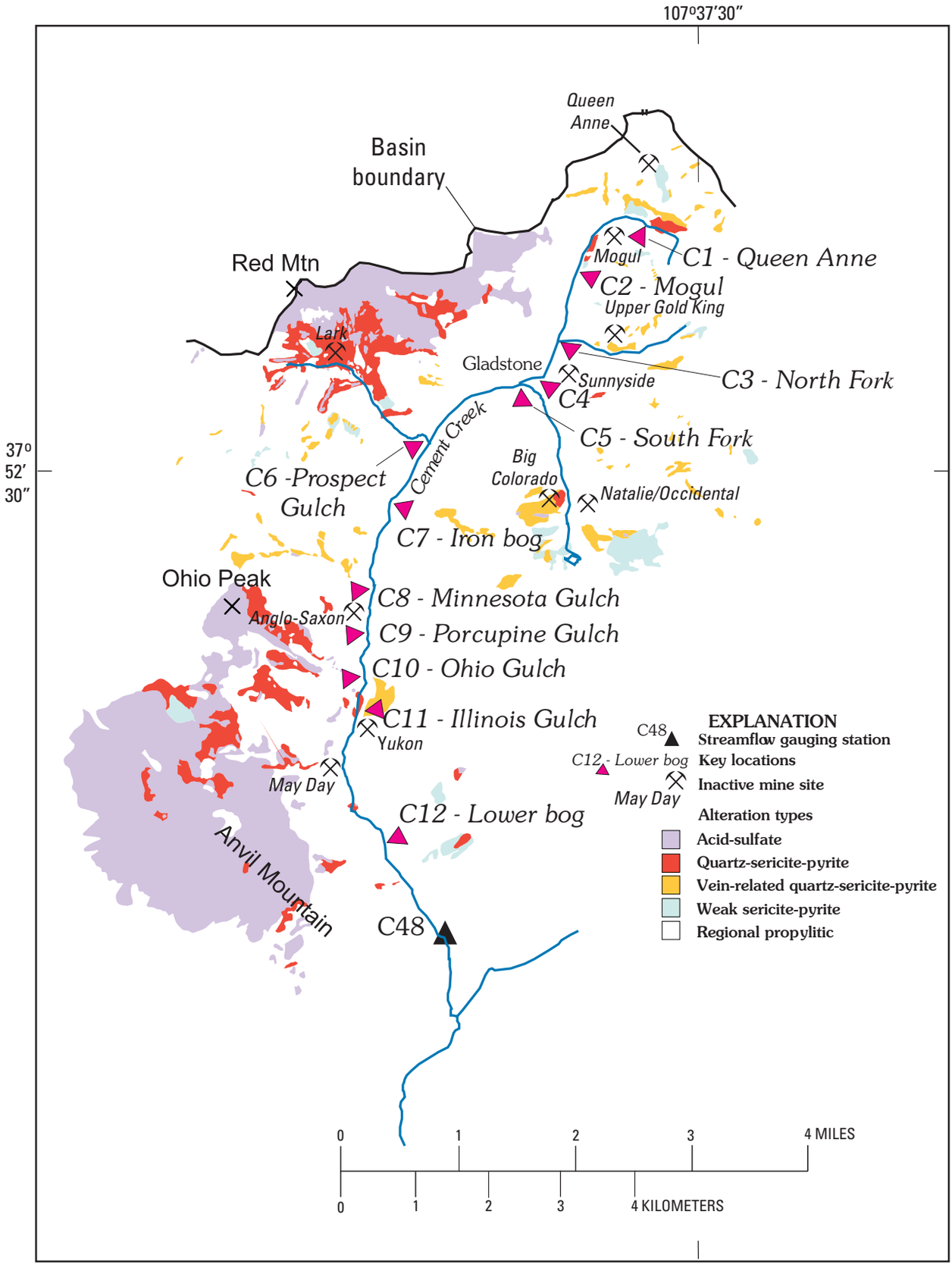

Figure 7. Location of study area, alteration zones, key locations, and principal sites of inactive mines, Cement Creek basin, 1996, 1999, and 2000.

Four mass-loading studies have been completed in Cement Creek. The first, in 1996, started a short distance upstream from the North Fork Cement Creek (C3) and continued to the U.S. Geological Survey stream gauging station 09358550 (C48) near the mouth (Kimball and others, 2002). The second, in 1999, started high in the basin, upstream from the Queen Anne mine (upstream from C1), and continued to a site downstream from the South Fork (C5) of Cement Creek. Also in 1999, a shorter injection study was done in Prospect Gulch (Wirt and others, 1999). In 2000, part of the 1996 study reach was revisited, starting upstream from Ohio Gulch (C10), and continuing to a point downstream from the May Day mine (Wright, Kimball, and Runkel, this volume, Chapter E23). This last study had the purpose of evaluating effects of remediation at the May Day tailings. Some factors complicate the combination of these data sets into one long view of the Cement Creek basin. First, in 1996 there was active treatment of water from Cement Creek at the Sunnyside mine at Gladstone, and the water that was returned to Cement Creek after the treatment had a much higher pH and lower base-metal concentrations than the water upstream from the treatment (fig. 8). This high pH decreased because of many acidic inflows, and with the inflow from Prospect Gulch, the pH was again very acidic. Second, the stream chemistry changed upstream from North Fork Cement Creek between sampling in 1996 and 1999 (fig. 8). The pH decreased substantially. A detailed discussion of these changes and their implications is in Appendix 2. Third, pH downstream from Illinois Gulch (C11) increased more in 2000 than in 1996 (fig. 8).

Chemical Characterization of Synoptic Samples

The chemical composition of synoptic samples in the Cement Creek basin varied greatly. The combined data set was analyzed by PCA to define groups with similar chemical composition.

Inflows

Six groups of inflow samples were distinguished by PCA analysis. Inflow groups generally reflect the extent of water-rock interaction with particular alteration mineral assemblages (Kimball and others, 2002; Bove and others, 2000; Mast and others, 2000). Samples representing the median values of each group are listed in table 3. Samples of inflow group 1 were the least affected by interaction with alteration minerals, as indicated by relatively low concentrations of all the constituents and high values of pH. Concentrations of sulfate and the metals were particularly low with respect to other inflow groups (table 3). Samples from inflow group 5 also had high pH, but had higher concentrations of sulfate and other constituents than samples from group 1, suggesting that they had some interaction with alteration minerals.

Samples in each of the other groups indicated a wide range of interaction with alteration mineral assemblages. Groups 2, 3, and 6 (fig. 9*A*) had the lowest pH values and the highest concentrations of metals (table 3). Among these acidic samples, group 3 had the highest concentrations of copper (fig. 9*C*) and zinc (fig. 9*D*). Sample sites of groups 2 and 3 included the Mogul mine (C2), North Fork Cement Creek (C3), Prospect Gulch (C6), Ohio Gulch (C10), and the Yukon tunnel (just downstream from C11, fig. 7; site designations also available in table 5). Each of these samples represents water from subbasins with V-QSP alteration, and most have come from locations of mining (fig. 7). Thus, group 2 likely represents many of the mine-related inflows.

Samples represented in group 4 included high-pH–high-sulfate concentration inflows (table 3) such as Elk tunnel (CE-4493), Porcupine Gulch (C9), and Illinois Gulch (C11). These samples had high concentrations of calcium, manganese, and strontium (table 3), which may reflect the presence of neutralizing carbonate minerals from propylitic alteration minerals. However, the high manganese concentrations could indicate the influence of other alteration mineral assemblages. Metal concentrations could have been lowered because of the higher pH.

Samples from inflow group 6 occurred between South Fork Cement Creek (C5) and Prospect Gulch (C6), in the vicinity of the iron bog (C7) and also at the lower bog (C12; CE-9543). These samples are distinct because of high concentrations of silica, aluminum, and iron (table 3), but copper and zinc concentrations were low compared to those of samples from inflow group 3. This difference might suggest that these inflows of group 6 drain alteration assemblages that have lower base metal content. Many of the ferricretes in Cement Creek and other basins of the watershed study area predate mining, and the type of inflow represented by group 6 could be typical of sources for water that formed the ferricretes (Wirt and others, this volume, Chapter E17).

Stream

Principal changes in stream chemistry of Cement Creek occurred at the same locations as the major changes in pH (figs. 7 and 9*A*). Five groups of stream samples are represented by the samples in table 4, but this excludes those samples from 1996 between South Fork (C5) and Prospect Gulch (C6) that were affected by the active treatment. Excluding those samples, the overall variation in pH of the stream was from 6.83 at the most upstream site to 3.32 at a site downstream from the North Fork inflow (C3). At the beginning of the study reach, the high pH decreased below 6.5 downstream from the first sampled inflow (upstream from C1). The next major decrease in pH was below the inflow from the Mogul mine (C2), where pH dropped below 4.5. Samples collected in 1999 and 2000 indicated that pH remained less than 4.5 along the remainder of Cement Creek (fig. 8). The decrease in pH at 11,245 m (CE-8218; end of blue diamonds, fig. 8) reflects a difference between samples collected in 2000 (higher pH upstream) and 1996 (lower pH downstream), an artifact of joining the two data sets.

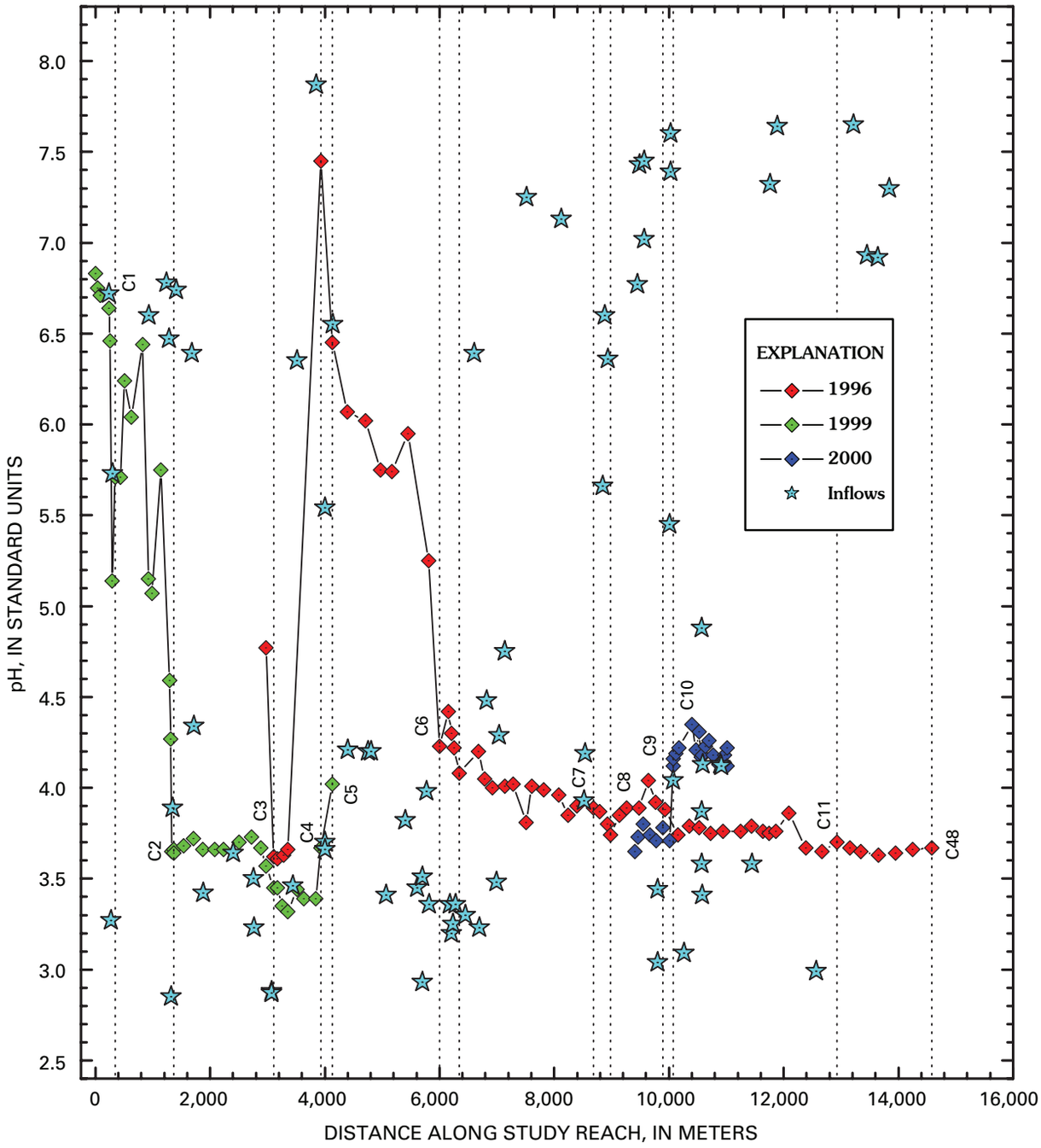

Figure 8. Variation of pH with distance for three mass-loading studies, Cement Creek basin, 1996, 1999, and 2000. Labels on vertical lines refer to locations in figure 7.

Concentrations of major ions varied in downstream steps, similar to the pattern of pH (table 4). Upstream from the Mogul mine (C2; groups 1 and 2, table 4), concentrations were relatively low, but they increased substantially downstream from the Mogul mine (group 3, table 4). The next step occurred downstream from the North Fork (C3; still group 3, table 4). Inflow from the Sunnyside mine (C4) caused a substantial increase (group 4, table 4). A final step occurred downstream from Porcupine Gulch (C9, group 5, table 4).

Substantial colloidal iron concentrations (fig. 9*B*) occurred along the entire study reach but were greater than dissolved iron concentrations upstream from the Mogul mine inflow (C2). Colloidal aluminum also was important upstream from the Mogul mine inflow (C2). Values of pH in these reaches were consistent with the formation of iron and aluminum oxyhydroxide-mineral colloids, according to calculations with PHREEQC (Parkhurst and Appelo, 1999). Downstream from the Mogul mine inflow (C2), pH was less than 3.7, which

Table 3. Chemical composition of selected inflow samples representing groups defined by principal component analysis, Cement Creek basin, 1996, 1999, and 2000.

[RBI, right bank inflow; LBI, left bank inflow; concentrations in milligrams per liter; diss, dissolved; <, less than]

Group	1	2	3	4	5	6
Sample identification	ROSS-1187	ROSS-2711	MD-852	MD-1230	CE-8860	CE-3180
Source	RBI	LBI	LBI	RBI	LBI	RBI
Downstream distance, in meters	1,237	2,761	10,261	10,678	11,887	6,207
Chemical character of group	High pH, low sulfate	Acidic, moderate sulfate	Acidic, high sulfate and metal concentrations	Acidic, moderate concentrations	High pH, moderate concentrations	Acidic, high concentrations
Number of samples	10	10	3	21	11	22
Site description	Drains across road	Draining Fe bog and Red and Bonita mine	Seeps down gradient of Yukon tunnel	Ferricrete spring	Inflow	Inflow
pH, in standard units	6.78	3.50	3.09	4.46	7.64	3.20
Calcium	19.4	25.8	165	103	41.3	164
Magnesium	1.35	3.90	19.7	5.28	2.94	9.74
Sodium	.69	2.28	4.18	2.74	1.19	4.31
Sulfate	22.4	88.3	722	275	52.9	582
Chloride	.06	.25	.52	.54	.37	.94
Silica, diss	3.46	23.3	61.0	20.3	6.97	44.1
Aluminum, diss	.063	12.5	25.9	2.93	.041	8.19
Cadmium, diss	<.001	.049	.052	.005	<.001	.041
Copper, diss	<.002	.499	1.71	.012	.001	.006
Iron, diss	<.002	.270	9.64	.029	.026	8.46
Lead, diss	.023	.023	.345	.023	.023	.023
Manganese, diss	.015	1.81	15.7	.651	.123	1.41
Nickel, diss	<.003	.016	.050	.005	.003	.021
Strontium, diss	.174	.221	1.83	1.38	.391	1.32
Zinc, diss	.021	9.16	10.6	.377	.024	.521

rendered aluminum soluble, and colloid formation did not occur. Iron, however, was still insoluble and ferrihydrite or schwertmannite colloids occurred. Dissolved iron and aluminum were dominant along most of the remaining study reach, but colloidal iron increased downstream from the inflow of Illinois Gulch (C11) as a result of the higher pH. The similarity of iron concentrations for 1996 and 2000 between C9 and C10 (fig. 9*B*) might not be expected because most of the iron was removed from the stream water by the mine treatment in 1996 (Kimball and others, 2002). To have nearly equal concentrations is consistent with the geochemical control of dissolved iron concentrations by colloidal formation. This was indicated by the simulation of Walton-Day and others (this volume, Chapter E24).

For copper (fig. 9*C*), important differences appeared among data from 1996, 1999, and 2000. Concentrations of copper were high downstream from North Fork in 1996 but much lower upstream from North Fork (Kimball and others, 2002). Copper concentrations in samples collected in 1999 were much higher upstream from North Fork. This, and other significant chemical changes upstream from North Fork between 1996 and 1999, are discussed in Appendix 2.

Another difference occurred downstream from South Fork (C5), where the dissolved copper concentration was 0.02 mg/L in 1996 (Kimball and others, 2002, table 3) but was 0.65 mg/L in 1999. Finally, in the interval between 9,409 and 11,018 m higher copper concentrations occurred in 2000 than in 1996 (fig. 9*C*). These likely represent differences caused by the lack of treatment at the Sunnyside mine in 2000. Walton-Day and others (this volume) simulated the transport of copper along Cement Creek, using the results of the 1999 sampling and the calibration with inflow loads from 1996. These simulations indicated that the higher copper below South Fork (C5) would be 0.27 mg/L at the beginning of the May Day study reach. This prediction is substantially higher than the 0.076 mg/L at 9,409 m measured in 2002 (Wright, Kimball, and Runkel, this volume; see fig. 9*C*, this report). Sorption of copper at the low pH near 4.0 would be minimal (Walton-Day and others, 2000), so this could indicate coprecipitation of copper with the iron colloids. Walton-Day and others (2000) suggested that this could occur in mixing zones, where higher values of pH might be locally important, even though the overall pH of the stream remains low (Kimball and others, 2002).

The pattern of zinc concentration had many similarities with that of copper (fig. 9*D*). Although zinc concentration was 2.6 mg/L upstream from North Fork (C3) in 1996, the concentration at that point in 1999 was 10.9 mg/L. Downstream from South Fork (C5), zinc concentration was 0.82 mg/L in 1996 and 4.27 mg/L in 1997, reflecting the treatment that occurred

during the 1996 sampling. At the start of the May Day study reach (9,409 m, fig. 9*D*), zinc concentration was near 1.0 mg/L in 1996 and 1.24 mg/L in 2000. The simulation of Walton-Day and others (this volume) predicts a concentration of about 2.3 mg/L for the beginning of the May Day study reach. The lower observed concentration in 2000 likely is obtained from the effects of mixing zone processes, as suggested for copper (Walton-Day and others, 2000; Kimball and others, 2002).

Mass-Load Profiles

Constructing profiles of mass loading with the combined data sets required some assumptions about the effects of inflows along the study reach. Loading profiles from the 1999 study reach were used to the point downstream from South Fork (C5). After that point, the change in load for stream segments of the 1996 study reach were applied to the new load at C5. This assumes that areas of loss and gain were the same downstream from the mine in 1999 as they were in 1996, which essentially is the same assumption used for the solute-transport simulations (Walton-Day and others, this volume).

A summary of the mass-load calculations for selected constituents, and the sum of cumulative instream load for selected sections of the study reach, are given in table 5. The summary indicates the great variation in the magnitude of cumulative instream load. Iron mass load was greater than 1,000 kg/day, and aluminum was about half that amount. These loads are substantially greater than those in the upper Animas River basin, indicating the importance of the acid-sulfate and quartz-sericite-pyrite altered rock that crops out in the Cement Creek basin. Mass loading of base metals also was substantial for copper, lead, and zinc, but both copper and zinc loads were less than in the upper Animas River basin. Although lower in magnitude than copper and zinc loads, the mass loads of cadmium and lead were important.

Principal Locations of Loading

Normalized loads indicate the patterns of loading along the study reach (fig. 10). Normalization is with respect to the cumulative instream load in table 5. Constituents that are most conservative during transport had normalized values near 1 at the end of the study reach, including copper (because of the low pH of Cement Creek), manganese, strontium, and sulfate. Loads of reactive constituents, including zinc, cadmium, aluminum, iron, and lead decreased along the study reach. Three general patterns of load profiles emerged among the solutes (fig. 10; table 5). Copper and zinc loads increased substantially in the upper part of the study reach at the Mogul mine inflow (C2) and the North Fork (C3) (fig. 10*A*). Cadmium load also increased, but not as much as copper and zinc. Instead, downstream from the inflow of South Fork (C5), cadmium load increased similar to loads of aluminum and iron (fig. 10*B*). Aluminum and iron loads increased at many locations, but particularly at the iron bog (C7) and the lower bog (C12), and at 13,953 m (fig. 10*B*), where lead load also increased substantially. Finally, manganese, strontium and sulfate mostly increased at Sunnyside mine (C4), Minnesota Gulch (C8), and Yukon tunnel (downstream from C11; fig. 10*C*).

Despite differences in details among the load profiles, the metal loads collectively indicated the areas where most of the metal loads entered the stream. Although it might seem that loads from these sources could be divided into mined and unmined areas, mined and unmined sources exist in almost every subbasin along Cement Creek (Wright and Nordstrom, 1999). Therefore, such a distinction is difficult. The summary of cumulative instream load in table 5 is similar to that presented for sampled instream load by Kimball and others (2002), but table 5 reports load calculations with an analysis of load error that was not applied in Kimball and others (2002). The principal locations of loading were defined by the same stream segments in both reports, except that some areas with little or no loading were combined to simplify table 5. Such a large number of contributing segments indicates the widespread effects of alteration and mining in the Silverton caldera (Bove and others, 2000). Considering the patterns of all these constituents (table 5; fig. 10), the principal locations of loading include:

1. Mogul mine (C2): This was the major source for cadmium, copper, and zinc, but loads of aluminum, iron, manganese, and sulfate also were substantial.

2. North Fork Cement Creek (C3): The North Fork of Cement Creek was the second greatest source of copper and zinc. In 1996 it was the greatest source of copper (Kimball and others, 2002).

3. Sunnyside mine (C4): Effluent from the Sunnyside mine (the American tunnel) was the greatest source of strontium, and the loads of manganese and sulfate were substantial. These are the constituents that also had substantial loads from the treatment that was in place in 1996 (Kimball and others, 2002).

4. South Fork (C5): Inflow from South Fork Cement Creek was a considerable source for loads of iron, manganese, strontium, and sulfate.

5. Prospect Gulch (C6) and iron bog (C7): Kimball and others (2002) noted the substantial increase in many metal loads that occurred along a broad area around Prospect Gulch starting upstream from Prospect Gulch at CE-2785, and continuing downstream to CE-3185. This area includes both Prospect Gulch (C6) and the iron bog (C7). An adit contributed some drainage at CE-3425. Substantial mining took place in Prospect Gulch, and there are outcrops containing acid-sulfate and quartz-sericite-pyrite alteration assemblages in its headwaters (fig. 7). Taken together, this area was a substantial source of aluminum, cadmium, copper, iron, manganese, and sulfate. Because of the importance of Prospect Gulch to mass loading in Cement Creek, more detailed studies were done there and are summarized herein.

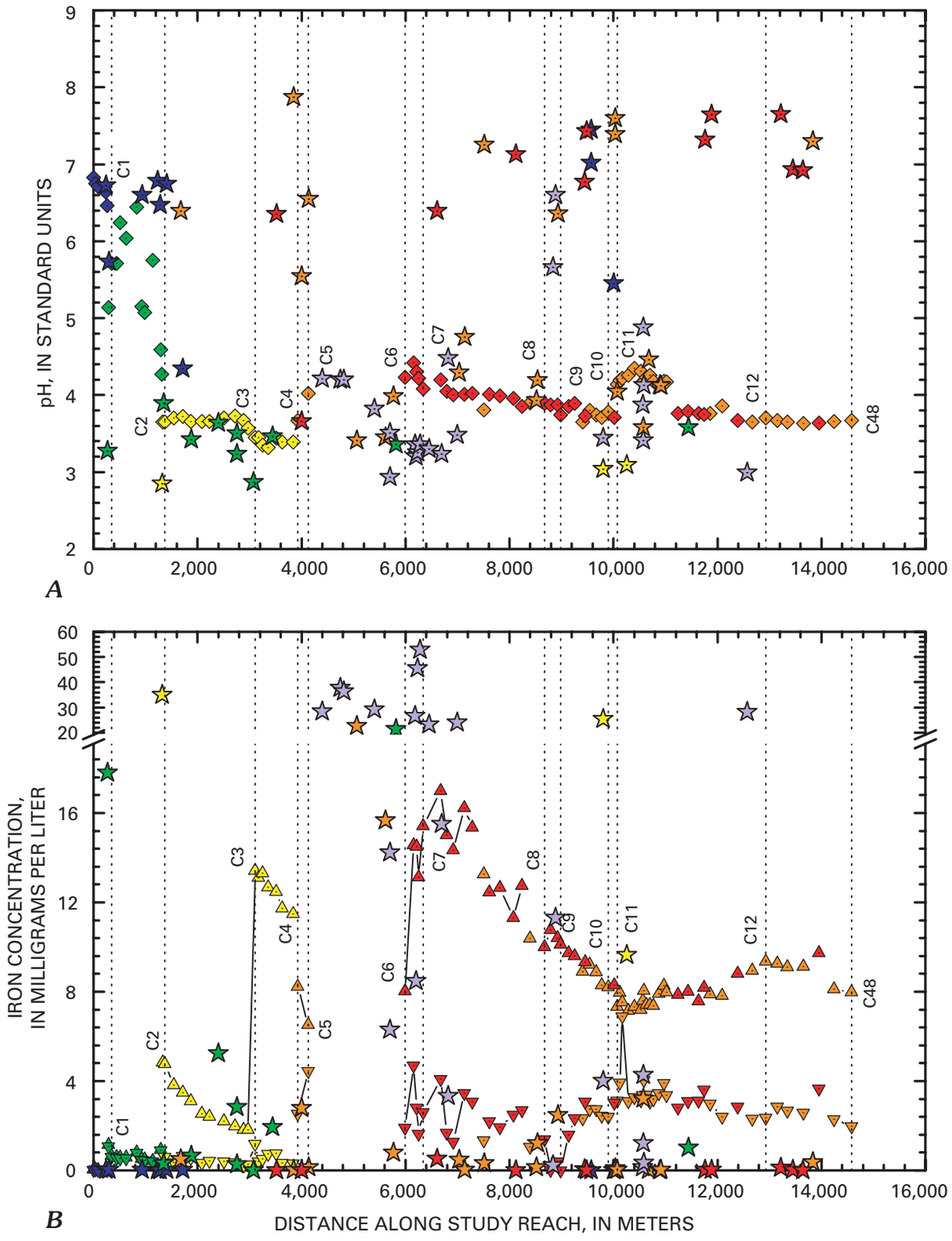

Figure 9. Variation of *A*, pH; of dissolved and colloidal concentrations of *B*, iron; and total-recoverable concentrations of *C*, copper; and *D*, zinc with distance, Cement Creek basin, 1996, 1999, and 2000. Groups of stream samples (diamonds, upward triangles, dissolved; downward triangles, colloidal), and inflows (stars) are indicated by colors: 1, blue, 2, green; 3, yellow; 4, orange; 5, red; 6, lavender. Groups were determined by principal component analysis, and their chemistry is summarized in tables 3 and 4. Labels on vertical dashed lines refer to locations in figure 7. *C*, *D*, Blue line, acute toxicity standard; red line, chronic toxicity standard.

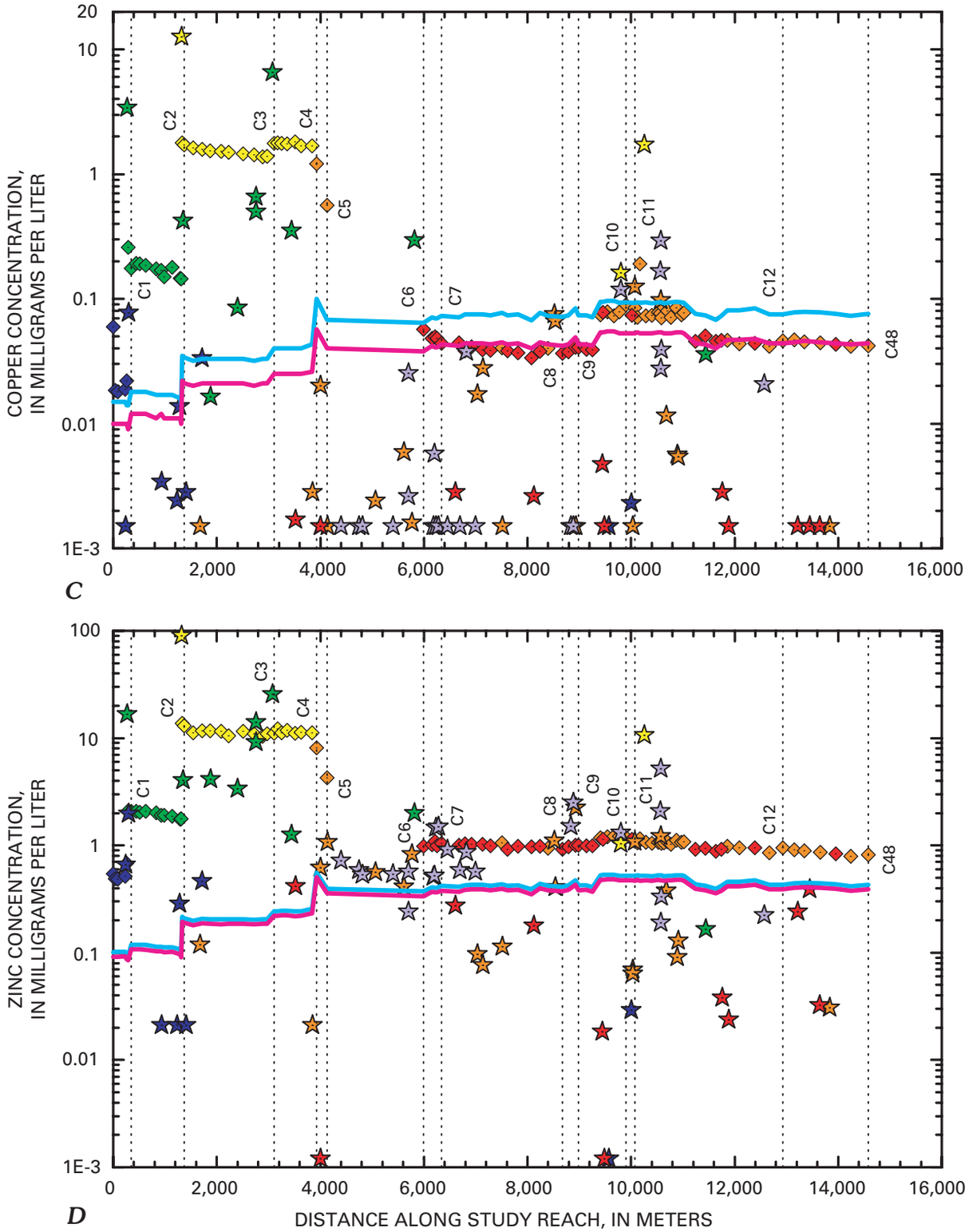

Figure 9—Continued. Variation of total-recoverable concentrations of *C*, copper; and *D*, zinc with distance, Cement Creek basin, 1996, 1999, and 2000. Groups of stream samples (diamonds, upward triangles, dissolved; downward triangles, colloidal), and inflows (stars) are indicated by colors: 1, blue, 2, green; 3, yellow; 4, orange; 5, red; 6, lavender. Groups were determined by principal component analysis, and their chemistry is summarized in tables 3 and 4. Labels on vertical dashed lines refer to locations in figure 7. Blue line, acute toxicity standard; red line, chronic toxicity standard.

Table 4. Chemical composition of selected stream samples representing groups defined by principal component analysis, Cement Creek basin, 1996, 1999, and 2000.

[Concentrations in milligrams per liter; diss, dissolved; coll, colloidal; <, less than]

Group	1	2	3	4	5
Sample identification	ROSS-0234	ROSS-0345	ROSS-3272	MD-712	CE-6107
Downstream distance, in meters	234	345	3,358	10,121	9,134
Character	Upstream from Queen Anne mine inflow	From Queen Anne mine inflow to Mogul mine inflow	From Mogul mine inflow to South Fork Cement Creek	From Prospect Gulch to downstream from Porcupine Gulch	Upstream from Ohio Gulch to end of study reach
Number of samples	5	11	19	31	28
Site description	Above inflow from talus	Below Queen Anne inflow	At treatment intake for Sunnyside	Down 88 m from Illinois Gulch	200 m downstream from Porcupine Gulch
pH, in standard units	6.64	5.71	3.32	4.19	3.85
Calcium	29.3	30.9	48.6	205	149
Magnesium	2.58	3.61	5.38	7.63	8.39
Sodium	0.79	0.77	1.48	3.97	3.38
Sulfate	24.6	34.5	80.9	536	460
Chloride	0.04	0.05	0.16	0.58	2.88
Silica	1.61	2.58	5.01	31.3	27.4
Aluminum, diss	.050	.722	8.63	5.37	5.15
Aluminum, coll	.313	.462	.020	.111	.382
Cadmium, diss	.003	.010	.153	.012	.050
Cadmium, coll	<.001	<.001	<.001	<.001	<.001
Copper, diss	.019	.175	1.76	.071	.039
Copper, coll	.048	.021	.004	<.001	.003
Iron, diss	.003	.036	11.9	4.03	8.13
Iron, coll	.035	.617	.743	3.92	1.60
Lead, diss	<.023	<.023	.026	<.023	.023
Lead, coll	<.023	<.023	<.023	<.023	.023
Manganese, diss	.123	1.22	4.11	1.78	2.67
Manganese, coll	<.001	<.001	.174	.010	.107
Nickel, diss	.003	.004	.018	.008	.015
Nickel, coll	<.003	<.003	<.003	<.003	<.003
Strontium, diss	.246	.169	.384	2.23	1.53
Strontium, coll	.018	.016	.008	.008	.112
Zinc, diss	.515	2.08	11.8	1.06	.992
Zinc, coll	.007	.005	.183	<.001	.082

Prospect Gulch is a steep-gradient mountain catchment that is strongly affected by natural acidity from pyrite weathering. Metal content in the stream water is a composite of multiple sources affected by hydrologic, geologic, climatic, and anthropogenic conditions. We identified sources of metals from various drainage areas using tracer-injection and synoptic-sampling methods during base flow on September 29, 1999. Tracer data were interpreted by Wirt and others (1999) in conjunction with detailed geologic mapping, topographic profiling, geochemical characterization, and the occurrence and distribution of trace metals to identify sources of ground-water inflows.

Samples of water affected by mining in Prospect Gulch characteristically had some of the lowest pH values and highest concentrations of aluminum, sulfate, and iron; but they also contained elevated dissolved metals from ore-bearing vein minerals such as copper, zinc, cadmium, nickel, and lead. In comparison, weathering of regional acid-sulfate mineral assemblages produced moderately low pH waters elevated in sulfate, aluminum, and iron, but generally lacking in copper, cadmium, nickel, and lead. Occurrences of the base metals were helpful in identification of ground-water sources and flow paths. For example, cadmium was greatest in inflows associated with drainage from inactive mine sites and was absent in inflows that were unaffected by past mining activities; thus cadmium appears to be an important indicator of the effect of mining in this setting.

The reach of Prospect Gulch most strongly affected by mining contributed substantial percentages of the total sulfate, aluminum, and iron loads, and also large percentages of the copper and zinc loads for the entire Cement Creek basin (Wirt and others, 1999). An acidic spring near the mouth of Prospect Gulch yielded much of the stream discharge, sulfate, aluminum, and iron loads but only small loads of copper and zinc. Watershed-scale remediation efforts targeted at reducing loads of sulfate, aluminum, and iron at inactive mine sites will likely be limited in their influence because of the major sources of these constituents in Prospect Gulch, which are predominantly

Table 5. Summary of load calculations and cumulative instream load for selected subreaches, Cement Creek basin, 1996 and 1999.

[Distance, in meters along study reach; Al, aluminum; Cd, cadmium; Cu, copper; Fe, iron; Mn, manganese; Pb, lead; Sr, strontium; Zn, zinc; SO_4, sulfate; all values in kilograms per day, except percents; rank of loading for each element indicated by number in parentheses; blank entries indicate loading less than load error]

	Al	Cd	Cu	Fe	Mn	Pb	Sr	Zn	SO_4
Cumulative instream load	531	3.83	14.0	1,039	210	6.94	77.7	166	35,000
Cumulative inflow load	148.7	1.15	11.4	374	97.2	0.35	97.7	83.7	21,200
Percent inflow load	28.0	30.1	81.2	35.9	46.3	5.1	>100	50.4	60.7
Unsampled inflows	382	2.67	2.64	666	113	6.59	0.00	82.5	13,800
Percent unsampled inflow	72.0	69.9	18.8	64.1	53.7	94.9	<1	49.6	39.3
Attenuation	206	1.18	0.03	436.7	59.4	4.39	7.17	38.2	5,700
Percent attenuation	38.8	30.7	<1	42.0	28.3	63.3	9.24	23.0	16.3

Area or site designation	Distance	Al	Cd	Cu	Fe	Mn	Pb	Sr	Zn	SO_4
ROSS-0345 Queen Anne (C1)	345	3.68	0.042	0.620 (4)	2.02	3.77	0.014	0.559	6.31	312
ROSS-1317A Mogul mine (C2)	1,367	32.3 (4)	.994 (1)	8.30 (1)	25.8	19.0 (3)	.214	.707	61.6 (1)	665
ROSS-3057 North Fork (C3)	3,107	23.9		3.87 (2)	96.5 (3)	8.59	.000	.872	37.0 (2)	560
ROSS-3845 Sunnyside mine (C4)	3,931					16.2	.159	20.8 (1)		5,660 (1)
ROSS-4047 South Fork (C5)	4,133	20.4			64.7	13.3		12.9 (4)		2,810 (3)
CE-2425 Upstream from Prospect Gulch	5,452	14.9	.868 (2)		47.5	2.95	.631 (4)		2.35	1,230
CE-3185 Prospect Gulch area (C6)	6,212	74.8 (2)	.484 (3)	.852(3)	229 (1)	19.1 (2)	.259	5.97 (5)	8.07	2,650 (4)
CE-3317 Iron bog (C7)	6,344	22.2	.169		68.9 (4)	6.20			1.71	
CE-5215 Upstream from Minnesota Gulch	8,242	16.2			134 (2)	17.2 (5)	.752 (3)		2.70	2,630 (5)
CE-5767 Minnesota Gulch area (C8)	8,794	87.4 (1)	.308 (5)	0.402 (5)	57.1	33.4 (1)	.000	18.7 (2)	13.3 (3)	1,960
CE-6107 Porcupine Gulch area (C9)	9,134		.440 (4)			12.2	.481 (5)		7.56 (4)	2,650 (4)
CE-6742 Upstream from Ohio Gulch	9,769	15.8	.306			4.65	.422		4.75	889
CE-6907 Ohio Gulch (C10)	9,934	31.3 (5)			33.4	18.0 (4)			4.02	
CE-7131 Illinois Gulch (C11)	10,158		.215					17.2 (3)		2,520
CE-7331 Yukon tunnel	10,358	25.8				14.5	.422		6.13	
CE-7501 Topeka Gulch (May Day mine)	10,528				36.4					1,470
CE-9360 Upstream from lower bog	12,387	65.4 (3)			54.5	8.07				
CE-9905 Lower bog area (C12)	12,932	32.1 (4)		.000	68.7 (5)	12.8	1.34 (2)		6.79 (5)	4,100 (2)
CE-11558 End of study reach (C48)	14,585	64.9 (3)	.000	.000	36.0		1.48 (1)			1,900

discharged from nonmining sources. Remediation goals targeting reductions in loads of copper and other base metals may have better success, however, because changes in these loads are disproportionately higher than increases in discharge over the same reach, and a substantial fraction of the source of these metals is from mine-influenced reaches.

6. Minnesota Gulch area (C8, fig. 7): The area around Minnesota Gulch contributed substantial loads of aluminum, iron, manganese, lead, and sulfate. This appears to be related to the vein-related QSP (V-QSP) alteration in that subbasin.

7. Porcupine Gulch area (C9, fig. 7)*:* Segments around Porcupine Gulch contributed cadmium, lead, and sulfate.

8. Ohio Gulch (C10, fig. 7): The stream segment ending at 6,907 m accounted for the load added by Ohio Gulch, which was important for aluminum and manganese. There also was an iron load, but it was not as great as in other areas.

9. Illinois Gulch (C11, fig. 7): Loading from Illinois Gulch was represented in a single stream segment (C11), where loads of strontium and sulfate were substantial.

10. Yukon tunnel (downstream from C11, fig. 7): Seeps that were not visible in 1996 were sampled in 2000; the results of that sampling helped us to separate loading of the Yukon tunnel from that of Illinois Gulch. The loads of aluminum and manganese were substantial here.

11. Lower bog (C12, fig. 7): Significant loading of aluminum, iron, manganese, lead, and sulfate occurred in the area of the lower bog. This small bog is located where a fracture zone crosses the stream. It is a setting similar in appearance to the iron bog (C7; Bruce Stover, Colorado Department of Minerals and Geology, oral commun., 1999). No mines were developed in this fault area; only prospects were observed. This area likely represents a nonmining contribution to the load of Cement Creek.

12. Gauge at C48: Most of the load accounted for at the last stream segment occurred at 13,953 m. Substantial percentages of the aluminum and lead loads were contributed in this segment. Although this stream segment passed the load error test, the dramatic increase and subsequent decrease might be attributed to sampling error of some kind, particularly because this area is not near mine sites or mapped altered areas.

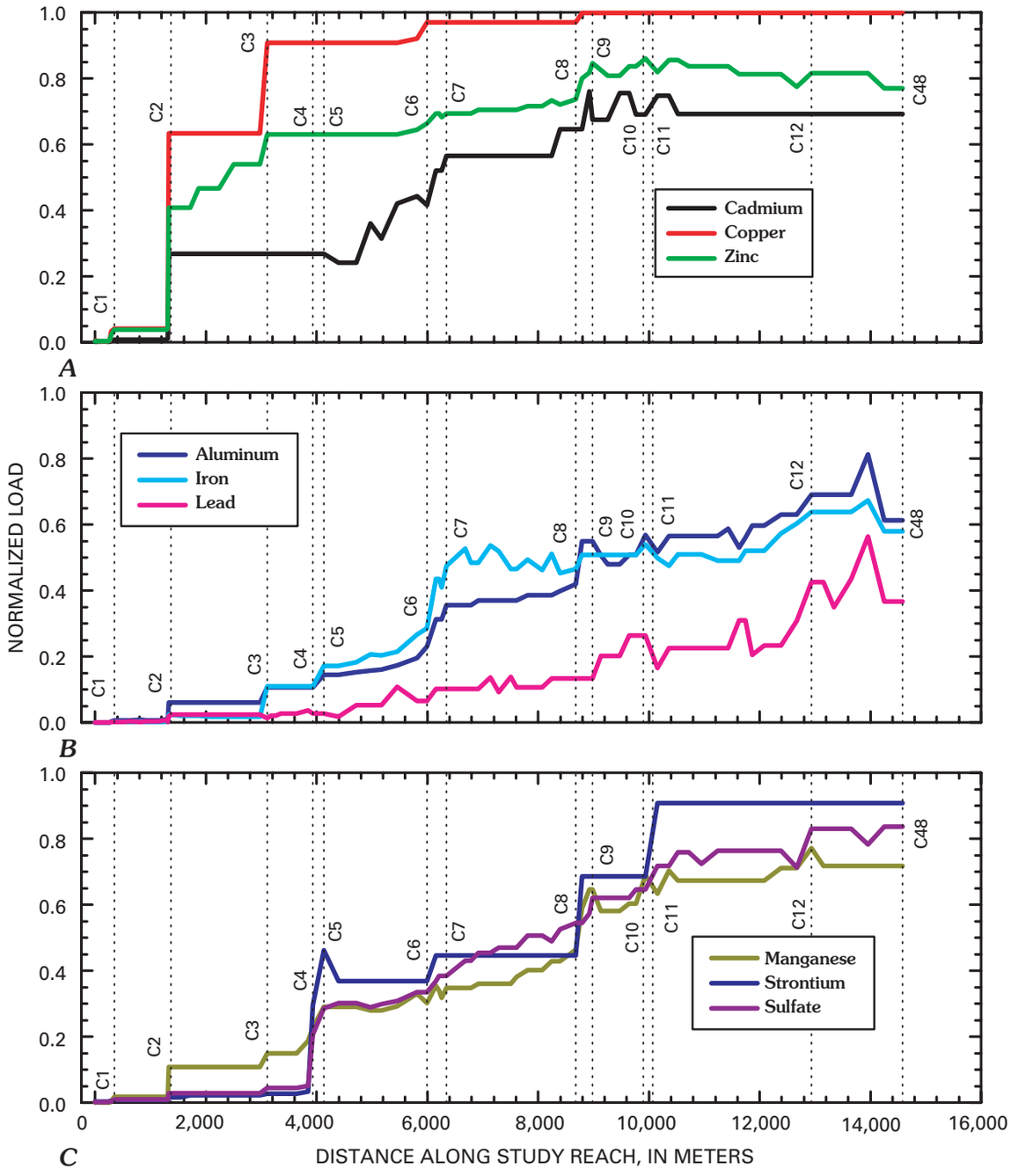

Figure 10. Variation of normalized instream loads for *A*, cadmium, copper, zinc; *B*, aluminum, iron, lead; *C*, manganese, strontium, and sulfate with distance, Cement Creek basin, 1996 and 1999. Labels on vertical lines refer to locations of substantial change along the study reach in table 5.

Unsampled Inflow

Unsampled inflow was important for mass loading in Cement Creek. Over half the cumulative instream loads for aluminum, cadmium, iron, manganese, lead, and zinc entered the stream as unsampled inflow (table 5). Only copper and sulfate had smaller unsampled inflow. This indicates two aspects of the geology in the Cement Creek basin. First, there are a large number of outcrops of the AS- and QSP-altered rocks, and many of these may contribute loading to the stream through dispersed, subsurface inflow, most likely through the large alluvial fans at the mouths of many side drainages. These fans also could contain substantial amounts of unweathered, altered rock that could be contributing to these loads. Second, there are areas where fracture flow is important for the contribution of mass load to the stream, principally the Prospect Gulch area (C6) and the lower bog area (C12).

Kimball and others (2002) indicated several important areas where unsampled inflow occurred in the Cement Creek basin. These included the area around Prospect Gulch (C6), the area around Minnesota Gulch (C8), the Yukon tunnel area (downstream from C11), and the lower bog (C12). Another important area was near the end of the study reach, near 13,953 m. From results of the work upstream from North Fork in 1999, two areas can be added: (1) substantial unsampled inflow upstream from the Mogul mine inflow (C2), which could indicate that drainage from the mine seeps into the ground and enters the stream upstream from the visible inflows; (2) unsampled inflow near North Fork (C3) (better observed in 1999 than in 1996). The normalized load profiles indicate additional, smaller inflows (fig. 10). Although these smaller inflows may not be substantial sources of metal load individually, together they represent a large, dispersed contribution to the metal loads, and they may complicate remediation goals.

Attenuation of Load

Net attenuation of constituent loads ranged from less than 1 percent for copper to 63 percent for lead (table 5). Copper, strontium, and sulfate were the most conservative in Cement Creek: all three showed less than 20 percent attenuation. Copper commonly is attenuated in streams affected by mine drainage, but at a pH less than 4.5 in Cement Creek, copper is mostly conservative. Aluminum, cadmium, iron, manganese, and zinc had from 20 to 50 percent attenuation. These results differ from those of Kimball and others (2002) because the accounting here used the total metal concentrations rather than the filtered concentrations.

Not many areas occurred along the study reach where attenuation took place for all the elements simultaneously (fig. 10). The greatest amount of attenuation occurred downstream from the Sunnyside mine discharge in 1996, but no attenuation was measured in the same reach in 1999, when treatment was temporarily stopped during the mass-loading study. The normalized loading curves for the combined data sets do not show the 1996 attenuation (fig. 10). Attenuation occurred in several other areas as follows:

Area	Attenuation
Near Minnesota and Porcupine Gulches	Substantial for aluminum, cadmium, and manganese
Downstream from Illinois Gulch	Aluminum, manganese, lead, zinc (Kimball and others, 2002; Walton-Day and others, 2002)
Last few segments of study reach	Aluminum, iron, lead, zinc, and sulfate

From about 6,000 m to 10,000 m, a reach that includes Illinois Gulch, some of the attenuation could result from higher pH waters along the left bank (east side of the canyon) that drain the propylitized rocks.

Summary

With many outcrops of AS- and QSP-altered rock in the Cement Creek basin, loadings of many constituents were substantial. Cement Creek had a pH less than 4.5 along much of the study reach, and so changes between dissolved and colloidal phases were not substantial. Important changes occurred between sampling in 1996 and 1999 and are detailed in Appendix 2.

Mineral Creek Basin, 1999

Three tracer injections were needed to assess the 15 km study reach of Mineral Creek. Basic details of all three studies are combined here to give a framework for the entire Mineral Creek basin. The study reach started on a tributary to Mineral Creek near Red Mountain Pass. The injection was upstream from the Junction mine inflow (M1, fig. 11), which collects water from the Longfellow mine and the Koehler tunnel, and continued downstream to the U.S. Geological Survey stream gauging station 09359010 (M34), near the confluence with the Animas River (figs. 1 and 11). The upstream injection ended just upstream from Mill Creek (M6). The middle injection started at this same location and continued to the site just upstream from South Fork (M11). The lower injection started upstream from South Fork (M11), and continued to the gauging station (M34). Overall, there were 84 stream segments and 65 sampled inflows. Locations where changes in stream chemistry occurred are indicated by the labels M1 through M34 in figure 11 and subsequent figures.

For each of the three injections, the bromide tracer provided a clear tracer signal that was elevated above the low background concentrations (fig. 12). Calculated stream discharge from the tracer dilution indicates that the greatest increases in stream discharge occurred at Mill Creek, Middle Fork Mineral Creek, South Fork, and along the section of stream from South Fork to Bear Creek (fig. 12).

Chemical Characterization of Synoptic Samples

The chemical character of stream water in Mineral Creek is dominated by distinct changes in response to a few key inflows (fig. 13). Many substantial changes in pH and constituent concentrations occurred in the upstream part of the study reach, from M1 to M6, where the stream was relatively small. Thus, small inflows had a large effect on concentrations. Inflow from the Longfellow mine and the Koehler tunnel are combined herein and called the Junction mine inflow (M1) for this discussion. The inflow caused a substantial decrease in pH from greater than 6.5 to less than 3.0 (fig. 13*A*). Subsequent inflows downstream from M1 caused the pH to increase back to values greater than 6.0. Many inflows from M1 to M6 had substantial concentrations of iron, copper, and zinc, and the concentrations in the stream were high.

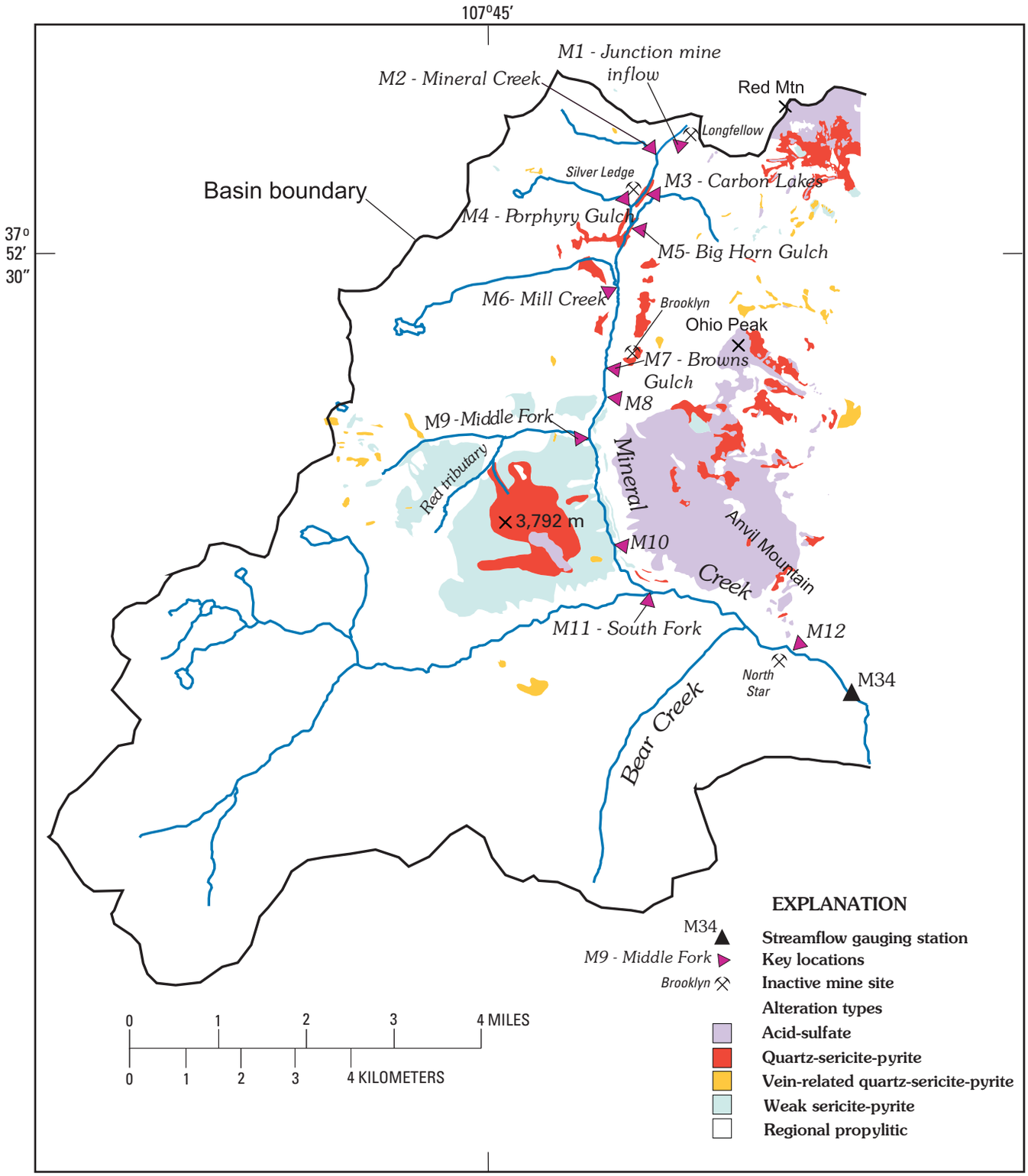

Figure 11. Location of study area, alteration zones, key locations, and principal sites of inactive mines, Mineral Creek basin, 1999.

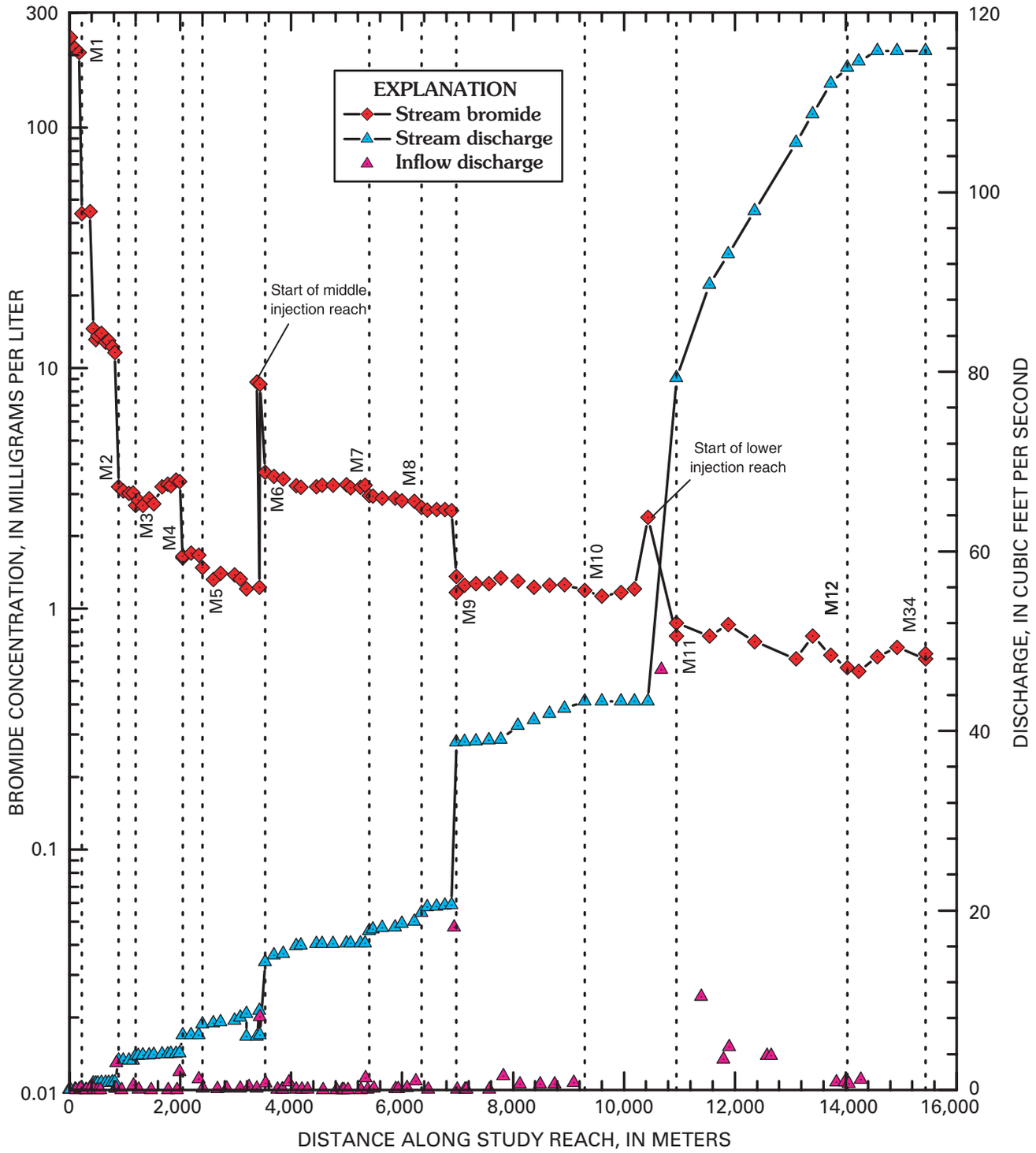

Figure 12. Variation of injected bromide concentration and calculated discharge with distance, Mineral Creek basin, September 1999. Note the start of the two downstream injection reaches where bromide concentration is higher than at the end of each upstream injection reach.

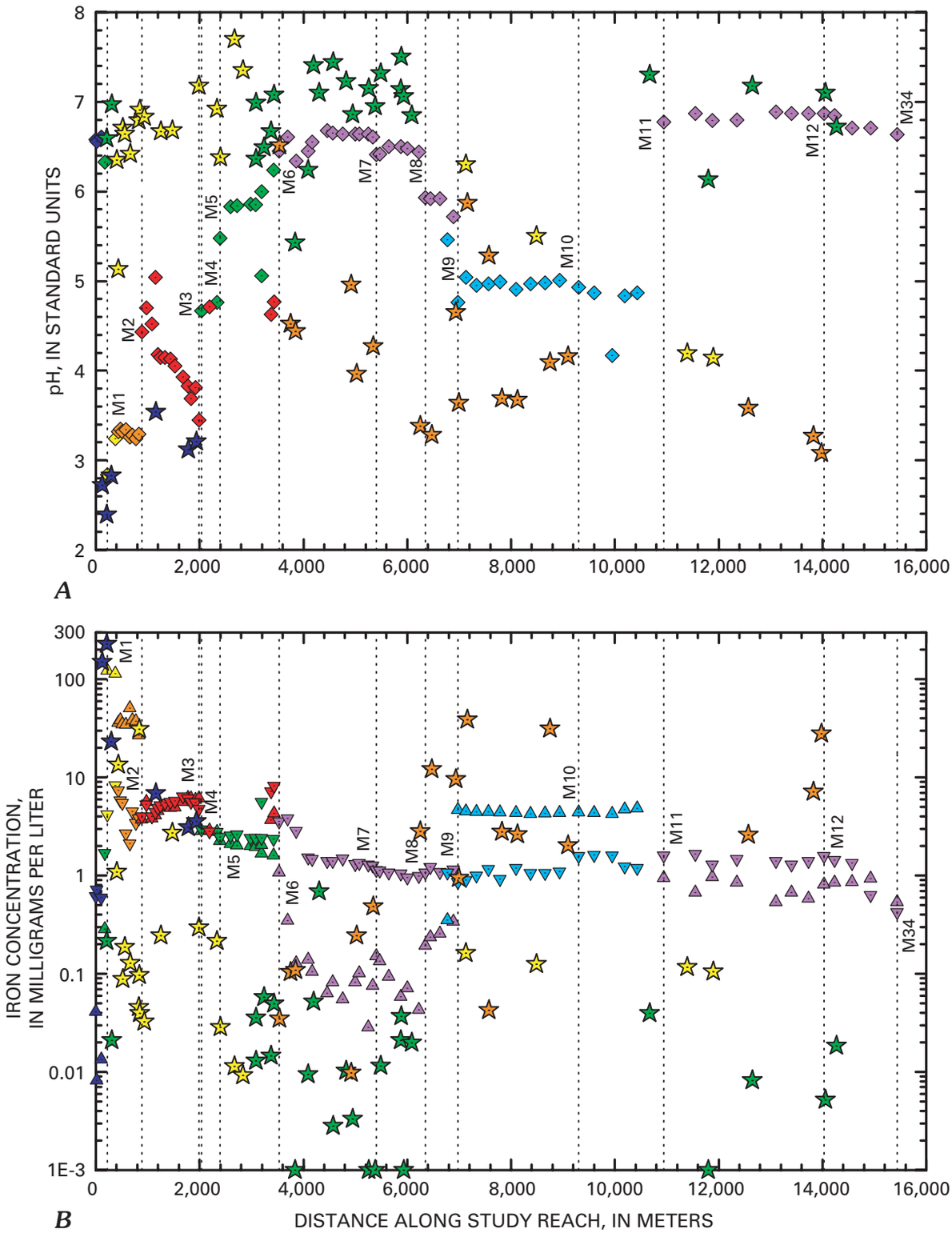

Figure 13. Variation of *A*, pH; of dissolved and colloidal concentrations of *B*, iron; and total-recoverable concentrations of *C*, copper, and *D*, zinc with distance, Mineral Creek basin, 1999. Groups of stream samples (diamonds or upward triangles, dissolved; downward triangles, colloidal), and inflows (stars) are indicated by colors: 1, blue (darker); 2, green; 3, yellow; 4, orange; 5, red; 6, purple; 7, cyan (lighter). Groups were determined by principal component analysis; their chemistry is summarized in tables 6 and 7. Labels on vertical dashed lines refer to site locations in figure 11. *C*, *D*, Blue line, acute toxicity standard; red line, chronic toxicity standard.

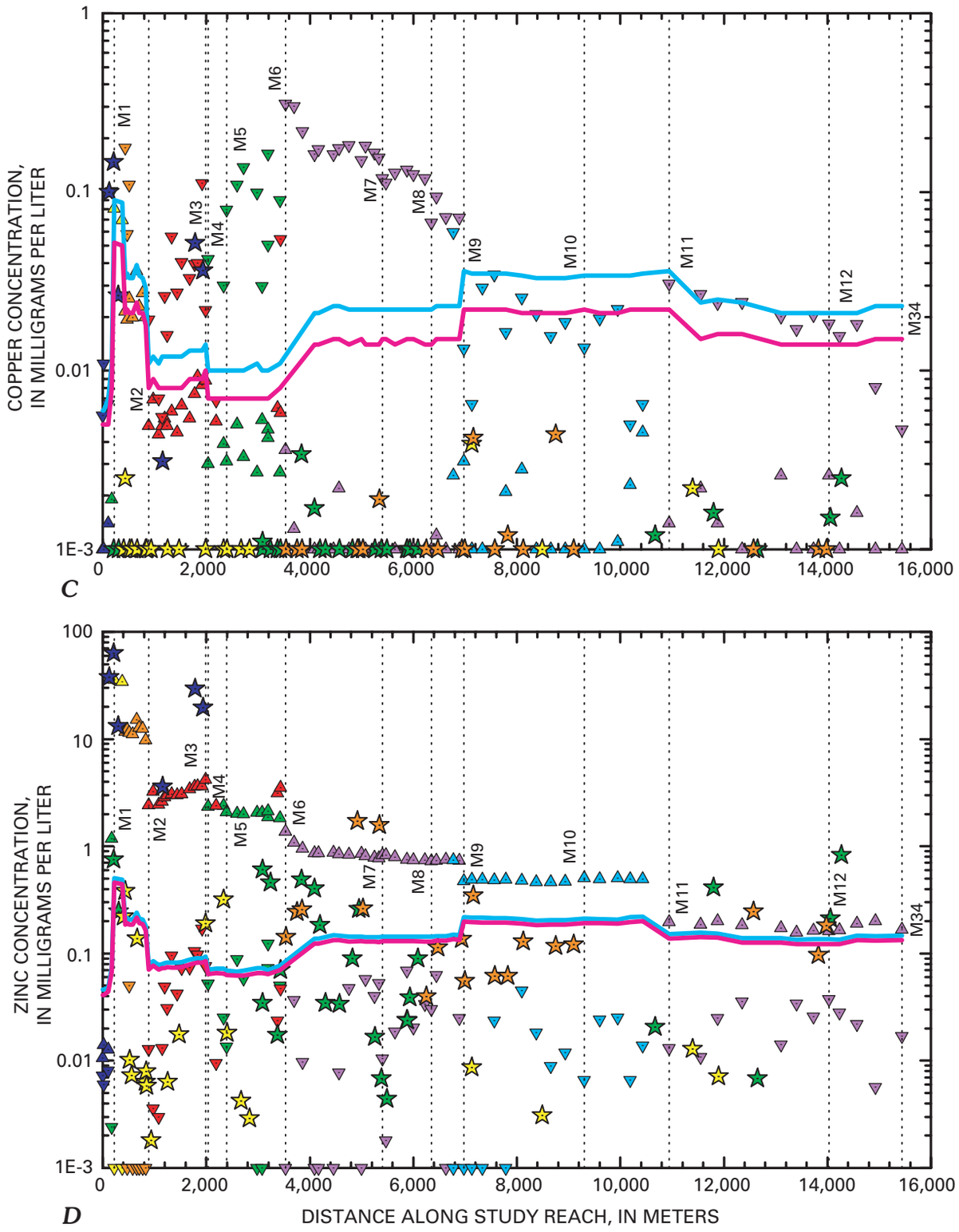

Figure 13—Continued. Variation of total-recoverable concentrations of *C*, copper, and *D*, zinc with distance, Mineral Creek basin, 1999. Groups of stream samples (diamonds or upward triangles, dissolved; downward triangles, colloidal), and inflows (stars) are indicated by colors: 1, blue (darker); 2, green; 3, yellow; 4, orange; 5, red; 6, purple; 7, cyan (lighter). Groups were determined by principal component analysis; their chemistry is summarized in tables 6 and 7. Labels on vertical dashed lines refer to site locations in figure 11. Blue line, acute toxicity standard; red line, chronic toxicity standard.

Inflows

Classification of inflow samples, based on PCA, is illustrated by the chemical composition of representative samples from each of four inflow groups (table 6). The chemical composition of samples in the groups range from acidic (inflow groups 1 and 4) with high sulfate concentrations to near neutral with lower sulfate concentrations (inflow groups 2 and 3, table 6). Sulfate concentrations among these representative samples are very different, ranging from 6.81 to 346 mg/L (table 6). The most acidic, sulfate-rich samples (inflow group 1) also had some of the highest base metal concentrations. The four groups of inflows in this report do not directly relate to groups or categories suggested by Mast and others (2000) and Mast and others (this volume, Chapter E7). The classification of Mast and others (2000) sought to evaluate the potential for the effects of mining activity on water quality of seeps and springs throughout the Animas River watershed study area, and was constructed on the basis of field observations, topographic maps, geologic maps, geologic and mining publications, aerial photographs, and PCA. Inflow samples from the tracer studies differ from the data of Mast and others (2000) in that the tracer inflow samples were collected at the stream rather than at the sources away from the stream to obtain a representation of the water quality that directly affects the stream chemistry. The tracer inflow samples do not meet the goals of the Mast and others (2000) study.

Variations in the chemistry of inflows reflect the differences that result from weathering of the particular alteration suites in the Mineral Creek basin (Bove and others, this volume). The sample at the Junction mine inflow (M1, inflow group 1) is influenced by weathering of the AS-altered rocks and breccia pipes that are rich in copper and zinc sulfides (Bruce Stover, Colorado Department of Minerals and Geology, written commun., 1999). This produces the high concentrations of almost all the metals, but especially copper and zinc. The inflow from Middle Fork Mineral Creek (M9, group 4) is influenced by weathering of QSP-altered rocks on peak 3,792 m (fig. 11), which produces very high

Table 6. Chemical composition of selected inflow samples representing groups defined by principal component analysis, Mineral Creek basin, 1999.

[Sample identification, key to samples in database; distance, in meters along study reach; specific conductance in microsiemens per centimeter; all concentrations in milligrams per liter; <, less than; NM, no measurement]

Group	1	2	3	4
Chemical character	Acidic, high sulfate and metal concentrations	Near neutral, moderate sulfate and metal concentrations	Near neutral, low sulfate and metal concentrations	Acidic, moderate sulfate and metal concentrations
Number of samples	6	26	20	19
Site description	Small spring near highway 550	Draining marsh from alluvial fan	From culvert under highway 550	Draining over ferricrete and moss
Downstream distance, in meters	297	5,883	518	6,994
Sample identification	MIN3-00121	MIN2-05667	MIN3-00292	MIN2-06768
pH, in standard units	2.83	7.50	6.71	3.64
Specific conductance	958	262	59.0	392
Calcium	43.0	38.3	8.39	36.4
Magnesium	7.16	2.85	.69	4.19
Sodium	4.47	3.84	1.48	3.88
Potassium	<.001	.87	.51	1.32
Alkalinity	<.001	NM	33.6	<.001
Sulfate	346	93.4	6.81	148
Chloride	.96	.46	.94	1.55
Fluoride	.56	.43	<.001	.18
Silica as SiO_2	23.4	9.67	2.39	16.9
Aluminum	10.5	.016	.058	3.56
Arsenic	.078	.008	.002	.026
Cadmium	.047	<.001	<.001	<.001
Copper	4.43	.002	.003	.005
Iron	23.1	.037	.088	.943
Lead	.092	.006	.008	.045
Lithium	.044	<.001	.001	<.001
Manganese	4.35	.064	.006	.524
Nickel	.042	<.001	<.001	.004
Strontium	.659	.228	.125	.265
Zinc	13.2	.024	.010	.055

aluminum and iron concentrations. A few other inflows (inflow group 4 between M9 and M12) also had high base-metal concentrations, and like the Junction mine inflow had high zinc to aluminum mole ratios. The zinc to aluminum ratio helps us distinguish between drainage from the AS and QSP alteration zones. Samples of water draining the AS alteration zones are relatively high in zinc concentration, whereas samples of water draining QSP alteration zones, such as Middle Fork Mineral Creek (M9), are relatively lower in zinc and higher in aluminum concentration.

Stream

Classification of stream samples into groups that have similar chemistry yielded seven distinguishable groups along the 15 km study reach (table 7). Unlike the groups of inflow samples, these groups of stream samples indicate sequential chemical changes along the study reach. Groups assigned by the multivariate analysis differ slightly from the sequential order downstream; however, the groups are ordered in table 7 according to their sequential occurrence in downstream order. PCA for stream samples used both dissolved and colloidal concentrations. Calcium and sulfate were the major ions throughout the study reach (table 7). Values of pH were less than 4.5 in several sections of the study reach (fig. 13*A*), and alkalinity was absent in those sections. The highest instream concentration of iron exceeded 100 mg/L (fig. 13*B*); concentrations of copper (fig. 13*C*) and zinc (fig. 13*D*) were greater than 15 mg/L and 35 mg/L, respectively, in stream group 3. Concentrations of arsenic, cadmium, and lead were relatively high also. There were measurable colloidal concentrations of all the metals, and the colloidal concentrations of iron and copper were greater than dissolved concentrations in several sections along Mineral Creek (fig. 13). The method for determining colloidal concentrations usually is not sensitive enough to measure colloidal concentrations of arsenic, cadmium, nickel, and lead, but these concentrations were measurable in Mineral Creek (Kimball and others, 1995).

Each of the metal concentrations, and especially the partitioning between dissolved and colloidal phases, varied considerably along the study reach in response to inflows of differing pH (fig. 13 and table 7). Details of these spatial patterns help to indicate the chemical reactions that affect the metal loading and transport. Metals affected the most by colloid formation were aluminum, arsenic, copper, iron, and lead. Those least affected were manganese and zinc.

Iron colloids (fig. 13*B*) affect the transport and partitioning of other metals (Kimball and others, 1992, 1995). Sorption of arsenic and lead to the abundant colloidal iron has been simulated for the upstream injection reach (Runkel and Kimball, 2002). Downstream from the Junction mine inflow (M1) where pH was less than 3.0, iron was not yet diluted or partitioned to the colloidal phase. As pH increased downstream, the streambed became coated with iron colloidal material along much of the study reach, particularly downstream from inflows that had higher pH (downstream from M2, M3, M6, and M11). Dissolved iron concentrations substantially decreased downstream from the inflow of Mill Creek (M6) and South Fork (M11), but they increased downstream from Middle Fork Mineral Creek (M9). Colloidal concentrations were substantial in groups 2 through 7; they were substantially greater than dissolved iron in stream groups 4, 5, 6, and 7 (table 7). A notable decrease in colloidal iron concentration was evident at the last two stream sites along the study reach (fig. 13*B*). Colloidal aluminum concentrations also showed a decrease in these samples.

Because of the AS and QSP alteration of bedrock in the Middle Fork Mineral Creek subbasin and the low pH of the stream water, aluminum concentrations were unusually high in Mineral Creek (table 7). Dynamic changes between dissolved and colloidal aluminum occurred at the locations where pH changed across a value of about 5.3 (fig. 13*A*). In general, when pH was less than 5.5 (stream groups 3, 4, 5, and 7), aluminum was mostly transported in the dissolved phase; when pH was greater than 5.3 (stream groups 1, 2, and 6), colloidal aluminum exceeded dissolved aluminum. This behavior is consistent with the observations of aluminum solubility by Nordstrom and Ball (1986) for waters affected by mine drainage. The greatest changes occurred downstream from the Junction mine inflow (M1), the inflow of Mill Creek (M6), the inflow of Middle Fork Mineral Creek (M9), and the inflow of South Fork (M11). The pattern was similar to that of iron (fig. 13*B*). Because these changes occurred within the time frame of transport through an individual stream segment, the rate of precipitation and dissolution reactions had to be on the order of seconds to minutes.

Important similarities were observed between the spatial variations of copper (fig. 13*C*) and iron (fig. 13*B*) concentrations. Copper concentration increased at many, but not all, of the same locations as iron, which suggests either that some sources of iron did not include copper mineralization or that copper had been removed before it reached the stream. Colloidal copper concentrations became increasingly more important downstream from Big Horn Gulch (M5) and Mill Creek (M6). At M8, no increase in total-recoverable copper occurred, but instead an increase in dissolved copper was observed, indicating partitioning from colloidal to dissolved phases. The change was consistent with the decrease in pH that occurred at M8 (fig. 13*A*). No significant increase in copper took place downstream from Middle Fork Mineral Creek, and yet Mast and others (2000) found substantial sources of copper load in Middle Fork subbasin that most likely was from QSP veins. Thus, the relatively low concentration of copper in the Middle Fork Mineral Creek sample from this synoptic study likely reflects the removal of copper between the informally named Red tributary and the mouth of Middle Fork. Dissolved copper concentrations were greater than acute and chronic standards (Colorado Department of Public Health and Environment, 2000) along the entire study reach, except downstream from the South Fork, where the concentration was less than the acute standard (fig. 13*C*).

Table 7. Chemical composition of selected stream samples representing groups defined by principal component analysis, Mineral Creek basin, 1999.

[Sample identification, key to samples in database; distance, in meters along study reach; specific conductance in microsiemens per centimeter; all concentrations in milligrams per liter; diss, dissolved; coll, colloidal; <, less than; NM, no measurement]

Group characteristic	Group 1 Upstream from acid inflows; generally low concentrations	Group 3 Downstream from Junction mine inflow; high concentrations from inflow	Group 4 From highway 550 culvert to inflow of Mineral Creek; dilution of high concentrations	Group 5 Mineral Creek to Porphyry Gulch; substantial colloidal concentration	Group 2 From Porphyry Gulch to Mill Creek; colloidal iron higher than dissolved iron	Group 6 From Mill Creek to Middle Fork and downstream from South Fork; higher pH and colloidal concentrations, upstream	Group 7 From Middle Fork to South Fork; high dissolved and colloidal concentrations
Number of samples	3	2	8	17	11	34	15
Sample identification	MIN3-UP103	MIN3-00050	MIN3-00550	MIN3-01450	MIN3-02170	MIN2-03945	MIN2-09372
Downstream distance	103	226	776	1,676	2,396	4,171	9,598
pH, in standard units	6.61	2.84	3.24	3.93	5.48	6.55	4.87
Specific conductance	286	1,531	638	226	139	270	414
Calcium	10.3	59.9	24.7	15.9	15.3	43.8	62.6
Magnesium	2.14	10.7	3.63	1.65	1.55	2.06	5.12
Sodium	.64	7.72	4.40	2.23	1.69	2.92	3.30
Potassium	.40	1.09	1.88	.61	.62	.82	.18
Alkalinity	36.0	<.001	<.001	<.001	NM	14.85	NM
Sulfate	14.3	664	234	81.2	55.2	111	198
Chloride	.51	2.64	1.86	.98	.67	.62	.68
Fluoride	.01	1.76	.52	.16	.07	.32	.69
Silica	1.34	9.33	4.21	2.54	2.19	3.93	7.39
Aluminum, diss	.012	15.0	5.26	1.39	.232	.012	2.18
Aluminum, coll	.133	<.001	<.001	.198	.531	.332	1.97
Arsenic, diss	.008	2.12	.303	.010	.118	.007	.018
Arsenic, coll	.006	.530	.565	.274	<.001	.020	<.001
Cadmium, diss	.002	.143	.048	.010	.005	.002	<.001
Cadmium, coll	.003	.015	.007	.006	.005	.005	<.001
Copper, diss	.007	15.0	5.25	1.48	.658	.073	.089
Copper, coll	.007	<.001	<.001	.033	.080	.173	.020
Iron, diss	.013	123	37.6	5.68	2.25	.106	4.36
Iron, coll	.598	4.20	3.46	6.44	2.48	1.48	1.62
Lead, diss	.005	.109	.066	.003	.052	<.001	.022
Lead, coll	.004	<.001	<.001	.011	.041	.051	.017
Manganese, diss	.055	5.34	1.71	.472	.289	.260	.567
Manganese, coll	.026	<.001	<.001	.024	.003	<.001	.051
Nickel, diss	<.003	.035	.004	.007	<.003	<.003	<.003
Nickel, coll	<.003	.021	.003	<.003	<.003	<.003	<.003
Strontium, diss	.249	1.77	.748	.372	.299	.584	.620
Strontium, coll	.004	<.001	<.001	.008	.011	.011	.068
Zinc, diss	.013	35.6	12.5	3.41	2.07	.861	.495
Zinc, coll	.008	<.001	<.001	.074	.014	<.001	.024

Concentrations of zinc were remarkably high in Mineral Creek; the highest concentration was 35.6 mg/L, downstream from the Junction mine inflow (M1), and the median dissolved concentration was 0.829 mg/L (fig. 13*D*). Dissolved concentrations exceeded both acute and chronic standards along the entire study reach (Colorado Department of Public Health and Environment, 2000). Zinc concentrations consistently decreased downstream from each major inflow, and each downstream group of samples, from 2 through 7, had lower dissolved zinc concentrations (table 7). Downstream from South Fork (M11 to M34) zinc was partitioned to the colloidal phase. Even with a small amount of partitioning to colloids, zinc concentration in the bed material, including biofilm, can be substantial because the streambed integrates colloidal concentrations through time (Kimball and others, 2002).

Arsenic is an important component of the arsenopyrite found in the AS-altered rocks (D.B. Yager, written commun., 2003). Although concentrations were not measurable along much of the study reach (table 7), dissolved arsenic concentration was high in stream group 2, which was downstream from the Junction mine inflow (M1). In groups 3 and 4, colloidal arsenic concentration was greater than the dissolved concentration, suggesting the sorption of arsenic to iron colloids (Runkel and Kimball, 2002). This process has been described in streams affected by mine drainage by Fuller and Davis (1989) and Fuller and others (1993). This association of arsenic and other toxic metals with colloidal material could provide a means for arsenic's introduction into the food web (Besser and others, 2001). Arsenic is also elevated in bed sediments near locations M1 and M2 (Church, Fey, and Unruh, this volume).

Concentrations of dissolved lead were similar to those of arsenic; measurable concentrations of colloidal lead occurred downstream from the Junction mine inflow (M1; table 7), and were detectable for the first 3,500 m of Mineral Creek. Two relatively high inflow concentrations occurred at 1,781 and 1,921 m; both inflows were near the Silver Ledge mine (upstream from M4, fig. 11). Downstream from Mill Creek (M6), however, their concentrations mostly were less than detection along the rest of the study reach.

Manganese did not partition to the colloidal phase; its pattern was similar to that of zinc (fig. 13*D*). Downstream from South Fork (M11, stream group 6, table 7), where other metals transformed to the colloidal phase, manganese mostly remained in the dissolved phase. Manganese concentration is a good indication of metal sources because manganese comes from the weathering of gangue minerals in some alteration zones and is not highly reactive once in solution. Variation of manganese was similar to variation of other metals until the inflow of Mill Creek (M6); downstream from that point were substantial increases in concentration at Browns Gulch (M7) and Middle Fork (M9).

Variation of strontium concentrations along the study reach differed from that of the other metals (table 7). Strontium did not partition to the colloidal phase. Downstream from Mill Creek (M6), strontium concentrations increased substantially. Where there were large increases in concentration of other metals downstream from Middle Fork (M9), strontium concentration did not increase. These differences imply a source for strontium that was different from the alteration assemblages that provided other metals, mined or unmined. Strontium likely comes from substitution for calcium in plagioclase of propylitized intermediate-composition lavas of the San Juan Formation and Silverton Volcanics (D.B. Yager, written commun., 2003). Thus, its source is not always associated with the alteration zones that produced ores in the watershed.

Mass-Load Profiles

A summary of the loading calculations for each constituent and the sum of cumulative instream load for selected sections of the study reach are given in table 8. Cumulative instream loads varied substantially, from more than 30,000 kg/day for sulfate to less than 5 kg/day for arsenic. Normalized loading profiles indicate three general patterns among the solutes: (1) arsenic, copper, and zinc mostly increased in the upper part of the study reach, upstream from Mill Creek (M6; fig. 14*A*); (2) aluminum, iron, and manganese mostly increased from the inflow of Middle Fork (M9, fig. 14*B*); and (3) strontium and sulfate increased at these and other locations (fig. 14*C*).

The first load pattern is illustrated by zinc (fig. 14*A*). The Junction mine inflow (M1) was the single largest load among all the stream segments, but the sum of cumulative instream load along the reaches to M2 and M3 was 35.0 kg/day, greater than the amount from the Junction mine inflow (table 8). Much of this zinc loading was from AS alteration in rocks that crop out near Red Mountain Pass (Bove and others, this volume) and the breccia pipes that also crop out near the stream (Bruce Stover, Colorado Division of Mines and Geology, written commun., 1999). Two inflows near the Silver Ledge mine also contributed to the zinc load in this part of Mineral Creek (upstream from M4). Between Middle Fork (M9) and the gauge at M34 a substantial increase in zinc load was observed, which was likely a result of weathering areas of QSP alteration in the Middle Fork Mineral Creek subbasin (Mast and others, 2000), and AS-altered rock that crops out on Anvil Mountain (fig. 11).

Loading for arsenic mostly occurred upstream from Mill Creek (M6, fig. 14*A*). To some extent, patterns of cadmium and nickel mass loading (not shown in fig. 14*A*) resembled that of arsenic, but their concentrations were too variable to calculate reliable mass-loading profiles. Loads for arsenic that are listed in table 8 only include the subreach down to Mill Creek (M6). Some indications of loading for arsenic were observed at Porphyry Gulch (M4) and downstream from South Fork (M11 to M34), near the AS-altered rock of Anvil Mountain (fig. 11).

Inflow from Middle Fork Mineral Creek (M9) dominated the second pattern (fig. 14*B*). This load is a result of weathering in the QSP alteration zone of peak 3,792 m (fig. 11; Mast and others, 2000; Mast and others, this volume). Iron and aluminum both had the same general pattern, particularly with the dynamic changes in partitioning between dissolved and colloidal phases (shown for iron in fig. 13*B*). The normalized load profile for aluminum (fig. 14*B*) does not indicate this partitioning because the total instream load did not change greatly; the partitioning occurred in the water column and total aluminum concentrations remained nearly constant. A substantial increase in pH with the inflow of South Fork Mineral Creek (pH 7.2) was responsible for partitioning essentially all the aluminum to the colloidal phase. An increase at M12 was observed, near the Anvil Mountain alteration, but over a short distance downstream from there most of the colloidal load was removed.

The third pattern included both strontium and sulfate loads (fig. 14*C*). In addition to substantial mass loading from Middle Fork Mineral Creek (M9), increases came from Mill

Table 8. Summary of load calculations and cumulative instream load for selected subreaches, Mineral Creek, September 1999.

[Distance, in meters along study reach; Al, aluminum; As, arsenic; Cu, copper; Fe, iron; Mn, manganese; Sr, strontium; Zn, zinc; SO_4, sulfate; all values in kilograms per day, except percents; rank of load for each constituent indicated by number in parentheses after load value; blank entries indicate loading less than load error. Note that "below" and "above" indicate "downstream from" and "upstream from"]

	Al	As	Cu	Fe	Mn	Sr	Zn	SO_4
Cumulative instream load	526	4.18	27.4	910	102	128	99	30,638
Cumulative inflow load	418	1.82	10.7	731	53	71.2	52.1	24,574
Percent inflow	80	44	39	80	52	56	53	80
Unsampled inflow	107	2.35	16.7	180	49	57.0	46.7	6,064
Percent unsampled	20	56	61	20	48	44	47	20
Attenuation	359	2.58	18.5	521	15	13.8	39.6	1,857
Percent attenuation	68	62	68	57	15	11	40	6

Description	Distance	Al	As	Cu	Fe	Mn	Sr	Zn	SO_4
Below Junction mine inflow (M1)	226	7.99	1.41 (2)	7.99 (2)	67.6 (5)	2.84	0.941	18.9 (2)	353
Below Mineral Creek (M2)	888	3.35	.882 (3)	3.54 (3)	37.1	0.486	1.72	7.85	234
Above Porphyry Gulch (upstream from M4)	1,989	6.59	1.48 (1)	9.04 (1)	70.1 (4)	1.81	0.804	27.1 (1)	436
Below Porphyry Gulch (M4)	2,041								72.1
Below Big Horn Gulch (M5)	2,396		0.398 (4)				1.16		40.4
Below Mill Creek (M6)	4,090					4.25	17.8 (4)		3,370 (4)
Below Browns Gulch (M7)	5,406	29.3 (5)				8.17 (5)	6.87	3.40	912 (5)
Below left bank drainage (M8)	6,350	29.4 (4)			14.0		0.0	0.0	412
Below Middle Fork (M9)	6,981	293 (1)		1.15	450 (1)	36.2 (1)	31.9 (1)	10.5 (5)	14,200 (1)
Below acid springs (M10)	9,298	51.2 (3)		2.63 (4)	159 (3)	11.2 (4)	3.53	9.74	
Below South Fork (M11)	10,943	28.5			42.9		28.3 (2)	2.95	6,360 (2)
Below Anvil Mountain alteration (near M12)	14,033	105 (2)		0.775	160 (2)	21.0 (2)	21.6 (3)	11.7 (4)	4,220 (3)
Mineral Creek at gauge (M34)	15,436			1.74 (5)		16.2 (3)	13.5 (5)	17.1 (3)	

Creek (M6) and South Fork (M11). Strontium represents the weathering of carbonate-bearing propylitized rocks in Middle Fork subbasin (D.B. Yager, written commun., 2003). There also were locations where these constituents were not lost like the others, and along with manganese (fig. 14*B*) they were the most conservative during transport.

Principal Locations of Loading

Cumulative instream loads for each constituent are the best estimate of the total loading along the study reach (table 8). Although different patterns appear among loading profiles of the metals, their similarities identify certain locations as the most important for metal loading. Cumulative instream load for individual stream segments have been summed for the subreaches identified in figure 11. Subreaches that contributed the greatest load to Mineral Creek are indicated by ranks in the table.

The three patterns of loading for Mineral Creek suggest those areas of the study reach where the majority of loading occurred. In upstream to downstream order, these sources are as follows:

1. Junction mine inflow (M1), Red Mountain mining district, and associated AS alteration (fig. 11). Downstream from Junction mine inflow (M1) to Porphyry Gulch (M4) substantial sources enter the stream from dispersed, ground-water inflows. These sources account for the majority of arsenic, copper, and zinc (fig. 14*A*).

2. Middle Fork Mineral Creek (M9) contributes the greatest loads of aluminum, iron, manganese, strontium, and sulfate. Upstream from Middle Fork, there also are substantial loads of aluminum, manganese, and sulfate from Browns Gulch (M7), and the subbasin at M8.

3. AS-altered rock that crops out in Anvil Mountain downstream from South Fork Middle Creek (fig. 11). This was most important for zinc loading.

Unsampled Inflow

More than 40 percent of the loads of arsenic, copper, manganese, strontium, and zinc occurred as unsampled inflow (table 8). The most important location for unsampled inflow along the Mineral Creek study reach was between M1 and M3, near the upper part of the study reach. This area was responsible for much of the loading for arsenic, copper, and zinc (fig. 14*A*). Data in Runkel and Kimball (2002) also indicate that this area was an important source of lead. Unsampled inflows also occurred near Anvil Mountain where there was substantial outcrop of AS-altered rock (near M12, fig. 11).

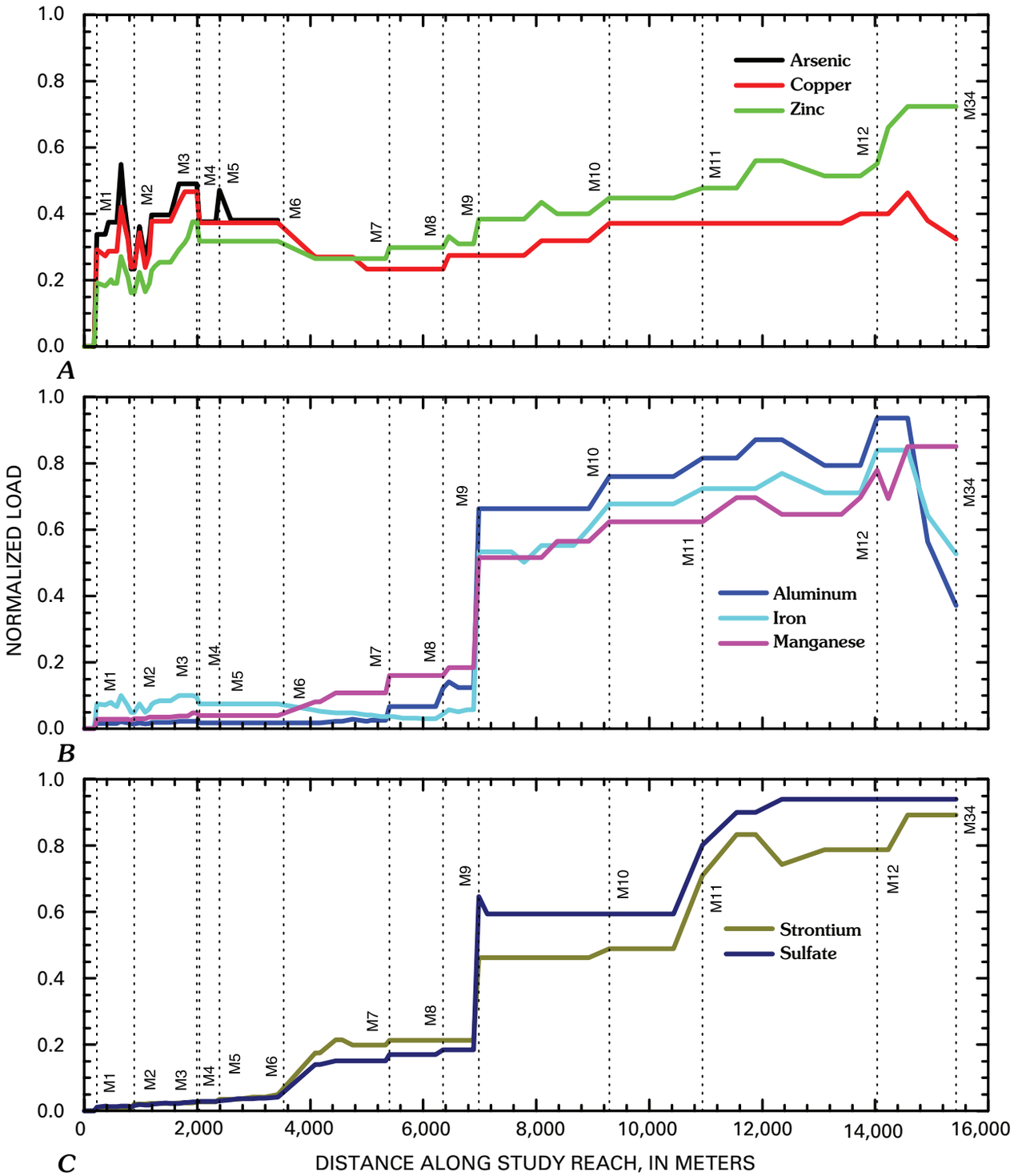

Figure 14. Variation of normalized instream loads for *A*, arsenic, copper, zinc; *B*, aluminum, iron, manganese; *C*, strontium, and sulfate with distance, Mineral Creek basin, September 1999. Labels on vertical lines refer to locations of substantial change along the study reach of figure 11 and table 8.

Attenuation of Load

The net attenuation of metal loads ranged from 6 percent for sulfate to 68 percent for aluminum and copper (table 8). Spatially, most of the attenuation occurred at three locations along the study reach. Downstream from the inflow of Mill Creek (M6), substantial attenuation of copper occurred. There could have been sorption of copper onto the iron colloidal material with the increase in pH in this part of the stream. Downstream from the inflow of Middle Fork (M9), sulfate was attenuated. The removal of sulfate could have been associated with the formation of aluminum hydroxysulfates and schwertmannite. Finally, a large amount of attenuation took place for aluminum, copper, and iron loads in the last few segments of the study reach, downstream from M12 (fig. 11). The cause of this loss is not clear, but it could be related to inflow from Bear Creek, 1,922 m upstream, which drains a large component of propylitized rocks (Yager and Bove, 2002). These areas of attenuation could result in substantial input of metals to the food web (Besser and others, 2001).

Summary

Loadings of aluminum, copper, iron, manganese, and zinc into Mineral Creek were substantial. The mass-loading studies support the conclusions of Mast and others (2000) that much of this loading was from nonmining sources, but there were very substantial loads from the Junction mine inflow (M1) and near the Silver Ledge mine (upstream from M4). Few streams have such dynamic chemical reactions causing the partitioning of metals back and forth between dissolved and colloidal phases (fig. 13*B, C*). These reactions were rapid enough to occur during stream transport of a few hundred meters downstream from the inflows that affected the changes.

Elk Park Basin, 1998—Summary of Watershed Contributions

The Elk Park study reach, near Silverton, Colo., was selected in order to include the confluences of Cement Creek and Mineral Creek with the Animas River. Downstream from these confluences, the study reach extended to Elk Park (fig. 15). This section combines the results of a mass-loading study in 1997 that began upstream from the mouth of Cement Creek (C48) and continued to the A72 gauge downstream from Silverton, and results from a study that began at the stream gauging station in Mineral Creek (M34) and continued to Elk Park in 1998 (fig. 15). The two studies had overlapping sites that allowed for scaling of the loads calculated from each. In the Elk Park study reach, problems occurred with copper contamination in ultrafiltrate samples; thus, total-recoverable concentrations are used for load calculations and the 0.45-µm concentrations are used as the dissolved concentration in this study reach. The objectives of combining the studies were (1) to evaluate the relative contributions of the three main basins of the Animas River upstream from Silverton, (2) to quantify the chemical and physical processes that affect metals in the mixing zones along the study reach, and (3) to quantify the transport of dissolved and colloidal metals in the reach of the Animas River from Silverton to Elk Park. Transport of metals downstream from the Silverton area, to a large degree, is facilitated by iron and aluminum colloids that form in the mixing zones as these three major tributaries of the Animas converge (Church and others, 1997; Schemel and others, 2000).

The systematic decrease of chloride concentration along the study reach represented dilution by inflows. In 1997, discharge at several sites along the upstream part of the study reach was measured by the area-velocity method as well as tracer dilution because the stream was divided into several braids downstream from Cement Creek (from 1,818 m to 1,998 m). A synoptic discharge profile was calculated from chloride concentrations for both data sets (fig. 16). Background concentrations of chloride were low compared to the injected concentrations. The increase of chloride downstream from Deer Park Creek (E5) is unexplained. In that stream segment we had to use conservative solutes like calcium, strontium, and sulfate to estimate the increase in flow from Deer Park Creek (E5) (Bencala and McKnight, 1987). The discharge profile indicates a gain of 166 ft^3/s. Stream segments with sampled inflows contributed 123 ft^3/s, or 74 percent of the total increase. The remaining 26 percent of the increase in streamflow was contributed as dispersed, subsurface inflow.

Chemical Characterization of Synoptic Samples

Inflows

The spatial variation of concentrations distinguished four groups of inflow samples (table 9). Inflows from Cement Creek (C48, inflow group 1) and Mineral Creek (M34, inflow group 2) were distinct from all of the other inflow samples and also from each other. Cement Creek (C48) was acidic at pH 4.11, and thus, aluminum and copper mostly occurred in the dissolved phase; iron was split between the dissolved and colloidal phases. Owing to the neutralization of Mineral Creek by the inflow of the South Fork (M11), Mineral Creek at the mouth (M34) is more basic with a pH of 6.87, and the colloidal concentrations of aluminum, copper, and iron were greater than the dissolved concentrations. Downstream from Mineral Creek, all the other inflow samples (inflow groups 3 and 4, table 9) had near-neutral pH, relatively low concentrations of metals, and low sulfate concentrations. These two groups of samples generally did not influence the stream to any great extent.

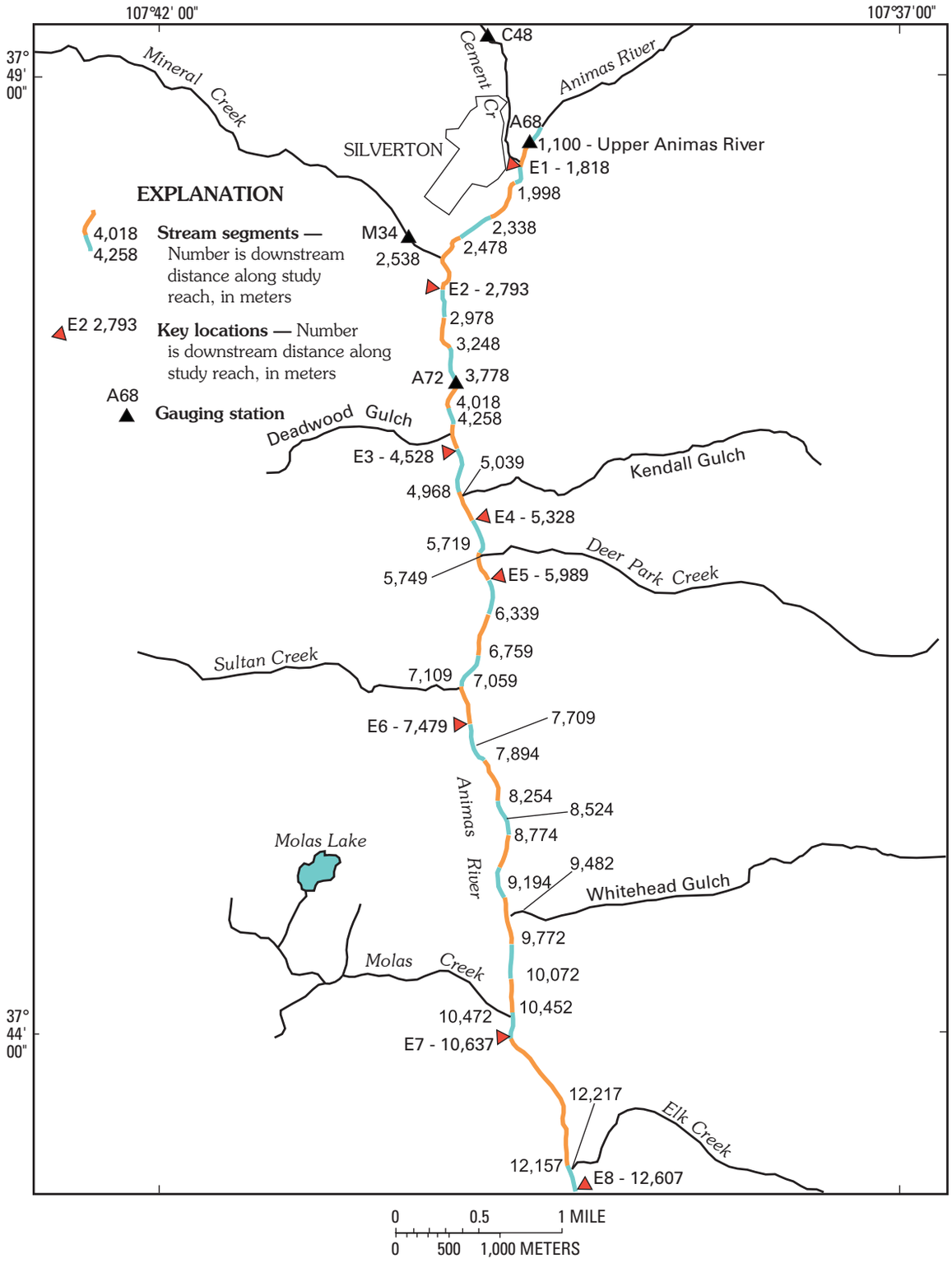

Figure 15. Location of study reach, stream segments, and key locations, Animas River, Silverton to Elk Park, August 1997 and 1998.

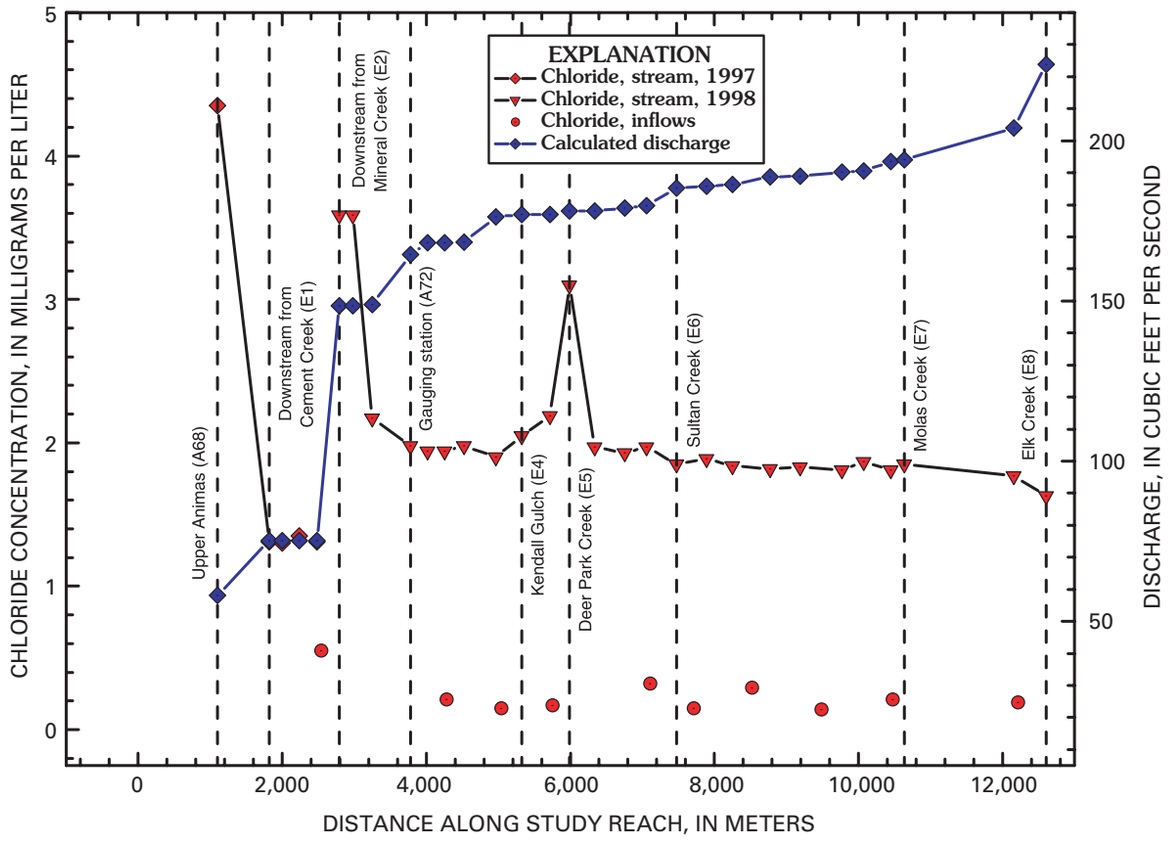

Figure 16. Variation of chloride concentration and discharge with distance, Animas River, Silverton to Elk Park, August 1997 and 1998.

Stream

The greatest changes in stream chemistry occurred downstream from Cement Creek (E1) and Mineral Creek (E2; figs. 15 and 17). Four distinct groups of stream samples were classified by PCA as a result of these changes (table 10). The Animas River at Silverton (A68) yielded a unique sample at the beginning of the study reach (stream group 1, table 10); the sample had a pH of 7.60. The acidic inflow from Cement Creek (inflow group 1; table 9) decreased the pH to less than 7.0 in samples between Cement Creek and Mineral Creek (stream group 2). Mineral Creek inflow (inflow group 2, table 9), was also slightly acidic, which caused the instream pH to decrease below 7.0 in the sample just downstream from Mineral Creek (E2); but the remaining samples between Mineral Creek and the end of the study reach had pH values near 7.0 (stream groups 3 and 4, table 10).

Instream concentrations of iron and copper (fig. 17*B*, *C*) increased downstream from the inflows of Cement Creek (E1) and Mineral Creek (E2). Iron concentration was highest downstream from Cement Creek (E1); iron was present mostly as colloidal (fig. 17, downward triangles), rather than dissolved (upward triangles). The sample from Cement Creek (C48) had 54 percent colloidal iron, and the sample from the upper Animas River (A68) had more than 99 percent colloidal iron. The sample collected downstream from Cement Creek (E1) had 87 percent colloidal iron. Schemel and others (2000) have documented the transformation of iron from the dissolved to the colloidal iron in this mixing zone. The maximum concentration of colloidal iron occurred downstream from Deer Park Creek (E5, fig. 17*B*), and concentrations consistently decreased downstream from there. The pattern of aluminum concentration was very similar to that of iron because both formed colloids in the mixing zones (Schemel and others, 2000).

The pattern of copper concentration was similar to the pattern of iron concentration (fig. 17*C*). The greatest increase was downstream from Cement Creek (E1), but the concentration also increased downstream from Mineral Creek (E2), which had the highest inflow concentration of copper (inflow group 2, table 9). Downstream from Cement Creek (E1) and Mineral Creek (E2) copper was predominantly in the colloidal phase, which likely was copper sorbed to the abundant iron colloids (Runkel and Kimball, 2002). Copper concentrations remained nearly constant along the remainder of the study reach (fig. 17*C*), but the concentration in bed sediment increased (Church and others, 1997), suggesting that some colloidal copper was lost to the bed. Total-recoverable

Table 9. Chemical composition of selected inflow samples representing groups defined by principal component analysis, Animas River, Silverton to Elk Park, August 1997 and 1998.

[Phase: Diss, dissolved; Coll, colloidal; all concentrations in milligrams per liter; (97), 1997 only; <, less than; NM, not measured]

	Phase	Inflows			
		1	2	3	4
Site description		Cement Creek at mouth (97)	Mineral Creek at mouth (97)	Deer Park Creek	Whitehead Gulch
Distance (m)		1,166	2,538	5,749	9,482
pH, in standard units		4.11	6.87	7.74	7.91
Calcium	Diss	155	47.2	21.4	20.5
Magnesium	Diss	7.77	3.83	2.59	2.04
Sodium	Diss	6.27	2.34	1.32	1.54
Alkalinity, as $CaCO_3$	Diss	<1	NM	NM	50.1
Sulfate	Diss	473	131	11.9	13.2
Chloride	Diss	4.35	.550	.170	.140
Silica	Diss	12.4	5.38	1.62	1.80
Aluminum	Diss	4.53	.025	.020	.020
	Coll	.403	1.71	.020	.020
Cadmium	Diss	<.001	<.001	<.001	<.001
	Coll	<.001	<.001	<.001	.002
Copper	Diss	.021	.003	.013	.005
	Coll	<.002	.046	<.002	<.002
Iron	Diss	2.97	.237	.007	.002
	Coll	3.92	2.07	.009	.009
Manganese	Diss	1.59	.254	.001	.000
	Coll	.086	.002	.001	.001
Nickel	Diss	.006	<.003	.005	<.003
Lead	Diss	.037	<.023	<.023	.034
	Coll	<.023	<.023	<.023	<.023
Strontium	Diss	1.62	.412	.193	.222
	Coll	.084	.008	.012	<.008
Zinc	Diss	.620	.212	.025	.007
	Coll	.028	.032	<.001	<.001

concentrations of copper were near the chronic toxicity standard, but dissolved copper was lower than both standards along the entire study reach.

Concentrations of dissolved zinc decreased slightly with the inflow of Cement Creek (E1) but with the increase in colloidal zinc concentration, the total zinc increased (fig. 17*D*). There was a decrease in both dissolved and colloidal concentrations with the inflow of Mineral Creek (E2). A decrease in dissolved zinc concentration upstream from Deer Park Creek (E5) corresponded to an equal increase in colloidal zinc concentration. This corresponds to an increase in colloidal iron in the same location (fig. 17*B*). Both dissolved and colloidal zinc concentrations remained mostly constant for the remainder of the study reach. Dissolved concentrations of zinc exceeded the acute and chronic standards along the entire study reach.

Other metal concentrations were also distinct among the groups of stream samples (table 10). Manganese concentrations systematically decreased from group to group downstream. Lead concentrations were less than detection in all the groups; however, bed sediment contained substantial lead (Church and others, 1997). Besser and others (2001) found that the colloidal concentrations of copper, lead, and zinc are significant to the aquatic health in these reaches of the Animas River.

Mass-Load Profiles

Because the Elk Park study includes all three upstream basins, it provides the opportunity to compare the basin contributions to the Animas River downstream from Silverton, and in doing so, to compare the principal locations of loading among the three upstream basins. The load profiles fall into two groups (fig. 18), those solutes that were affected by colloidal concentrations (including aluminum, copper, and iron), and those that were not (sulfate, strontium, manganese, and zinc). A summary of load calculations, indicating the change in cumulative instream load along selected sections of the study reach, is presented in table 11.

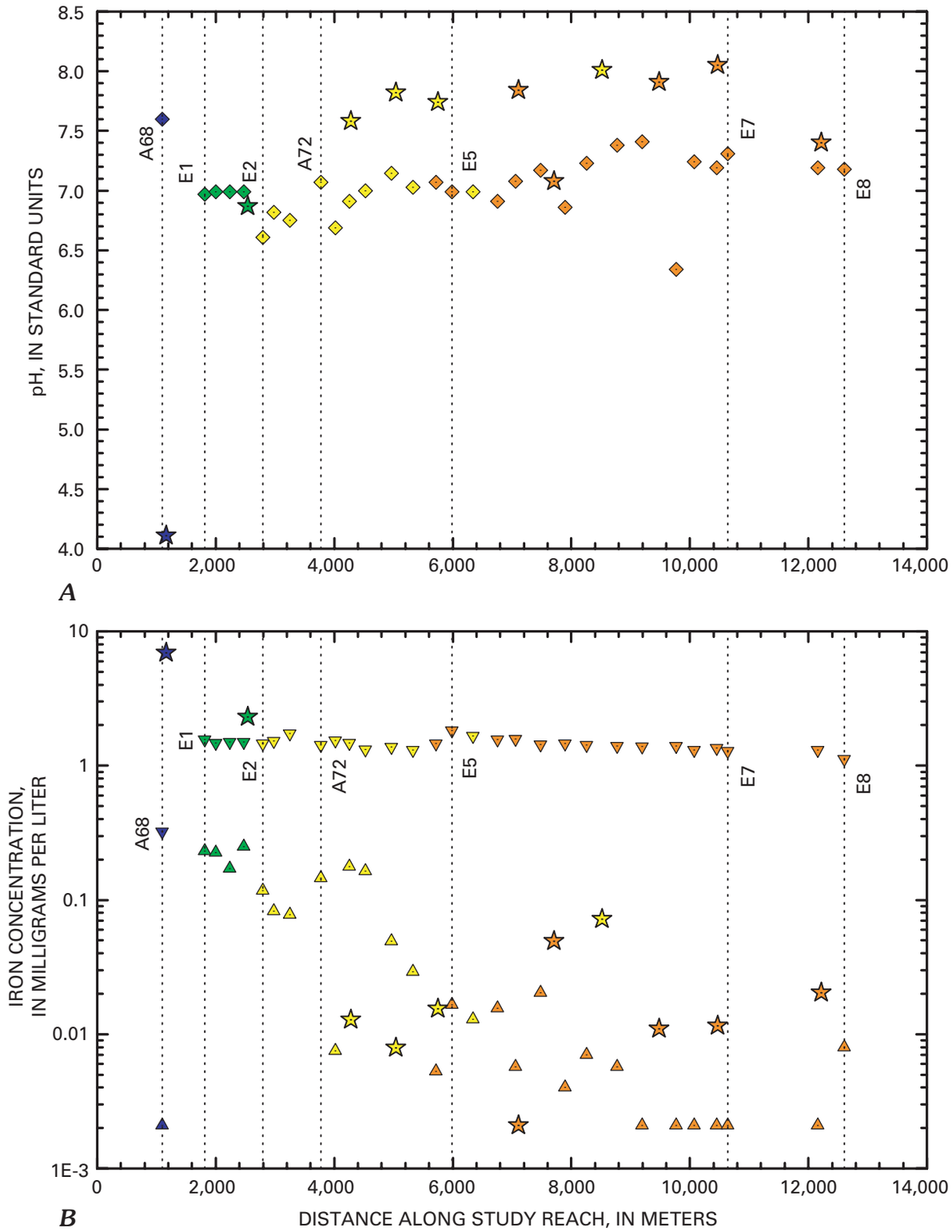

Figure 17. Variation of *A*, pH; of dissolved and colloidal concentrations of *B*, iron; and total-recoverable concentrations of *C*, copper; and *D*, zinc, with distance, Animas River, Silverton to Elk Park, August 1997 and 1998. Groups of stream samples (diamonds or upward triangles, dissolved; downward triangles, colloidal), and inflows (stars) are indicated by colors: 1, blue; 2, green, 3, yellow; 4, orange. Groups were determined by principal component analysis, and their chemistry is summarized in tables 9 and 10. Labels on vertical dashed lines refer to locations in figure 15. *C*, *D*, Blue line, acute toxicity standard; red line, chronic toxicity standard.

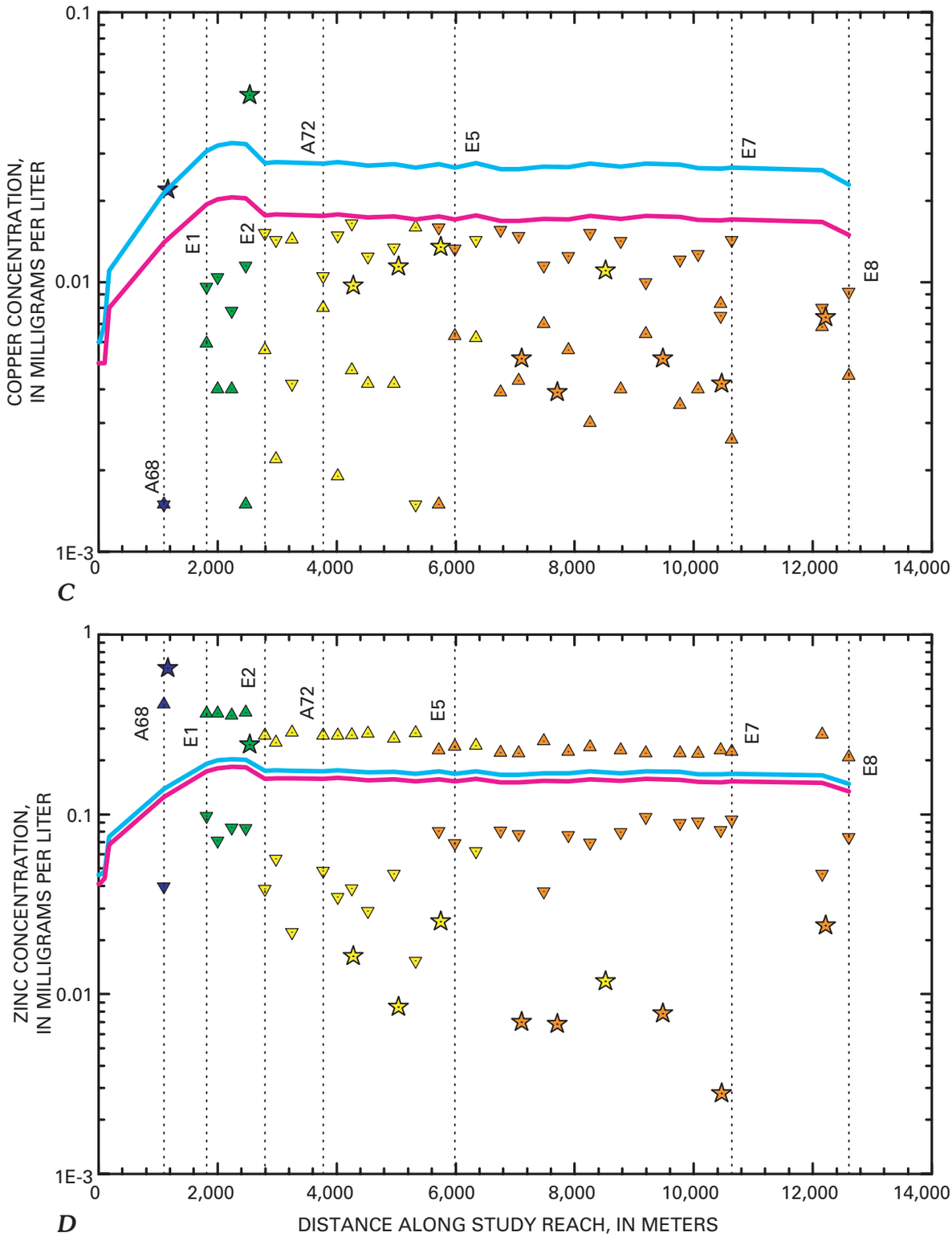

Figure 17—Continued. Variation of total-recoverable concentrations of *C*, copper; and *D*, zinc, with distance, Animas River, Silverton to Elk Park, August 1997 and 1998. Groups of stream samples (diamonds or upward triangles, dissolved; downward triangles, colloidal), and inflows (stars) are indicated by colors: 1, blue; 2, green, 3, yellow; 4, orange. Groups were determined by principal component analysis, and their chemistry is summarized in tables 9 and 10. Labels on vertical dashed lines refer to locations in figure 15. Blue line, acute toxicity standard; red line, chronic toxicity standard.

Table 10. Chemical composition of selected stream samples representing groups defined by principal component analysis, Animas River, Silverton to Elk Park, August 1997 and 1998.

[Phase: Diss, dissolved; Coll, colloidal; all concentrations in milligrams per liter; (97), 1997 only; <, less than; TR, tracer salt; NM, not measured]

	Phase	Stream			
		1	2	3	4
Site description		Animas River at Silverton A68 (97)	Upstream from Mineral Creek (97)	Downstream from Deadwood Gulch	Downstream from small inflow
Distance (m)		1,100	2,478	4,528	7,894
pH, in standard units		7.60	6.99	7.00	6.86
Calcium	Diss	45.8	68.7	56.6	55.3
Magnesium	Diss	2.72	3.83	3.73	3.69
Sodium	Diss	TR	TR	TR	TR
Alkalinity, as $CaCO_3$	Diss	NM	NM	19.7	27.4
Sulfate	Diss	90.0	174	161	153
Chloride	Diss	TR	TR	TR	TR
Silica	Diss	3.50	5.39	5.27	5.03
Aluminum	Diss	.020	.047	.038	.040
	Coll	.051	1.098	1.417	1.225
Cadmium	Diss	<.001	.004	.003	.003
	Coll	<.001	<.001	<.001	<.001
Copper	Diss	.002	.002	.004	.006
	Coll	<.002	.012	.012	.013
Iron	Diss	.002	.250	.164	.004
	Coll	.324	1.50	1.32	1.46
Manganese	Diss	1.20	1.12	.649	.594
	Coll	.026	.042	.027	.020
Nickel	Diss	<.003	.004	<.003	.004
Lead	Diss	<.023	<.023	<.023	<.023
	Coll	<.023	<.023	<.023	<.023
Strontium	Diss	.450	.697	.537	.527
	Coll	<.008	.018	.025	.015
Zinc	Diss	.409	.368	.282	.223
	Coll	.040	.084	.029	.077

The colloidal phase was the dominant form of transport for aluminum, iron, and copper (table 10). Inflows of Cement Creek (C48) and Mineral Creek (E2) added substantial aluminum load to the stream (fig. 18*A*). Mass-loading patterns of five metals, described next, illustrate the contributions of the different basins.

Aluminum

Aluminum loading for the Elk Park study reach reveals an important difference between two methods of accounting for a watershed load. The first method is to account for the load at the outlet of a basin, catchment, or watershed; this is a traditional way to account for load and has many uses. The second method is to account for load by using the cumulative instream load from the mass-loading analysis within the basin, catchment, or watershed. These two methods differ between a generalized view for the outlet method and a detailed view for the instream method. Mass-loading data from the Elk Park study reach (table 11) represent an outlet view, or the contributions of the Animas River, Cement Creek, and Mineral Creek by just accounting for the load observed in the Animas River. With the outlet view the Animas River contributes 1.6 percent of the cumulative load of aluminum (10.1 kg/day divided by 640 kg/day), Cement Creek contributes 33 percent, and Mineral Creek contributes 45 percent (table 11). The remaining 20 percent of load for aluminum along the Elk Park study reach comes from sources downstream from Mineral Creek (table 11). These sampled instream loads for individual stream segments along the Elk Park study reach differ substantially from the instream view that comes from the cumulative instream load determined for each of the upstream basins (tables 2, 5, and 8). For example, the inflow load for the Animas River in the Elk Park study was 10.1 kg/day (table 11), but the cumulative instream load for the Animas River from combining the California Gulch, Eureka, and Howardsville studies was 116 kg/day (table 2). The difference

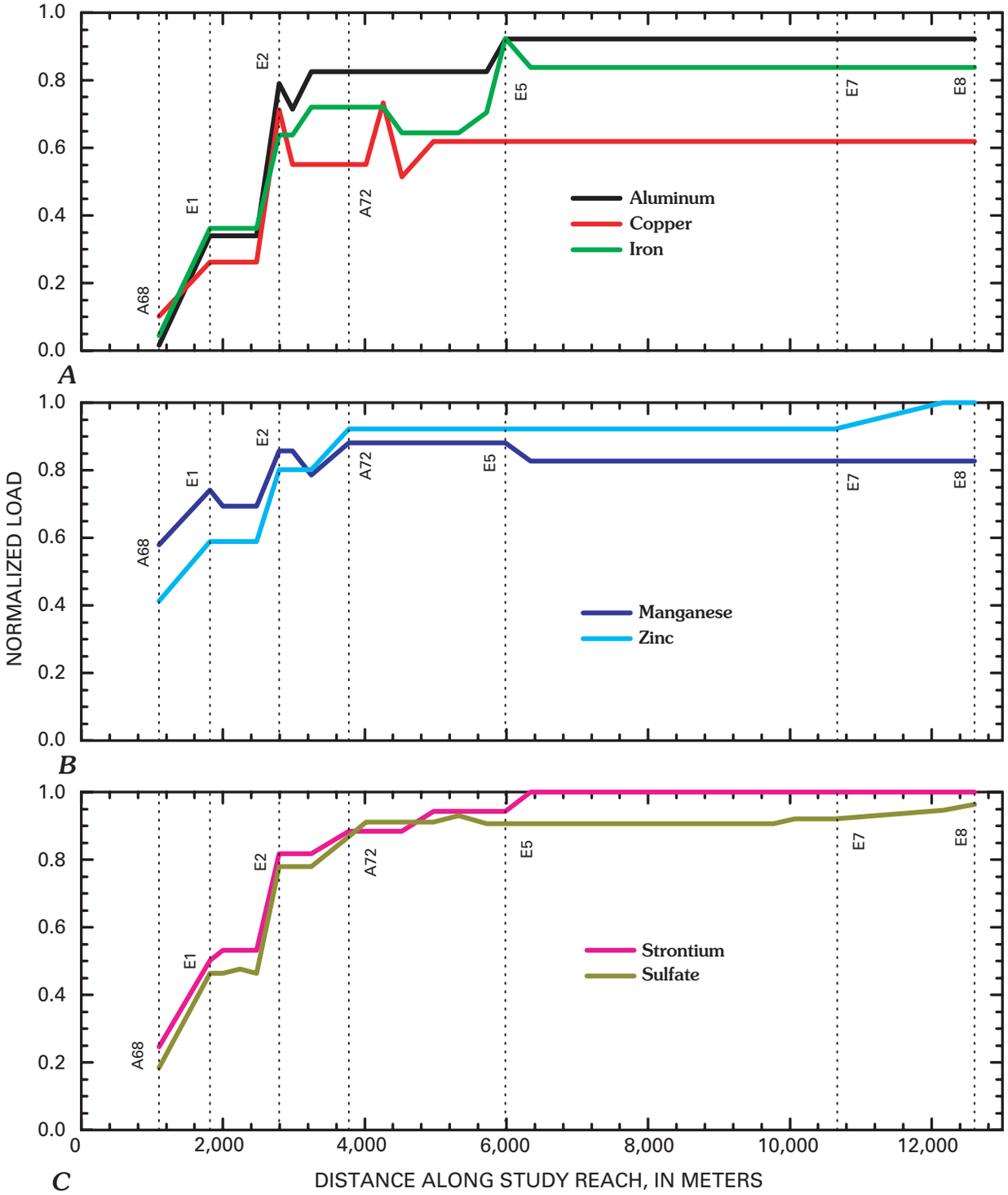

Figure 18. Variation of normalized instream loads for *A*, aluminum, copper, iron; *B*, manganese, zinc; *C*, strontium, and sulfate with distance, Animas River, Silverton to Elk Park, August 1997 and 1998. Labels on vertical lines refer to locations of substantial change along the study reach in figure 15.

Table 11. Summary of load calculations and change of instream load for selected sections of the study reach, Animas River, Silverton to Elk Park, August 1997 and 1998.

[Al, aluminum; Cu, copper; Fe, iron; Mn, manganese; Sr, strontium; Zn, zinc; SO_4, sulfate; distance, in meters; all loads in kilograms per day; number in parentheses indicates ranking of load for each constituent. Note that "below" and "above" indicate "downstream from" and "upstream from"]

	Al	Cu	Fe	Mn	Sr	Zn	SO_4
Cumulative instream load	640	11.2	914	300	241	144	68,890
Cumulative inflow load	532	11.5	746	290	207	132	56,893
Percent inflow	83.2	102	81.6	96.7	85.8	91.4	82.6
Unsampled inflow	108	<0	169	9.88	34.3	12.4	11,998
Percent unsampled	16.8	<1	18.4	3.29	14.2	8.59	17.4
Attenuation	49.4	4.28	148	52.1	0.00	0.00	2,510
Percent attenuation	7.72	38.1	16.2	17.4	0.00	0.00	3.64

Site	Dist	Al	Cu	Fe	Mn	Sr	Zn	SO_4
Animas River above Silverton (A68)	1,100	10.1 (5)	1.14 (3)	40.7 (5)	174 (1)	59.3 (3)	59.4 (1)	12,679 (3)
Downstream from Cement Creek (E1)	1,818	208 (2)	1.81 (2)	290 (1)	48.3 (3)	61.8 (2)	25.6 (3)	19,261 (2)
Downstream from Mineral Creek (E2)	2,793	289 (1)	5.06 (1)	253 (2)	49.4 (2)	75.8 (1)	30.6 (2)	22,520 (1)
A72 gauge (A72)	3,778	71.2 (3)	0.0	75.4 (4)	28.5 (4)	16.1 (4)	17.4 (4)	6,137 (4)
Below Deer Park Creek (E5)	5,989	62.7 (4)	0.8 (4)	185 (3)	0.0	14.0 (5)	0.0	2,604
Below Whitehead Gulch (E7)	9,772	0.0	0.0	0.0	0.0	13.9	0.0	0.0
Below Elk Park Creek (E8)	12,607	0.0	0.0	0.0	0.0	0.0	11.2 (5)	3,991 (5)

can be attributed to the attenuation of aluminum load that occurs upstream from the A68 gauge. Much of the aluminum load from the California Gulch study is effectively removed from the stream water through the braided reach downstream from Eureka (Paschke and others, 2005). Attenuation within the basin, upstream from the accounting site at the outlet, makes the apparent contribution from the upper Animas River basin at A68 (the outlet method) much smaller than the cumulative instream load from the detailed studies upstream from A68 (fig. 19*A*).

The large difference for aluminum and other metal loads (fig. 19) points out the difference between having the outlet view and the instream view. The outlet view gives an accounting of the load that affects the Animas River downstream from these basins, but it cannot indicate where the greatest sources of aluminum load occur. Indeed, some of the most substantial sources of constituent loading could go undetected using the outlet view because of the possible effects of attenuation. None of the detail that is necessary to make decisions about remediation is available. On the other hand, the instream view provides the detailed understanding that helps to facilitate decisions. This is all a matter of scale for a loading study. For example, the detailed loadings from the studies in the Animas River, Cement Creek, and Mineral Creek all use the outlet view to account for inflows within those basins along the study reaches. An appropriate scale must be selected depending on the questions being asked and the resources available for the study.

Taking the instream view from each of the basins, the principal locations of mass loading for aluminum can be compared among the basins for the entire watershed study area (fig. 20; table 12). The bars for aluminum load indicate that the load from Middle Fork Mineral Creek (M9) was the greatest of all sources, accounting for 23 percent of the combined cumulative instream loads (table 12). Combined with the other locations that are listed in table 12, these locations account for 73 percent of the total aluminum load. In Cement Creek, the Prospect Gulch area and the Minnesota Gulch area were both important for contributions of aluminum load. In the Animas River, downstream from Silverton, the area below the Mineral Creek confluence also was important.

Iron

Like aluminum loads, iron loads differ between outlet and cumulative instream views for each of the basins. The outlet loads only represent a fraction of the cumulative instream load that was determined for each of the basins (fig. 19*B*). Taking the more detailed view of the cumulative instream loads, Cement Creek contributed 49 percent of the load at A72 (gauge location, fig. 15), Mineral Creek contributed 43 percent, and the Animas River contributed 4 percent (table 12). These differences reflect the location of Cement Creek and Mineral Creek mostly within the altered rock of the Silverton caldera and the location of the upper Animas River more in areas that were affected by propylitic alteration and not AS or QSP alteration. This pattern also corresponds with the majority of ferricrete occurrences in the watershed (Yager and Bove, this volume, pl. 2). Substantial iron load entered the Animas River with the inflow of Deer Park Creek (E5, fig. 18). Most of the iron load downstream from Deer Park Creek was transported downstream. This might, in part, account for the iron stain on streamside boulders along much of the canyon. Iron stain

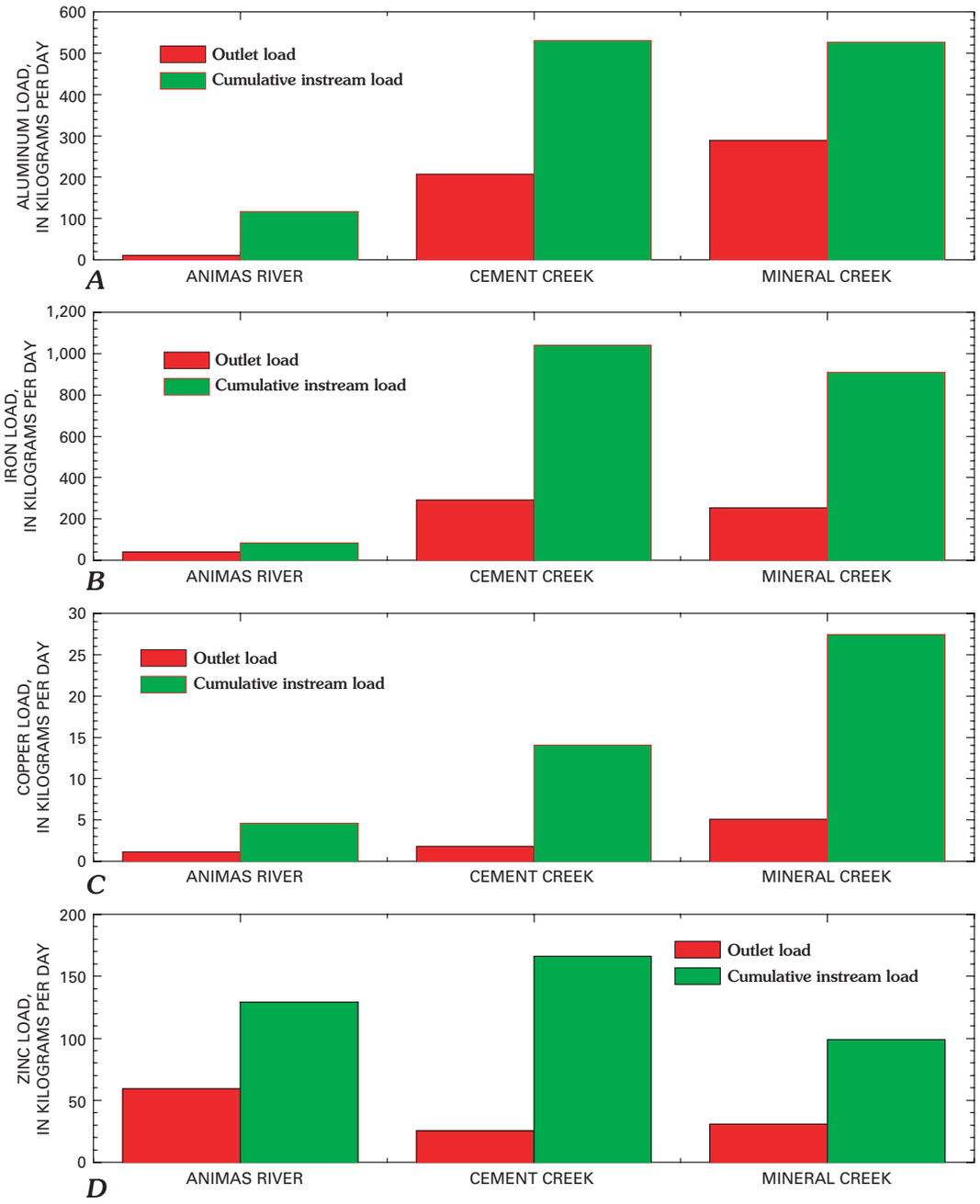

Figure 19. Comparison of sampled instream load for the Elk Park study reach (outlet load) with cumulative instream load for the individual basin studies for *A*, aluminum; *B*, iron; *C*, copper; *D*, zinc.

extended above stream level and most likely was deposited on the rocks during high flow. Church and others (1997) detailed how the colloidal iron load continued all the way into New Mexico, more than 180 km downstream.

Also like aluminum, iron was transported mostly in the colloidal phase (for example, see each stream group, table 10), and the segments that were important for aluminum loading also were important for iron loading (fig. 18*A*). On a watershed scale, mass loading of iron was dominated by the inflow from Middle Fork Mineral Creek, which was 21 percent of the watershed total upstream from the A72 gauge (fig. 21). In Cement Creek, Prospect Gulch contributed 11 percent and the iron bog contributed 6 percent of the watershed total. The contribution around Prospect Gulch was mostly unsampled inflow. In Mineral Creek, the Anvil Mountain area and the dispersed inflow above Porphyry Gulch each contributed more than 5 percent to the total iron load (fig. 21; table 12). The 23 locations in table 12 account

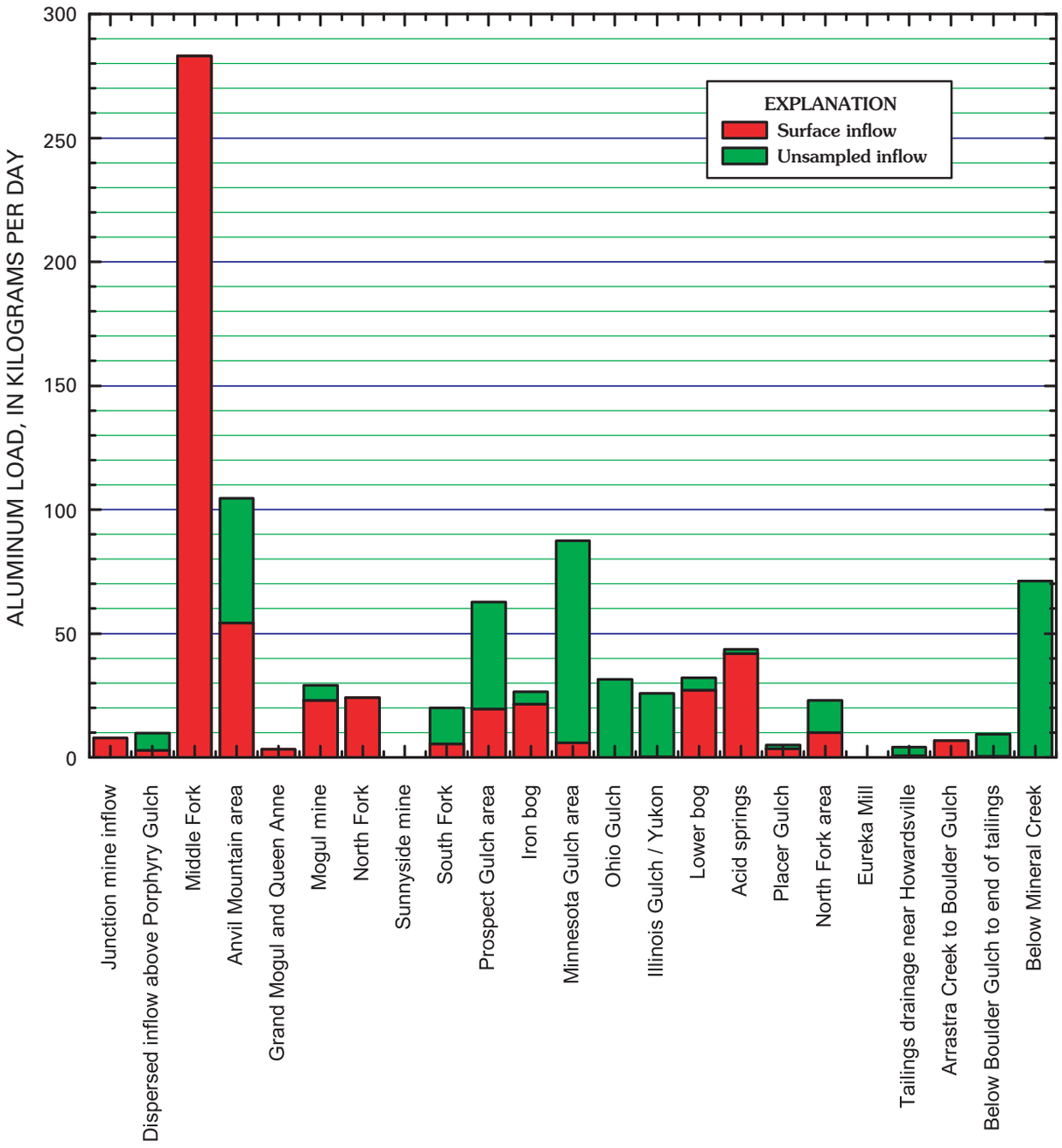

Figure 20. Areas of relative importance for aluminum mass loading, Animas River watershed study area.

for 74 percent of the cumulative instream load of iron. This is similar to the percentages for aluminum and zinc, and is lower than the percentage for copper because sources of iron throughout the watershed are more dispersed, and not just present with base-metal deposits.

Iron colloids in the Animas River watershed study area have a role in the transport of copper, zinc, and other metals (Schemel and others, 2000). The sequence of iron transformation has been studied in laboratory experiments (Grundl and Delwiche, 1993) and quantified in streams affected by mine drainage (Kimball and others, 1994). Steps of this transformation occur within the time frame of transport through individual stream segments in the Animas River, indicating rates of reaction on the order of seconds. The presence of high concentrations of colloidal iron can have two effects. First, the high concentrations of colloidal iron affect the streambed habitat as this material is trapped by algae on cobbles and fills interstices in the cobbles and gravels (Woodward and others, 1995; Clements, 1994). This decreases the pore space that is inhabited by benthic invertebrates. Second, the colloidal iron surface accumulates metals through sorption (Webster and others, 1998). Benthic invertebrates consume iron colloids

Table 12. Summary of mass loading for selected metals, Animas River watershed study area.

[Label, symbol used on maps and figures; Al, aluminum; Fe, iron; Cu, copper; Mn, manganese; Zn, zinc; all loads are in kilograms per day; numbers in parentheses indicate stream segments that were combined for these sums within each subbasin; blanks indicate no significant loading]

Basin	Label	Description	Al	Fe	Cu	Mn	Zn
Animas		Total (California Gulch + Eureka + Howardsville – overlaps)	116	82.9	4.60	333	129
Cement		Total (Upper + Lower minus North/South Forks)	531	1,040	14.0	210	166
Mineral		Total	526	910	27.4	102	99
Elk		Total (between A68 and A72, less Cement and Mineral)	71.2	75.4	0	28.5	17.4
		Total at A72	1,240	2,110	46	674	411
Basin		**Segment or area description**					
Mineral	M1	Junction mine inflow	7.99	67.6	7.99	2.84	18.9
Mineral	M4	Dispersed inflow upstream from Porphyry Gulch	9.94	107	12.6	2.30	35.0
Mineral	M9	Middle Fork	293	450	1.15	36.2	10.5
Mineral	Near M12	Anvil Mountain area	105	160	.78	21.0	11.7
Cement	C1	Grand Mogul and Queen Anne	3.68	2.02	.62	3.77	6.31
Cement	C2	Mogul mine	32.3	25.8	8.30	19.0	61.6
Cement	C3	North Fork	23.9	96.5	3.87	8.59	37.0
Cement	C4	Sunnyside mine				16.2	
Cement	C5	South Fork	20.4	64.7		13.3	
Cement	C6	Prospect Gulch area (2785, 2970, 3125, 3185)	74.8	229	.85	19.1	8.07
Cement	C7	Iron bog (3230, 3317)	22.2	68.9		6.20	1.71
Cement	C8	Minnesota Gulch area (5356, 5652, 5767)	87.4	57.1	.40	33.4	13.3
Cement	C10	Ohio Gulch	31.3	33.4		18	4.02
Cement	C11	Illinois Gulch / Yukon	25.8			14.5	6.13
Cement	C12	Lower bog (9643, 9905)	32.1	68.7		12.8	6.79
[1]Animas	Downstream from A1	Acid springs (790 through 1586)	43.5	0.959	0.20	105	15.9
Animas	A2	Placer Gulch (4448, 4762)	4.98	2.23	0.17	15.5	9.24
Animas	A3	North Fork area (5634 through 6128)	23.0	5.87	0.36	11.2	18.7
Animas	A4	Eureka Mill	1.51	.80	.46	2.07	6.67
Animas	A6	Tailings drainage near Howardsville	12.0	42.6	.43	35.5	27.8
Animas	A8 to A9	Arrastra Creek to Boulder Gulch	6.80	9.39	1.12	32.6	9.84
Animas	A9 to A10	Downstream from Boulder Gulch to end of tailings	9.22	0	0.79	87.9	14.9
Elk	A72	Downstream from Mineral Creek	71.2	75.4	0	28.5	17.4
		Total	910	1,567	40.0	586	318
		Percent of total	73	74	87	87	77

[1]Several of the Animas sums are calculated differently from sums in table 2.

along with algae in biofilm, introducing sorbed metals to the food chain. Colloidal iron has been shown to dissolve in the digestive system of fish and release metals (Gasser and others, 1996).

Copper

Even though problems of copper contamination arose for the ultrafiltrate samples, we could still calculate loads using the total-recoverable concentrations (fig. 18*A*). In general, the pattern of copper load resembled that of aluminum and iron because of the tendency of copper to be sorbed by colloidal solids at the near-neutral pH values of the Animas River (Smith, 1999). Accounting for copper load through the individual cumulative instream loads from the three upstream basins gives differences with the outlet view that are similar to the differences for aluminum and iron (fig. 19*C*). The copper load from the Mineral Creek basin was 60 percent of the total at A72. Cement Creek contributed 30 percent of the load and the Animas River contributed 4 percent. Large differences between the outlet view and the cumulative instream loads for copper again point out the need for a detailed spatial accounting to understand the scale of metal loading (fig. 19*C*).

The partitioning of copper was similar to that of iron because the relatively low pH inflow of Cement Creek had mostly dissolved copper, and the higher pH inflow of Mineral Creek had mostly colloidal copper. Dissolved copper from Cement Creek was transformed to colloidal copper in the mixing zone downstream (Schemel and others, 2000). Through the canyon to Elk Park, the total copper load increased at 4,258 m (fig. 15), but the source of this copper load was not obvious.

The 23 areas that are listed in table 12 account for 87 percent of the copper loading in the watershed study area. Among those areas, the Junction mine inflow (M1), the dispersed inflow above Porphyry Gulch (M4), the Anvil Mountain area (near M12), the Mogul mine (C2), and North

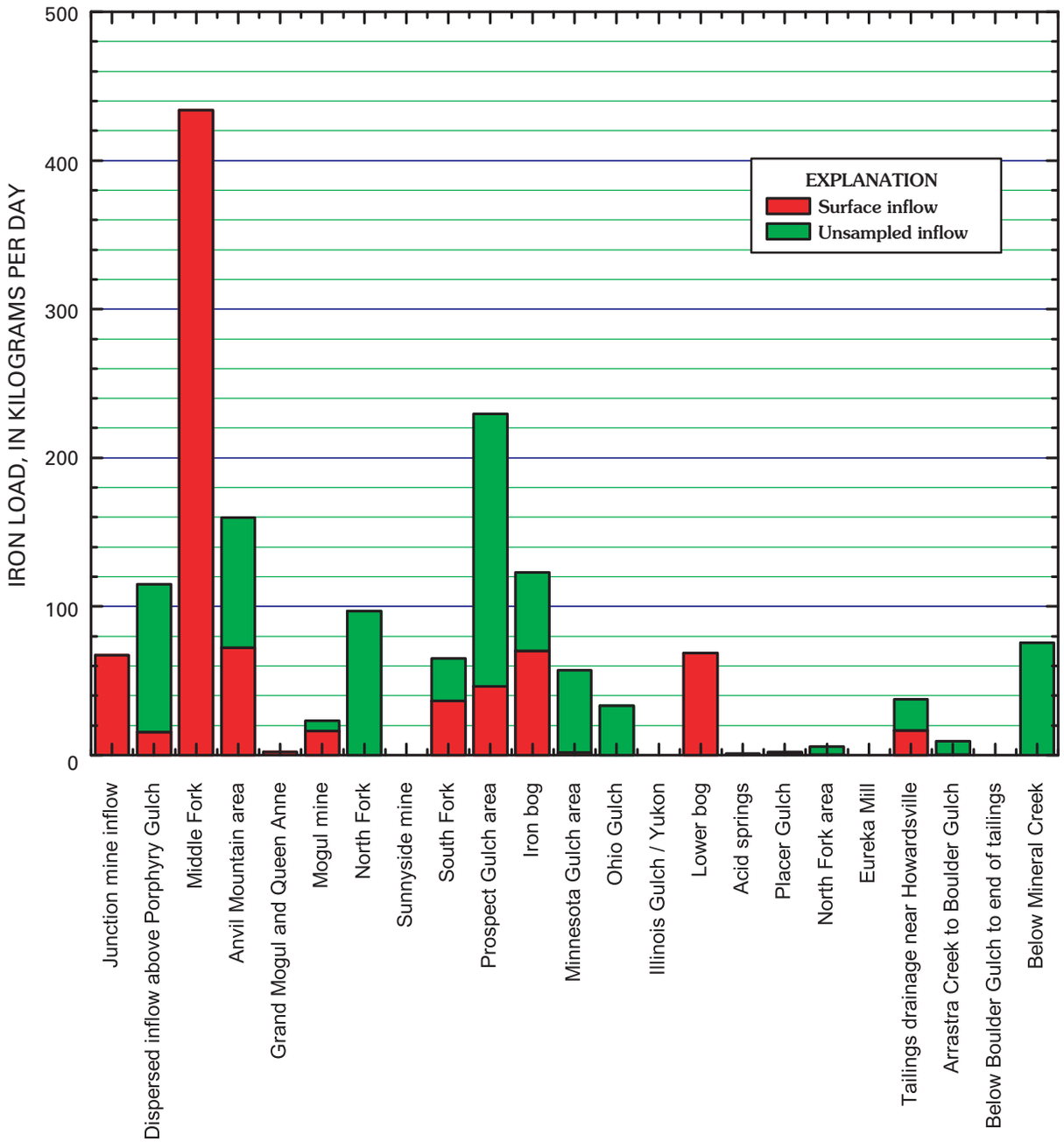

Figure 21. Areas of relative importance for iron mass loading, Animas River watershed study area.

Fork Cement Creek (C3) contributed the greatest loads (fig. 22). A substantial part of this mass loading is due to alteration zones dispersed throughout the watershed, which is reflected in the large portion of load that occurred as unsampled inflow.

Manganese

Dissolved manganese concentration was much greater than the colloidal concentration along the entire study reach (similar to zinc, fig. 17*D*; table 10). The normalized load profile of manganese indicates the large contribution from the upper Animas River basin (A68 gauge), and smaller loads from Cement Creek (E1) and Mineral Creek (E2). A substantial increase in manganese load also occurred near the A72 gauge. Through the Animas River canyon loss of manganese was minimal. Percent contribution for each of the basins, which was calculated by using the cumulative instream loads, indicates that 49 percent of the load at A72 comes from the upper Animas River, 31 percent from Cement Creek, 15 percent from Mineral Creek, and 4 percent from sources near A72 (table 12). The areas listed in table 12 accounted for 87 percent of the total load of manganese at A72.

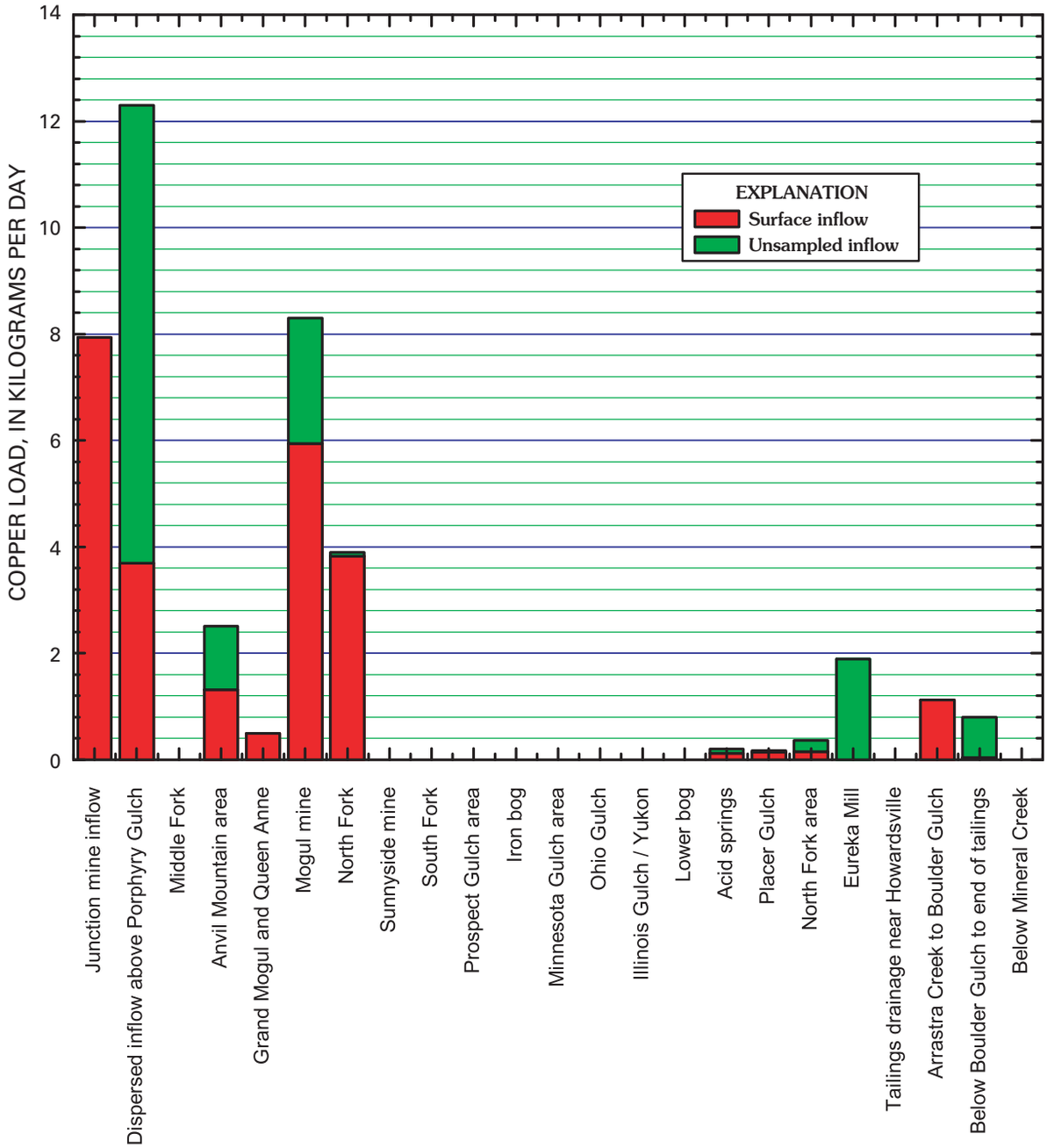

Figure 22. Areas of relative importance for copper mass loading, Animas River watershed study area.

Mass loading of manganese, slightly different from that of other metals, points out additional locations that are significant for metal loading in the watershed (fig. 23). The greatest contributions to manganese load are from the acid springs in California Gulch (downstream from A1; 15 percent), downstream from Boulder Gulch (A9 to A10, but not including Boulder Gulch) to the end of tailings in the upper Animas (13 percent), the Anvil Mountain area (near C12; 5 percent), and Middle Fork Mineral Creek (M9; 5 percent), and the tailings drainage near Howardsville (A6; 5 percent) (figs. 2, 7, 11). Manganese load principally results from the weathering of gangue minerals near the Eureka graben (Bove and others, this volume). Some of this load in the downstream subreach of the upper Animas River basin could be the result of the accumulated tailings piles that have been used to store tailings from many sites throughout the watershed study area.

Zinc

The pattern of zinc loading is comparable to the pattern of manganese, mostly because of the large contribution from the upper Animas River basin (fig. 18*B*). Dissolved zinc concentrations were much greater than colloidal concentrations along

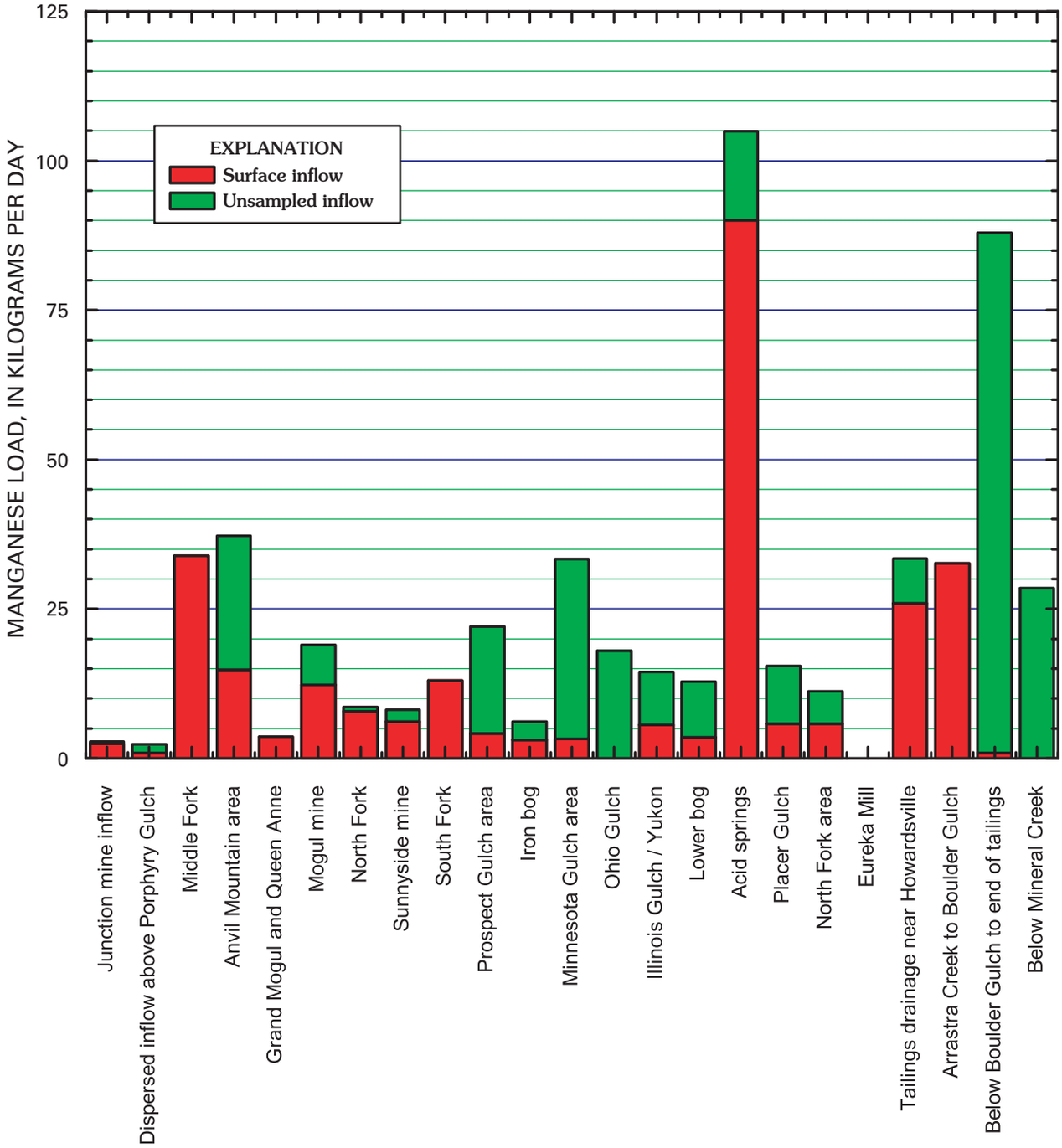

Figure 23. Areas of relative importance for manganese mass loading, Animas River watershed study area.

the entire study reach (table 10). Even though zinc transport was conservative along the Elk Park study reach (fig. 18*B*), attenuation of zinc was still substantial within the three upstream basins. This attenuation is indicated by the substantial differences for zinc in the comparison between the outlet view and the instream views (fig. 19*D*). The greatest contribution to the load of zinc at A72 was from Cement Creek, which contributed 40 percent. The Animas River contributed 31 percent and Mineral Creek contributed 24 percent (table 12). The greatest source of zinc was in the core of the Silverton caldera where the Eureka graben structures and other caldera-related base-metal-bearing structures were weathered or mined.

Mass loading of zinc was more evenly dispersed among the 23 areas, but the combined loading from these areas accounted for 77 percent of the cumulative instream load of zinc upstream from A72 (fig. 24; table 12). This

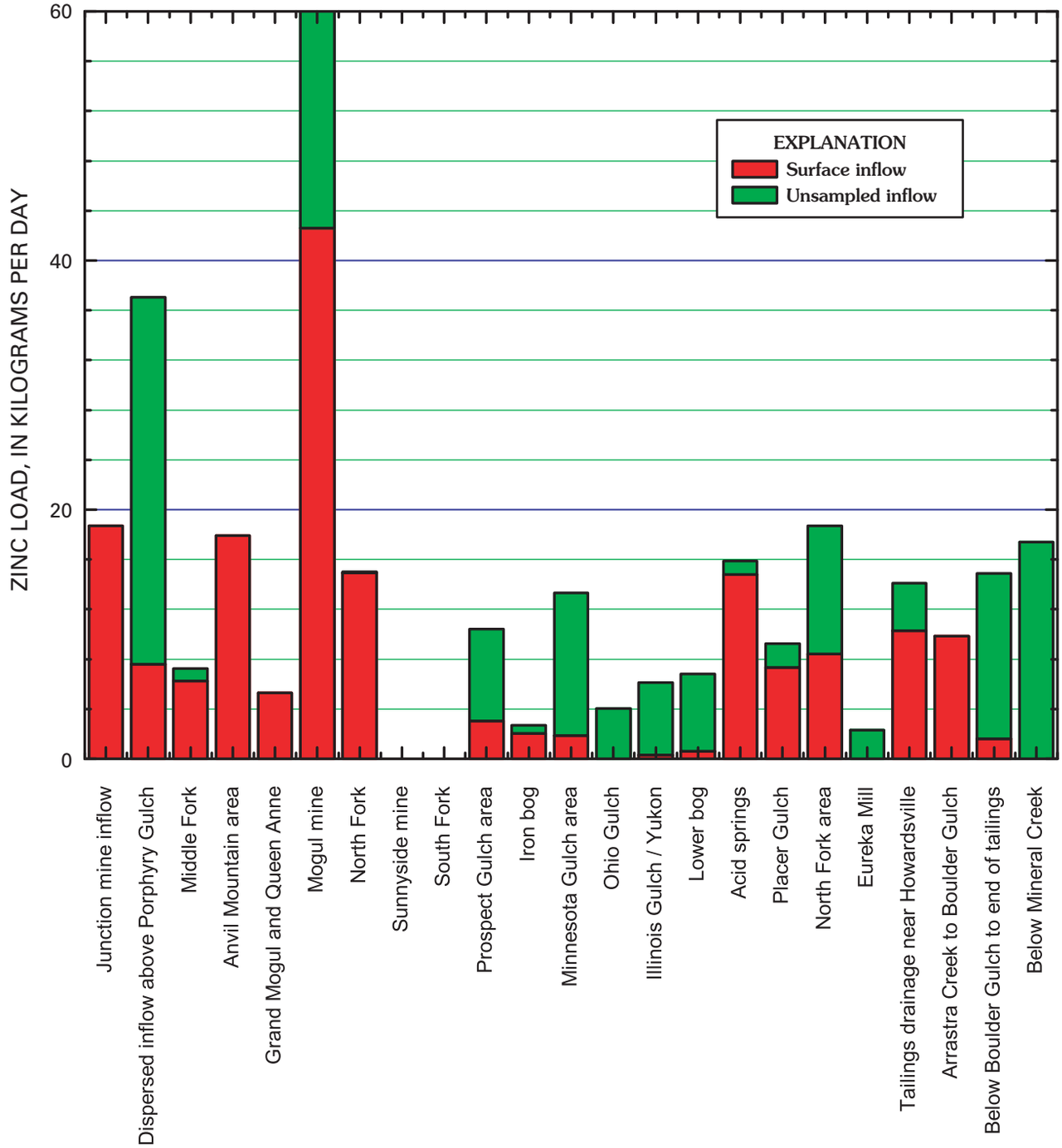

Figure 24. Areas of relative importance for zinc mass loading, Animas River watershed study area.

more dispersed pattern reflects the widespread occurrence of zinc in alteration zones. Areas with the greatest mass loading were the dispersed inflows upstream from Porphyry Gulch in Mineral Creek and the Mogul mine in Cement Creek. These two accounted for 9 and 14 percent of the cumulative instream zinc load, respectively. Several major contributions of zinc load occurred as unsampled inflow. Similar to the sources for copper loads, the dispersed inflows upstream from Porphyry Gulch in Mineral Creek had a substantial amount of unsampled inflow. In addition, the contributions in the upper Animas River basin, downstream from Boulder Gulch to the end of the capped tailings repositories, and in the Elk Park basin, below Mineral Creek, were principally unsampled inflow.

Summary and Conclusions

Tracer-injection and synoptic-sampling methods determined the locations and quantity of loading to three basins in the Animas River watershed. Much of the metal loading can be attributed to 23 specific areas in the watershed. Although these areas are prominent because of the large loads, numerous other sources exist, even though their loads were small in comparison to loads from these 23 areas. After transport in Cement Creek and the Animas River, many of the metals are partitioned between dissolved and colloidal phases by chemical reactions in mixing zones downstream from the confluence of these two streams. These reactions produce substantial colloidal material that affects the transport of metals that sorb to the colloids. Deposition of this material on the streambed provides a route for metals to enter the food web and affect the chronic toxicity in fish populations downstream. However, part of the colloidal load is transported for more than 100 km downstream, possibly affecting aquatic health for a long distance from the Animas River watershed study area.

Loading patterns that have been documented from the mass-loading studies have important implications for possible remediation. When a watershed is dominated by distinct sources, and those sources contribute such a high percentage of the total loads, it is obvious that the most effective remediation could be done by focusing efforts on those sources. Remediation efforts of the many smaller sources of metals would have limited influence on stream recovery if no improvements to the larger sources took place.

References Cited

Bencala, K.E., 1984, Interactions of solutes and streambed sediment—2, A dynamic analysis of coupled hydrologic and chemical processes that determine solute transport: Water Resources Research, v. 20, no. 12, p. 1804–1814.

Bencala, K.E., and McKnight, D.M., 1987, Identifying in-stream variability—Sampling iron in an acidic stream, *in* Averett, R.C., and McKnight, D.M., eds., Chemical quality of water and the hydrologic cycle: Chelsea, Mich., Lewis Publishers, Inc., p. 255–269.

Bencala, K.E., McKnight, D.M., and Zellweger, G.W., 1990, Characterization of transport in an acidic and metal-rich mountain stream based on a lithium tracer injection and simulations of transient storage: Water Resources Research, v. 26, p. 989–1000.

Bencala, K.E., Rathbun, R.E., Jackman, A.P., Kennedy, V.C., Zellweger, G.W., and Avanzino, R.J., 1983, Rhodamine WT dye losses in a mountain stream environment: Water Resources Bulletin, v. 19, p. 943–950.

Besser, J.M., Brumbaugh, W.G., May, T.W., Church, S.E., and Kimball, B.A., 2001, Bioavailability of metals in stream food webs and hazards to brook trout (Salvelinus fontinalis) in the upper Animas River watershed, Colorado: Archive of Environmental Contamination and Toxicology, v. 40, p. 48–59.

Besser, J.M., and Leib, K.J., 1999, Modeling frequency of occurrence of toxic concentrations of zinc and copper in the upper Animas River, *in* Morganwalp, D.W., and Buxton, H.T., eds., U.S. Geological Survey Toxic Substances Hydrology Program—Proceedings of the Technical Meeting, Charleston, South Carolina, March 8–12, 1999, Volume 1, Contamination from hardrock mining: U.S. Geological Survey Water-Resources Investigations Report 99–4018A, p. 75–81.

Blair, R.W., Jr., Yager, D.B., and Church, S.E., 2002, Surficial geologic maps along the riparian zone of the Animas River and its headwater tributaries, Silverton to Durango, Colorado, with upper Animas River watershed gradient profiles: U.S. Geological Survey Digital Data Series DDS–71, version 1.0, 1 CD-ROM.

Boggs, J.M., and Adams, E.E., 1982, Field study of dispersion in a heterogeneous aquifer—4, Investigation of adsorption and sampling bias: Water Resources Research, v. 28, no. 12, p. 3325–3336.

Bove, D.J., Mast, M.A., Wright, W.G., Verplanck, P.L., Meeker, G.P., and Yager, D.B., 2000, Geologic control on acidic and metal-rich waters in the southeastern Red Mountains area, near Silverton, Colorado, *in* ICARD 2000; Proceedings of the Fifth International Conference on Acid Rock Drainage, Volume 1: Society for Mining, Metallurgy, and Exploration, Inc., p. 523–533.

Broshears, R.E., Bencala, K.E., Kimball, B.A., and McKnight, D.M., 1993, Tracer-dilution experiments and solute-transport simulations for a mountain stream, Saint Kevin Gulch, Colorado: U.S. Geological Survey Water-Resources Investigations Report 92–4081, 18 p.

Burbank, W.S., and Luedke, R.G., 1969, Geology and ore deposits of the Eureka and San Juan Mountains, Colorado: U.S. Geological Survey Professional Paper 535, 73 p.

Church, S.E., Kimball, B.A., Fey, D.L., Ferderer, D.A., Yager, T.J., and Vaughn, R.B., 1997, Source, transport, and partitioning of metals between water, colloids, and bed sediments of the Animas River, Colorado: U.S. Geological Survey Open-File Report 97–151, 135 p.

Clements, W.H., 1994, Benthic invertebrate community responses to heavy metals in the Upper Arkansas River Basin, Colorado: Journal of the North American Benthological Society, v. 13, no. 1, p. 30–44.

Colorado Department of Public Health and Environment, 2000, The basic standards and methodologies for surface water, regulation no. 31 (5 CCR 1002-31): Colorado Department of Public Health and Environment, Water Quality Control Commission, p. 53–54. Available at URL: http://www.cdphe.state.co.us/regs/100231u.pdf/

Crowfoot, R.W., Paillet, A.W., Ritz, G.F., Smith, M.E., Jenkins, R.A., and O'Neill, G.B., 1997, Water Resources Data Water Year 1996—Volume 2, Colorado River Basin: U.S. Geological Survey Water-Data Report 96–2, 551 p.

Daultry, S., 1976, Principal components analysis: Concepts and Techniques in Modern Geography No. 8, 50 p.

Freeze, R.A., and Cherry, J.A., 1979, Groundwater: Englewood Cliffs, N.J., Prentice-Hall, Inc., 604 p.

Fuller, C.C., and Davis, J.A., 1989, Influence of coupling of sorption and photosynthetic processes on trace element cycles in natural waters: Nature, v. 340, p. 52–54.

Fuller, C.C., Davis, J.A., and Waychunas, G.A., 1993, Surface chemistry of ferrihydrite—2, Kinetics of arsenate adsorption and coprecipitation: Geochimica et Cosmochimica Acta, v. 57, p. 2271–2282.

Gasser, U.G., Walker, W.J., Dahlgren, R.A., Borch, R.S., and Burau, R.G., 1996, Lead release from smelter and mine waste impacted materials under simulated gastric conditions and relation to speciation: Environmental Science & Technology, v. 30, no. 3, p. 761–769.

Grundl, T., and Delwiche, J., 1993, Kinetics of ferric oxyhydroxide precipitation: Journal of Contaminant Hydrology, v. 14, p. 71–97.

Harvey, J.W., and Wagner, B.J., 2000, Quantifying hydrologic interactions between streams and their subsurface hyporheic zones, *in* Jones, J.A., and Mulholland, P.J., eds., Stream and ground waters: San Diego, Calif., Academic Press, 425 p.

Jarrett, R.D., 1992, Hydraulics of mountain rivers, *in* Yen, B.C., ed., Channel Flow Resistance Centennial of Manning's Formula; International Conference of the Centennial of Manning's and Kuichling's Rational Formula: Littleton, Colo., Water Resources Publications, p. 287–298.

Kaufman, L., and Rousseeuw, P.J., 1990, Finding groups in data—An introduction to cluster analysis: New York, Wiley, 368 p.

Kilpatrick, F.A., and Cobb, E.D., 1985, Measurement of discharge using tracers: U.S. Geological Survey Techniques of Water-Resources Investigations Book 3, Chap. A16, 52 p.

Kimball, B.A., Broshears, R.E., Bencala, K.E., and McKnight, D.M., 1994, Coupling of hydrologic transport and chemical reactions in a stream affected by acid mine drainage: Environmental Science & Technology, v. 28, p. 2065–2073.

Kimball, B.A., Callender, Edward, and Axtmann, E.V., 1995, Effects of colloids on metal transport in a river receiving acid mine drainage, Upper Arkansas River, Colorado, U.S.A.: Applied Geochemistry, v**.** 10, p. 285–306.

Kimball, B.A., McKnight, D.M., Wetherbee, G.A., and Harnish, R.A., 1992, Mechanisms of iron photoreduction in a metal-rich, acidic stream, St. Kevin Gulch, Colorado, U.S.A.: Chemical Geology, v. 96, p. 227–239.

Kimball, B.A., Nimick, D.A., Gerner, L.J., and Runkel, R.L., 1999, Quantification of metal loading in Fisher Creek by tracer injection and synoptic sampling, Park County, Montana, August 1997: U.S. Geological Survey Water-Resources Investigations Report 99–4119, 40 p.

Kimball, B.A., Runkel, R.L., Walton-Day, Katherine, and Bencala, K.E., 2002, Assessment of metal loads in watersheds affected by acid mine drainage by using tracer injection and synoptic sampling: Cement Creek, Colorado, U.S.A: Applied Geochemistry, v. 17, p. 1183–1207.

Lichte, F.E., Golightly, D.W., and Lamothe, P.J., 1987, Inductively coupled plasma-atomic emission spectrometry, *in* Baedecker, P.A., ed., Methods for geochemical analysis: U.S. Geological Survey Bulletin 1770, p. B1–B10.

Mast, M.A., Verplanck, P.L., Yager, D.B., Wright, W.G., and Bove, D.J., 2000, Natural sources of metals to surface waters in the upper Animas River watershed, Colorado, *in* ICARD 2000; Proceedings of the Fifth International Conference on Acid Rock Drainage, Volume 1: Society for Mining, Metallurgy, and Exploration, Inc., p. 513–522.

Mathsoft, 1999, S-PLUS 2000 guide to statistics, Volume 2: Seattle, Wash., Mathsoft, 582 p.

McKinnon, T.E., 2002, Sources and seasonal variability of metal and arsenic concentrations in the surface water of the Clark Fork River Basin: Missoula, Mont., University of Montana M.S. thesis, 115 p.

McKnight, D.M., Kimball, B.A., and Bencala, K.E., 1988, Iron photoreduction and oxidation in an acidic mountain stream: Science, v. 240, p. 637–640.

Nash, J.T., 2000, Geochemical studies of mines, dumps, and tailings as sources of contamination, upper Animas River watershed, Colorado: U.S. Geological Survey Open-File Report 00–104, 1 CD-ROM.

Nordstrom, D.K., and Ball, J.W., 1986, The geochemical behavior of aluminum in acidified surface waters: Science, v. 232, p. 54–56.

Parkhurst, D.L., and Appelo, C.A.J., 1999, User's guide to PHREEQC—A computer program for speciation, reaction-path, one dimensional transport, and inverse geochemical calculations: U.S. Geological Survey Water-Resources Investigations Report 99–4259, 310 p.

Paschke, S.S., Kimball, B.A., and Runkel, R.L., 2005, Quantification and simulation of metal loading to the upper Animas River, Eureka to Silverton, San Juan County, Colorado, September 1997 and August 1998: U.S. Geological Survey Scientific Investigations Report 2005–5054, 82 p.

Rantz, S.E., and others, 1982, Measurement and computation of streamflow—Volume 1, Measurement of stage and discharge: U.S. Geological Survey Water-Supply Paper 2175.

Runkel, R.L., and Kimball, B.A., 2002, Evaluating remedial alternatives for an acid mine drainage stream—Application of a reactive transport model: Environmental Science & Technology, v. 36, p. 1093–1101.

Seaman, J.C., Bertsch, P.M., Korom, S.F., and Miller, W.P., 1996, Physicochemical controls on nonconservative anion migration in coarse-textured alluvial sediments: Ground Water, v. 34, no. 5, p. 778–783.

Schemel, L.E., Kimball, B.A., and Bencala, K.E., 2000, Colloid formation and metal transport through two mixing zones affected by acid mine drainage near Silverton, Colorado: Applied Geochemistry, v. 15, p. 1003–1018.

Smith, K.S., 1999, Metal sorption on mineral surfaces—An overview with examples relating to mineral deposits, *in* Plumlee, G.S., and Logsdon, M.J., eds., The environmental geochemistry of mmineral deposits—Part A, Processes, techniques, and health issues: Society of Economic Geologists, p. 161–182.

Tate, C.M., Broshears, R.E., and McKnight, D.M., 1995, Phosphate dynamics in an acidic mountain stream—Interactions involving algal uptake, sorption by iron oxide, and photoreduction: Limnology and Oceanography, v. 40, no. 5, p. 938–946.

Taylor, J.R., 1997, An introduction to error analysis—The study of uncertainties in physical measurements, Second Edition: Sausalito, Calif., University Science Books, 327 p.

To, T.B., Nordstrom, D.K., Cunningham, K.M., Ball, J.W., and McCleskey, R.B., 1998, A new method for the direct determination of dissolved Fe(III) concentration in acid mine waters: Environmental Science & Technology, v. 33, no. 5, p. 807–813.

Walton-Day, Katherine, Runkel, R.L., Kimball, B.A., and Bencala, K.E., 2000, Application of the solute-transport models OTIS and OTEQ and implications for remediation in a watershed affected by acid mine drainage, Cement Creek, Animas River basin, Colorado, *in* ICARD 2000; Proceedings of the Fifth International Conference on Acid Rock Drainage, Volume 1: Society for Mining, Metallurgy, and Exploration Inc., p. 389–399.

Ward, J.R., and Harr, C.A., 1990, Methods for collection and processing of surface-water and bed-material samples for physical and chemical analyses: U.S. Geological Survey Open-File Report 90–140, 71 p.

Webster, J.G., Swedlund, P.J., and Webster, K.S., 1998, Trace metal adsorption onto an acid mine drainage iron(III) oxy hydroxy sulfate: Environmental Science & Technology, v. 32, no. 10, p. 1361–1368.

Wirt, Laurie, Leib, K.J., Bove, D.J., Mast, M.A., Evans, J.B., and Meeker, G.P., 1999, Determination of chemical-constituent loads during base-flow and storm-runoff conditions near historical mines in Prospect Gulch, upper Animas River Watershed, southwestern Colorado: U.S. Geological Survey Open-File Report 99–159, 36 p.

Woodward, D.F., Farag, A.M., Bergman, H.L., DeLonay, A.J., Little, E.E., Smith, C.E., and Barrows, F.T., 1995, Metals-contaminated benthic invertebrates in the Clark Fork River, Montana—Effects on age-0 brown trout and rainbow trout: Canadian Journal of Fisheries and Aquatic Science, v. 52, p. 1994–2004.

Wright, W.G., and Nordstrom, D.K., 1999, Oxygen isotopes of dissolved sulfate as a tool to distinguish natural and mining-related dissolved constituents: Rotterdam, Balkema, Tailings and Mine Waste 99, p. 671–678.

Yager, D.B., and Bove, D.J., 2002, Generalized geologic map of part of the upper Animas River watershed and vicinity: U.S. Geological Survey Miscellaneous Field Studies Map MF–2377, scale 1:48,000. Map PDF file available at URL http://pubs.usgs.gov/mf/2002/mf-2377/.

Zellweger, G.W., 1994, Testing and comparison of four ionic tracers to measure stream flow loss by multiple tracer injection: Hydrological Processes, v. 8, p. 155–165.

Zellweger, G.W., Avanzino, R.J., and Bencala, K.E., 1989, Comparison of tracer-dilution and current-meter discharge measurements in a small gravel-bed stream, Little Lost Man Creek, California: U.S. Geological Survey Water-Resources Investigations Report 89–4150.

Appendix 1. Methods

Sampling and Chemical Analysis

A general discussion of the sampling procedure is included here, although procedural details among the 10 studies actually varied as noted. Investigators began synoptic sampling at the downstream end of the study reach and moved upstream to avoid sampling suspended materials that they disturbed by walking in the streambed. Inflows and stream sites that were considered to be well mixed were sampled by using grab techniques. Sites that were not well mixed (commonly determined by specific-conductance measurements across the stream) were sampled by equal-width integration (Ward and Harr, 1990). An inflow is designated left or right bank looking downstream.

Samples were collected in 1.8-L bottles and were transported to a central processing area after being placed in black plastic bags, to avoid exposure to direct sunlight (McKnight and others, 1988). The collected samples for each study except the 1996 Cement Creek study were divided into raw (unfiltered) unacidified samples (RU), raw acidified samples (RA), filtered unacidified samples (FU), filtered acidified samples (FA), and ultra-filtered acidified samples (UFA). Filtration was with a tangential flow unit equipped with a 0.45-µm membrane for the FA and FU samples, and with 10,000-Dalton molecular-weight membranes for the UFA samples. Filtration equipment was acid-rinsed between samples and each new membrane was rinsed with reagent-grade water, followed by 250 mL of sample before collecting the filtrates. Aliquots for Fe speciation were placed in amber bottles and were preserved with concentrated HCl to fix the Fe(II)/Fe(III) ratio in UFA samples (To and others, 1998). Specific conductance and pH were determined from the RU sample. Aliquots for metal analysis were acidified to pH less than 2.0 with ultrapure HNO_3. Metal concentrations for the RA, FA, and UFA samples were determined by inductively coupled plasma–atomic emission spectrometry (Lichte and others, 1987). Anion concentrations were determined from FU samples by ion chromatography (Kimball and others, 1999). Total alkalinity was determined from the FU sample by titration.

Use of two filtration membranes provides for three operationally defined concentrations for each metal. The RA sample provides a measure of the total-recoverable metal concentration (dissolved+colloidal), and the UFA sample provides the dissolved metal concentration. Filtration for metals with the 0.45-µm membranes (FA) is used for comparison with the UFA filtration because aquatic standards commonly are in terms of 0.45-µm filtration. Colloidal metal concentrations are defined as the difference between the total-recoverable (RA) and the ultrafiltrate metal concentrations (UFA) (Kimball and others, 1995). For the 1996 Cement Creek study, there was only one filtration using a 0.1-mm filter and a pressure filtration system (Kimball and others, 2002). This filtration led to an operationally different, but comparable definition of dissolved and colloidal concentrations.

An unexpected result occurred with the filtration of samples collected for the Eureka study reach. Concentrations of dissolved copper in ultrafiltrates were consistently higher than concentrations of 0.45-µm-filtered copper and sometimes greater than the total-recoverable concentration. This likely indicates contamination of copper in the ultrafiltrate sample that did not occur in the other filtrates, nor for other metals. This contamination occurred in both mass-loading studies in 1998, and was a factor in the Elk Park study reach also. Generally, this only affected samples in which copper concentration was less than about 30 µg/L. Because of this contamination, the 0.45-µm concentration was used as the dissolved copper concentration for this study reach. Because total-recoverable concentrations were used to calculate loads, those calculations were not affected by the contamination.

Tracer Injections and Stream Discharge

Quantifying discharge in mountain streams by the traditional velocity-area method (Rantz and others, 1982) is compromised by the roughness of the streambed and the variability caused by pools and riffles (Jarrett, 1992). Further, a substantial percentage of discharge may be flowing through porous areas of the streambed that make up the hyporheic zone, a condition that may result in an underestimate of constituent loads (Zellweger and others, 1989). Measurement of discharge using the velocity-area method does not account for flow through the hyporheic zone. Another limitation of the velocity-area method for the characterization of metal loads is the time and personnel requirements associated with each discharge measurement. In the studies described herein, numerous (often, about 60) instream samples were collected during a single day to characterize stream chemistry at steady state. To perform velocity-area discharge measurements in conjunction with sample collection at the large number of sites that are needed is problematic, if not impossible.

An alternative means of estimating discharge used here is the tracer-dilution method (Kilpatrick and Cobb, 1985). The tracer-dilution method uses an inert tracer that is continuously injected into the stream at a constant rate and concentration. Given sufficient time, all parts of the stream including side pools and the hyporheic zone will become saturated with tracer and instream concentrations will reach a plateau (Kimball and others, 2002). Decreases in plateau concentration with stream length reflect the dilution of tracer by additional water entering the channel (surface- and groundwater inflow). Consideration of this dilution allows for the calculation of discharge at each stream site. Application of

the tracer-dilution method addresses both limitations of the area-velocity method because (1) the tracer enters porous areas of the streambed such that flow through the hyporheic zone is accounted for; and (2) the collection of tracer samples when plateau concentrations are achieved provides the ability to obtain discharge estimates at numerous locations.

Successful implementation of the tracer-dilution method is dependent on several key factors. (1) First and foremost, the injected tracer must be transported through the stream system in a conservative manner; that is, concentrations of the tracer should be unaffected by biogeochemical reactions. Tracers used include dyes and inorganic salts. The degree to which a given tracer is conservative is often a function of stream pH. Inorganic salts containing lithium, for example, are often used in acidic environments due to the conservative nature of lithium at low pH. In consideration of the range of pH found in the Animas River watershed, our investigations used a number of different inorganic salts in the individual studies described herein. Previous studies have documented the transport, chemistry, and toxicity of these inorganic tracers (Bencala and others, 1990; Broshears and others, 1993; Zellweger, 1994; Tate and others, 1995). (2) Another key factor is the ability to maintain a constant rate during the continuous tracer injection. For the studies described here, tracer injections were controlled with precision metering pumps linked to a Campbell CR-10 data logger. Use of the data logger provides a means to maintain a constant injection rate as battery voltage decreases. Additional details on specific tracer injections are included in the sections describing the basins.

Kilpatrick and Cobb (1985) presented a simple mass balance equation used to determine discharge when fluorescent dyes are used to implement the tracer-dilution method. Although the use of dyes is straightforward, their use is precluded in acidic waters due to sorption reactions that act to artificially dilute the added tracer (Bencala and others, 1983). Simple inorganic salts (sodium chloride, for example) were used instead. Use of these salt tracers necessitates the use of alternate equations for discharge determination, as described here. As in the work of Kilpatrick and Cobb (1985), these equations are based on a simple mass balance that considers the concentration and injection rate of the added tracer. Owing to the different types of tracers used in the Animas River studies, three different sets of equations are needed. Each equation set assumes that the concentration of the added tracer is much greater than the naturally occurring concentration. All concentration variables expressed herein refer to tracer concentrations at the time of synoptic sampling, except for those including the superscript “P,” which refers to a “presynoptic” sample.

Tracer-Dilution Case I: Uniform Background Concentrations

Inorganic salts containing lithium and bromide were used in several of the tracer injections. In mountain stream environments in which the rocks are mainly igneous, concentrations of lithium and bromide are typically low, with background concentrations at or near the detection limits. Spatial variability in background concentrations is also low, such that background concentrations are nominally uniform. Given the assumption of uniform background concentrations, stream discharge at any location downstream from the injection is given by:

$$Q_D = \frac{Q_{INJ} C_{INJ}}{C_D - C_B} \quad (1)$$

where

Q_D is stream discharge, in L/s,
Q_{INJ} is the injection rate, in L/s,
C_{INJ} is the injectate concentration, in mg/L,
C_D is the tracer concentration at plateau, in mg/L,

and

C_B is the naturally occurring background concentration, in mg/L.

Tracer-Dilution Case II: Non-Uniform Background with a Presynoptic Sampling

Due to their low background concentrations, lithium and bromide are ideal tracers for use in tracer-dilution studies. Inorganic salts containing lithium and bromide are relatively expensive, however, and alternate tracers may be preferable when discharge rates are high, or when the injection will be for a long period or will cover a long stream reach. Several studies described herein, therefore, involve the injection of sodium chloride, where the chloride ion is used as a conservative tracer. Because of the effects of natural sources and anthropogenic activities (road salting and dust management, for example), background chloride concentrations are neither low nor uniform in many situations.

Non-uniform background conditions may be addressed by the addition of presynoptic sampling, just prior to the start of the tracer injection. During presynoptic sampling, samples are collected at each of the stream sites that are to be sampled during the main synoptic. These presynoptic samples are analyzed for the tracer of interest (chloride, for example) and used to correct the observed tracer concentrations for the spatially variable background concentrations. Presynoptic and synoptic discharges are assumed equal, and stream discharge at any location downstream from the injection is given by:

$$Q_D = \frac{Q_{INJ} C_{INJ}}{C_D - C_D^P} \quad (2)$$

where

C_D^P is the presynoptic estimate of the naturally occurring background concentration, in mg/L, and all the other terms are defined as in equation 1.

Tracer-Dilution Case III: Non-Uniform Background without a Presynoptic Sampling

The final case concerns the use of a tracer with non-uniform background concentration, such as chloride, when a presynoptic either is not conducted or is invalid owing to a change in flow regimes. In this situation, non-uniform background concentrations are addressed by considering the tracer concentrations of the inflow waters entering the channel within each subreach. For some subreaches, these inflow waters will be well-defined surface inflows that are easily sampled during the main synoptic. In other subreaches, inflow waters may be primarily dispersed, ground-water inflows that are unsampled during the main synoptic. These subreaches require estimation of the tracer-inflow concentration, a process that can lead to considerable uncertainty in the discharge calculations.

Tracer-dilution estimates of discharge for this final case are made in downstream order, starting with the first synoptic site below the injection. Under the assumption that negligible inflow enters the stream between the injection site and the first synoptic site, stream discharge at the first synoptic site is given by:

$$Q_D = \frac{Q_{INJ} C_{INJ}}{C_D - C_0} \quad (3)$$

where

C_0 is the naturally occurring background concentration upstream of the injection, in mg/L, and all the other terms are defined as in equation 1. Discharge estimates for the remaining synoptic sites are given by:

$$Q_D = \frac{Q_U (C_U - C_L)}{C_D - C_L} \quad (4)$$

where

Q_U is the stream discharge for the synoptic site immediately upstream, in L/s,

C_U is the plateau tracer concentration for the synoptic site immediately upstream,

and

C_L is tracer concentration in the inflow waters entering a given subreach, in mg/L, and all the other terms are defined as in equation 1.

Synoptic Sampling and Analytical Methods

Synoptic sampling is needed to quantify water chemistry and discharge for instream load calculations. This sampling scheme is appropriate for streams and small rivers in which the most significant chemical gradients occur in the longitudinal direction. Under ideal conditions, samples at all of the sampling locations would be collected simultaneously, providing data for stream-water quality at steady state. Personnel limitations generally preclude simultaneous sample collection, but the synoptic studies described herein provide an approximate means of defining steady-state conditions. This approximation is achieved by collection of all the stream samples during a relatively short time period (less than 8 hours). When this is done under base-flow conditions, the effects of diurnal flow variation are minimized.

Stream sites along the study reach are spaced such that they bracket the sampled inflows and areas of likely subsurface inflow. Subreaches that are bracketed by two adjacent stream sites are referred to as stream segments. The intent of this bracketing is to capture the changes in load that are attributable to visible surface inflow and (or) dispersed subsurface inflow within each segment. Changes in stream chemistry and discharge between stream sampling sites reflect a net metal load for specific segments, but the loads cannot always be attributed to specific sources.

If stream sites downstream from inflows are considered well mixed, grab samples are collected. The extent of mixing is determined by pH or water conductance cross sections before sampling. Sites that are not well mixed are sampled by equal width integration (Ward and Harr, 1990). Water temperature is measured at the time of collection. Samples are transported to a central location for further processing, having been placed in black plastic bags to prohibit sunlight from altering the sample (McKnight and others, 1988). The collected samples are divided into several 125 mL bottles with different treatments at the central processing location: a raw (unfiltered) unacidified sample (RU), a raw acidified sample (RA), a filtered unacidified sample (FU), a filtered acidified sample (FA), and an ultra-filtered acidified sample (UFA).

Specific conductance and pH are determined from the RU sample within hours of sample collection. Tangential-flow filtration is used with 0.45-µm membranes (FU and FA samples) and 10,000-Dalton molecular weight membranes (UFA ultrafiltration sample). Metal concentrations for the RA, FA, and UFA samples are determined by inductively coupled plasma–atomic emission spectrometry (Lichte and others, 1987). Anion concentrations are determined from FU samples using ion chromatography (Kimball and others, 1999). Ferrous iron is determined colorimetrically from the UFA samples (Kimball and others, 1992), and total alkalinity is determined by titration.

Use of three processing treatments provides for different operationally defined concentrations for each metal. The unfiltered sample (RA) provides a measure of the total-recoverable metal concentration (dissolved+colloidal), whereas the ultrafiltrate concentration (UFA) is considered the dissolved metal concentration. The 0.45-µm concentration (FA) is used for comparison purposes, as a means of quantifying the colloids having a size between 0.45-µm and 10,000-Dalton molecular weight, but also to compare the ultrafiltrate concentrations to aquatic standards that are written with 0.45-µm filtration. Colloidal metal concentrations are defined as the difference between the total-recoverable (RA) and the ultrafiltrate metal concentrations (UFA) for stream samples (Kimball and others, 1995).

Appendix 2. Details of Upper Cement Creek Mass-Loading Studies

Upper Cement Creek Study Area and Experimental Design

The tracer injection and synoptic sampling for upper Cement Creek covered approximately 4,133 m of stream starting downstream from Ross Basin and continuing to just downstream from the confluence with South Fork Cement Creek near Gladstone (figs. 7 and 25). Synoptic sampling sites and their site numbers are listed in table 13. This stream reach included inflows from the Grand Mogul and Queen Anne mines at 271 and 298 m and the Mogul mine at 1,318 and 1,348 m. North Fork Cement Creek, which contains several inactive mines and is affected by mine drainage, joins Cement Creek at approximately 3,076 m (table 13). Treated effluent from the American tunnel/Sunnyside mine enters the stream at 3,853 m. The American tunnel effluent contains mine drainage that is collected from underground workings associated with the Sunnyside mine and that is treated and released to Cement Creek under a National Pollutant Discharge Elimination System (NPDES) permit (Chris Gates, Colorado Water Quality Control Commission, oral commun., 2001). This source will be referred to as Sunnyside mine effluent. South Fork Cement Creek enters Cement Creek at approximately 4,001 m. Numerous additional inactive mines and prospects exist in the basin (see Church, Mast, and others, this volume). Stream elevation ranges from approximately 3,600 m at the injection site to 3,170 m at the downstream end of the reach. Average stream gradient is approximately 10 percent. Geology of the basin is described in Yager and Bove (this volume) and Bove and others (this volume).

A total of 36 stream sites and 21 inflow sites were sampled. Stream-discharge measurements using a velocity meter were made at 3,844 m (T3), and 4,133 m. A Parshall flume located at the Sunnyside mine effluent provided an independent measure of that inflow. A few additional inflow and stream samples were collected during August 2000 to aid in water-quality characterization for the basin.

Discharge

Profiles of bromide at sites T1 (507 m), T2 (2,885 m), and T3 (3,844 m) are shown in figure 26. Discharge calculated by use of equations 3 and 4 is shown in table 14. Independent velocity meter and Parshall-flume measurements also are shown in table 14. Two problems with the tracer data necessitated our making adjustments to the data and using slightly different techniques to calculate discharge from the tracer data than indicated in equations 1–4: (1) tracer was not at plateau at all sites when synoptic samples were collected; (2) discharge estimates made using equations 1–4 do not compare favorably with independent measurements of discharge made using velocity meters and Parshall flumes.

The first problem with the tracer data is that the synoptic samples collected between the bottom of the reach and site T2 (2,885 m) were collected before the tracer concentration had reached plateau or steady-state values (fig. 26*A*). Plateau concentrations at T3 were reached at approximately 1415 hours (MDT) on September 20, whereas the synoptic sample at that site was collected at 0915 hours. In contrast, it appears that tracer concentrations at site T2 (2,885 m) reached plateau at about the same time the synoptic sample was collected (1100 hours). Therefore, the tracer concentrations in synoptic samples collected at all sites downstream from T2 are lower than they would have been had the tracer reached plateau. It is possible to correct this problem and adjust the tracer concentrations at sites between T2 and T3 with the help of a few assumptions.

The first assumption is that the concentration of bromide in the synoptic sample collected at site T2 (2.73 mg/L) represents plateau, or steady-state concentration. The second assumption is that the proportional change in bromide concentrations (Br_{prop}) between stream sites relative to the change in bromide concentrations between sites T2 and T3 would be the same before plateau as after plateau. At each site, Br_{prop} is defined as:

$$\frac{(C_{up} - C_{down})}{(C_{T2} - C_{T3})} = Br_{prop} = \frac{(C'_{up} - C'_{down})}{(C'_{T2} - C'_{T3})} \qquad (6)$$

where

C_{up} is the concentration of bromide in the synoptic sample collected at a stream site, in mg/L,

C_{down} is the concentration of bromide in the synoptic sample from the adjacent downstream site, in mg/L,

C_{T2} is the concentration of bromide in the synoptic sample collected at site T2, in mg/L,

C_{T3} is the concentration of bromide in the synoptic sample collected at T3, in mg/L,

C'_{up} is the plateau concentration of bromide at a stream site, in mg/L,

C'_{down} is the plateau concentration of bromide at the adjacent downstream site, in mg/L,

C'_{T2} is the plateau concentration of bromide at site T2, in mg/L,

and

C'_{T3} is the plateau concentration of bromide at T3.

Solving for C'_{down}:

$$C'_{down} = C'_{up} - \frac{(C'_{T2} - C'_{T3})}{(C_{T2} - C_{T3})}(C_{up} - C_{down}) \qquad (7)$$

We can solve for C'_{down} at 2,976 m using site T2 (2,885 m) as C_{up}: $C_{up} = C'_{up} = 2.73$ mg/L bromide; $C_{down} = 2.63$ mg/L bromide; $C_{T2} - C_{T3} = 0.64$ mg/L bromide; $C'_{T2} - C'_{T3} = 2.73 - 2.34$

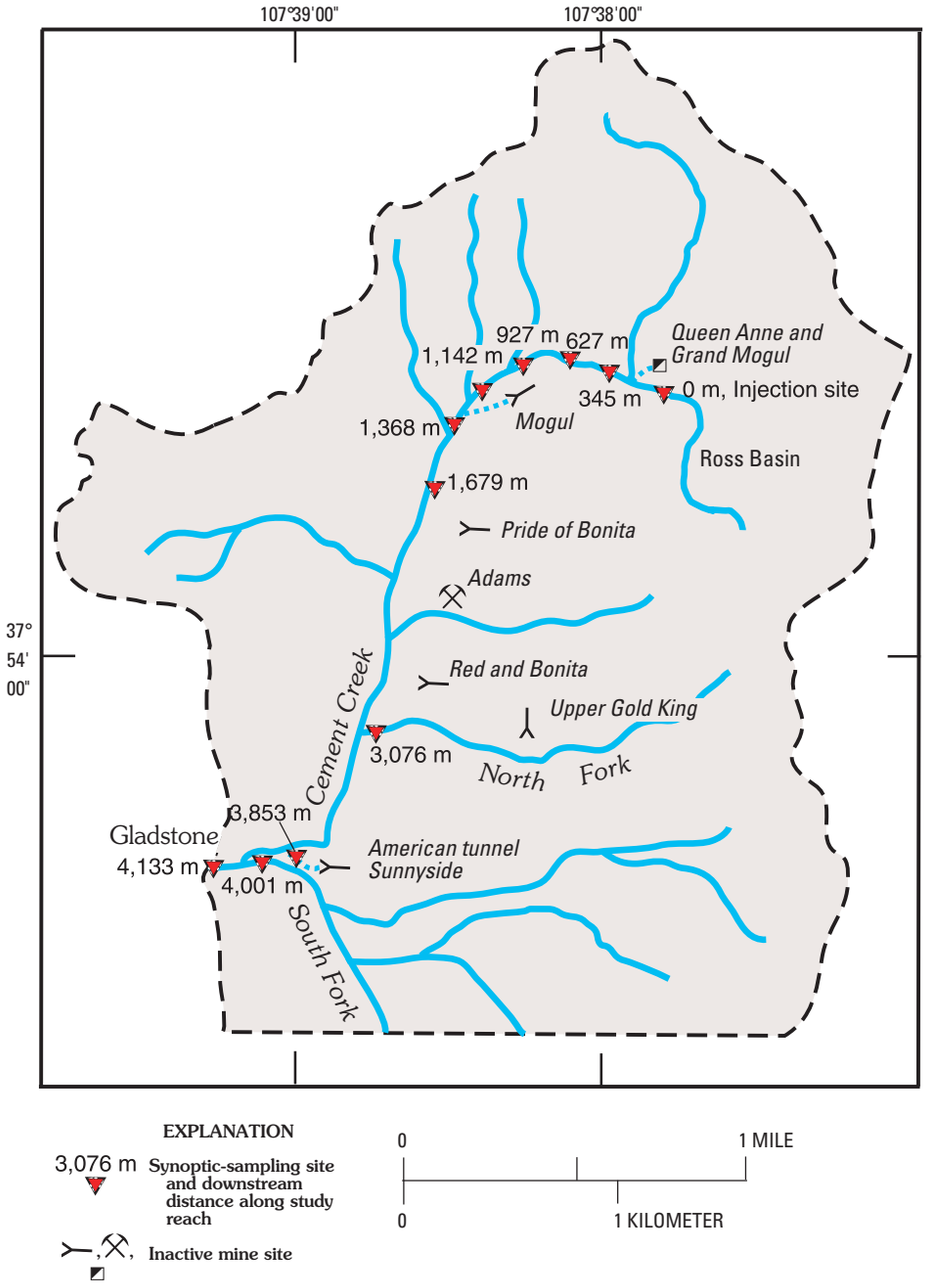

Figure 25. Location of selected synoptic sampling sites and inactive mines, upper Cement Creek, September 1999. Dashed blue line segments indicate drainage to stream.

(from fig. 26*B*) = 0.39 mg/L bromide. Therefore, the adjusted bromide concentration at 2,976 m is C'_{down} = 2.67 mg/L. The results of applying the correction moving downstream to T3 are listed in table 14, and shown graphically in figure 27. The adjustment procedure results in proportionally greater adjustments to the bromide concentration moving downstream. This type of proportional adjustment is appropriate considering that the samples were collected in an upstream direction, so the difference between the time the synoptic samples were collected and the time of plateau concentrations at each site decreased as sampling approached site T2.

The second problem with the tracer data is that the discharge values calculated from the tracer concentration are as much as three times greater than independent measurements of discharge made using velocity meters (table 14). This discrepancy indicates either a large hyporheic zone that carries one-half to two-thirds of the flow near the bottom of the stream reach, or a loss of tracer in the stream reach. To assign a large hyporheic zone to this stream seems unrealistic. The cross-sectional area of the hyporheic zone can be calculated using Darcy's law: $Q = KIA$, where K is the hydraulic conductivity (units length/time), I is the ground-water gradient

Table 13. Site identification, downstream distance, source, label, principal component classification, site description, and selected characteristics for stream and inflow sites, upper Cement Creek, September 1999.

[Site identification, reference to site in database; Distance, in meters along the study reach; Source: S, stream; RBI, right bank inflow; LBI, left bank inflow; Label, map and discussion label used in fig. 7; PCA group, classification from principal component analysis; pH in standard units; SO_4, sulfate, in milligrams per liter]

Site identification	Distance	Source	Label	PCA group	Site description	pH	SO_4
ROSS-0000	0	S		1	T0 transport site—up from injection site	6.83	73.4
ROSS-0041	41	S		1	First site below injection	6.75	73.3
ROSS-0084	84	S		1	After braids	6.71	73.6
ROSS-0234	234	S		1	Above inflow from talus	6.64	73.8
ROSS-0237	237	LBI		1	Draining talus slope	6.72	64.2
ROSS-0259	259	S		1	Below first inflow	6.46	69.0
ROSS-0271	271	RBI		3	From stope with Fe stain	3.27	205
ROSS-0293	293	S		1	Above Queen Anne inflow	5.14	77.8
ROSS-0298	298	RBI		3	Drainage from Queen Anne mine	5.73	143
ROSS-0345	345	S	C1	1	Below Queen Anne inflow	5.71	104
ROSS-0440	440	S		1	Above small mine dump	5.71	103
ROSS-0457	507	S		1	T1 transport site—above Texas crossing	6.24	101
ROSS-0577	627	S		1	Before first cascade of canyon	6.04	101
ROSS-0777	827	S		1	At head of deep canyon	6.44	98.3
ROSS-0877	927	S		1	At mouth of canyon	5.15	98.2
ROSS-0883	933	RBI		1	Drains prevailing fracture set	6.60	41.4
ROSS-0933	983	S		1	Below inflow for mixing	5.07	93.9
ROSS-1092	1,142	S		1	Above road to Mogul	5.75	94.5
ROSS-1187	1,237	RBI		1	Drains across road	6.78	44.7
ROSS-1237	1,287	RBI		1	Mossy inflow	6.47	34.8
ROSS-1242	1,292	S		1	Above first Mogul inflow	4.59	90.2
ROSS-1265	1,315	S		1	Above Mogul inflow—some Mogul inflow	4.27	83.9
ROSS-1268	1,318	LBI		2	Mogul mine inflow	2.85	1,010
ROSS-1283	1,333	S		2	Between Mogul inflows	3.65	203
ROSS-1298	1,348	LBI		3	Second, more dilute Mogul inflow	3.89	126
ROSS-1317	1,367	S	C2	2	Below Mogul inflows—replicate samples	3.65	200
ROSS-1361	1,411	RBI		1	Draining catchment	6.74	24.5
ROSS-1491	1,541	S		3	Below catchment inflow	0.00	189
ROSS-1629	1,679	LBI		3	Draining lineament	6.39	572
ROSS-1664	1,714	S		2	Below lineament inflow	3.72	193
ROSS-1669	1,719	LBI		1	Draining second fracture lineament	4.34	16.4
ROSS-1819	1,869	S		2	Above iron soil zone on right bank	3.66	182
ROSS-1834	1,884	RBI		3	Iron bog—dip sample	3.42	72.9
ROSS-2034	2,084	S		2	Below slumped soil zone on right bank	3.66	186
ROSS-2184	2,234	S		2	Near start of left bank iron soil zone	3.66	195
ROSS-2357	2,407	LBI		3	Draining iron soil zone on left bank	3.64	87.0
ROSS-2456	2,506	S		2	Below left bank iron soil zone	3.70	189
ROSS-2668	2,718	S		2	Below clean inflows	3.73	183
ROSS-2711	2,761	LBI		3	Draining iron bog and Red and Bonita mine	3.50	177
ROSS-2713	2,763	LBI		2	Second inflow draining iron bog	3.23	248
ROSS-2835	2,885	S		2	T2 transport site—below left bank iron soil zone	3.67	191
ROSS-2926	2,976	S		2	Above North Fork Cement Creek	3.57	191
ROSS-3026	3,076	LBI		2	North Fork	2.87	993
ROSS-3057	3,107	S	C3	3	30 m below North Fork	3.45	245
ROSS-3122	3,172	S		3	96 m below North Fork	3.45	236
ROSS-3205	3,255	S		3	129 m below North Fork	3.35	248
ROSS-3272	3,358	S		3	At treatment intake for Sunnyside	3.32	243
ROSS-3362	3,448	LBI		3	Pond at base of rocks	3.46	170
ROSS-3430	3,516	S		3	Above culvert at Sunnyside mine	3.44	234
ROSS-3432	3,518	LBI		3	Upper discharge pipe	6.35	288
ROSS-3547	3,633	S		3	Upstream of culvert	3.39	237
ROSS-3758	3,844	S		3	T3 transport site—above treatment inflow	3.39	267
ROSS-3767	3,853	LBI		3	Inflow from Sunnyside treatment	7.87	1,460
ROSS-3845	3,931	S	C4	3	Below Sunnyside treatment	3.67	610
ROSS-3915	4,001	LBI		3	South Fork Cement Creek	5.54	240
ROSS-3916	4,002	RBI		1	Inflow from iron-stained seep	3.66	198
ROSS-4047	4,133	S	C5	3	Below South Fork	4.02	407

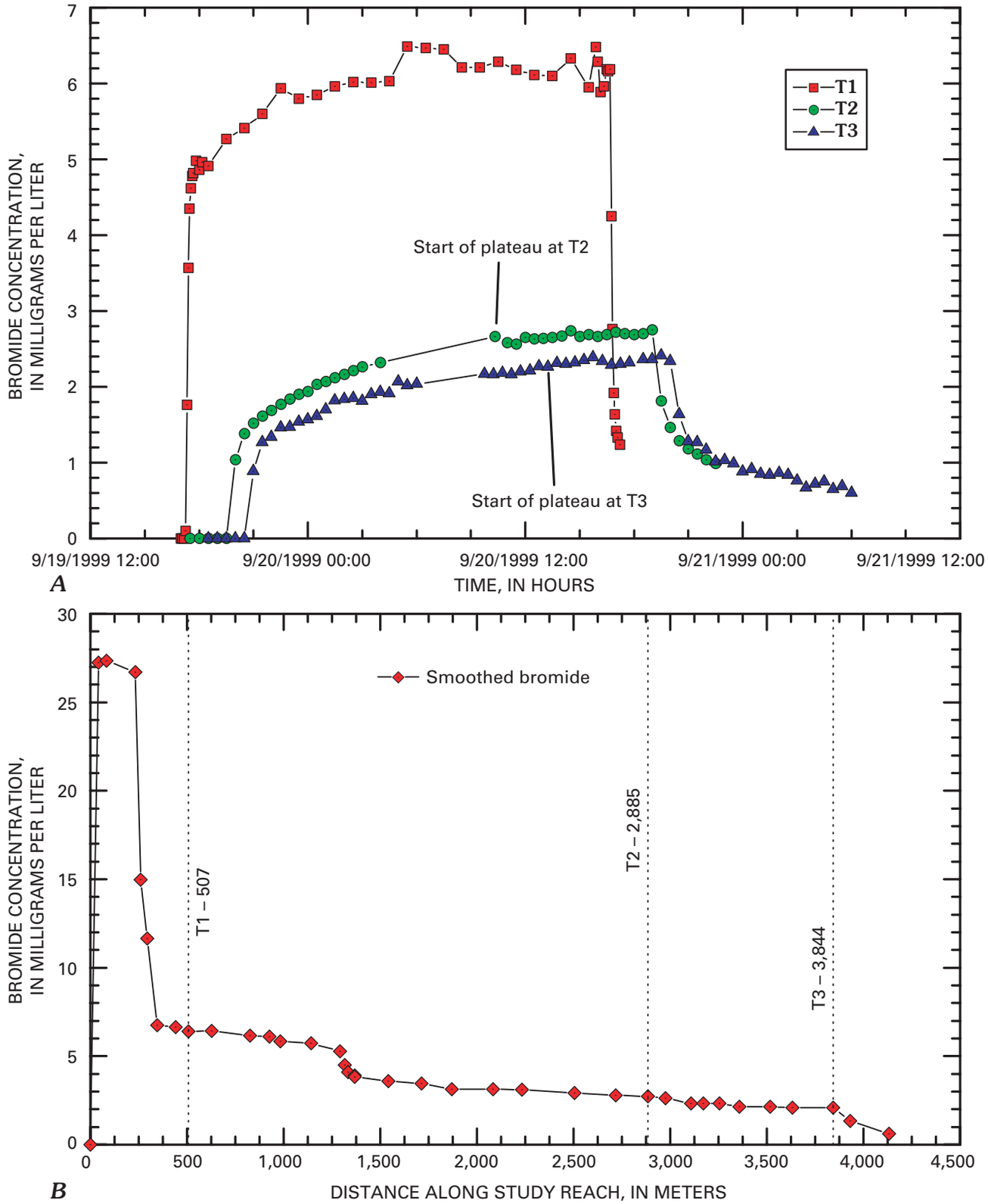

Figure 26. Variation of bromide concentration with *A*, time at three transport sites, and *B*, distance, upper Cement Creek, September 1999.

Table 14. Bromide concentrations, discharge based on velocity meter, Parshall flume measurements, and discharge calculated from tracer concentrations, upper Cement Creek, September 1999.

[Distance, along the study reach, in meters; all concentrations in milligrams per liter; all discharge in liters per second; NA, no analysis; dash, no measurement]

Distance	Smoothed bromide concentration	Initial discharge estimate	Discharge measured with velocity meter	Discharge (upstream velocity measurement plus Parshall flume measurement)	Adjusted bromide concentration	Adjusted discharge estimate	Discharge from CDMG[1]
0	0.00	21.0	--	--	0.0	8.68	--
41	27.2	21.0	--	--	27.2	8.68	17.9
84	27.3	20.9	--	--	27.2	8.70	--
234	26.7	21.4	--	--	26.7	8.85	--
259	15.0	39.3	--	--	15.0	15.8	--
293	11.7	50.5	--	--	11.7	20.3	14.8
345	6.75	87.2	--	--	6.75	35.0	--
440	6.65	88.5	--	--	6.65	35.5	--
507	6.41	91.9	--	--	6.41	36.9	--
627	6.42	91.7	--	--	6.39	37.0	--
827	6.17	95.5	--	--	6.17	38.3	--
927	6.12	96.3	--	--	6.12	38.6	--
983	5.83	101	--	--	5.83	40.6	--
1,142	5.74	103	--	--	5.74	41.2	[2]40.1
1,292	5.27	112	--	--	5.27	44.8	--
1,315	4.51	131	--	--	4.51	52.4	--
1,333	4.09	144	--	--	4.09	57.8	--
1,367	3.91	151	--	--	3.91	60.4	52.07
1,367 (replicate)	3.84	153	--	--	3.84	61.5	--
1,541	3.60	164	--	--	3.60	65.6	--
1,714	3.45	171	--	--	3.45	68.4	--
1,869	3.14	188	--	--	3.14	75.4	40.24
2,084	3.14	188	--	--	3.14	75.5	--
2,234	3.12	189	--	--	3.12	75.7	--
2,506	2.93	201	--	--	2.93	80.6	40.97
2,718	2.78	212	--	--	2.78	84.9	--
2,885 (T2)	2.73	216	--	--	2.73	86.6	50.74
2,976	2.63	224	--	--	2.67	88.6	--
3,107	2.32	254	--	--	2.48	95.4	--
3,172	2.32	254	--	--	2.48	95.4	--
3,255	2.32	254	--	--	2.48	95.4	32.62
3,358	2.13	277	--	--	2.36	100	--
3,516	2.13	277	--	--	2.36	100	--
3,633	2.01	293	--	--	2.34	101	--
3,844 (T3)	2.09	282	101	--	2.34	101	--
3,931	1.33	443	--	147	NA	147	[3]64.28
4,133	0.62	954	300	--	NA	300	123.5

[1]Jim Herron, Bruce Stover, and Paul Krabacher, Unpublished Cement Creek reclamation feasibility report, Upper Animas River Basin, Colorado Division of Minerals and Geology, 1998.

[2]Colorado Division of Minerals and Geology distance is 1,070 meters.

[3]Colorado Division of Minerals and Geology distance is 4,001 meters.

(dimensionless), and A is the cross-sectional area over which flow occurs (the area of the hyporheic or storage zone). In the hyporheic zone, I is assumed to be equal to the stream gradient, which in this case is 0.1. Values of K in sand and gravel range from 10^{-1} to 10^{2} cm/s (Freeze and Cherry, 1979, p. 29). At site T3, approximately 180 L/s discharge was unaccounted for by the velocity meter and may be flowing in the hyporheic zone. Assuming a hydraulic conductivity of 10 cm/s, which is approximately one-third stream velocity, the cross-sectional area of the hyporheic zone required to carry this flow is 18.3 m^2 or more than 60 times the cross-sectional area of the stream, which was measured as 0.296 square meters during the velocity-meter measurement. Considering the cemented and indurated nature of the streambed, this estimated hydraulic

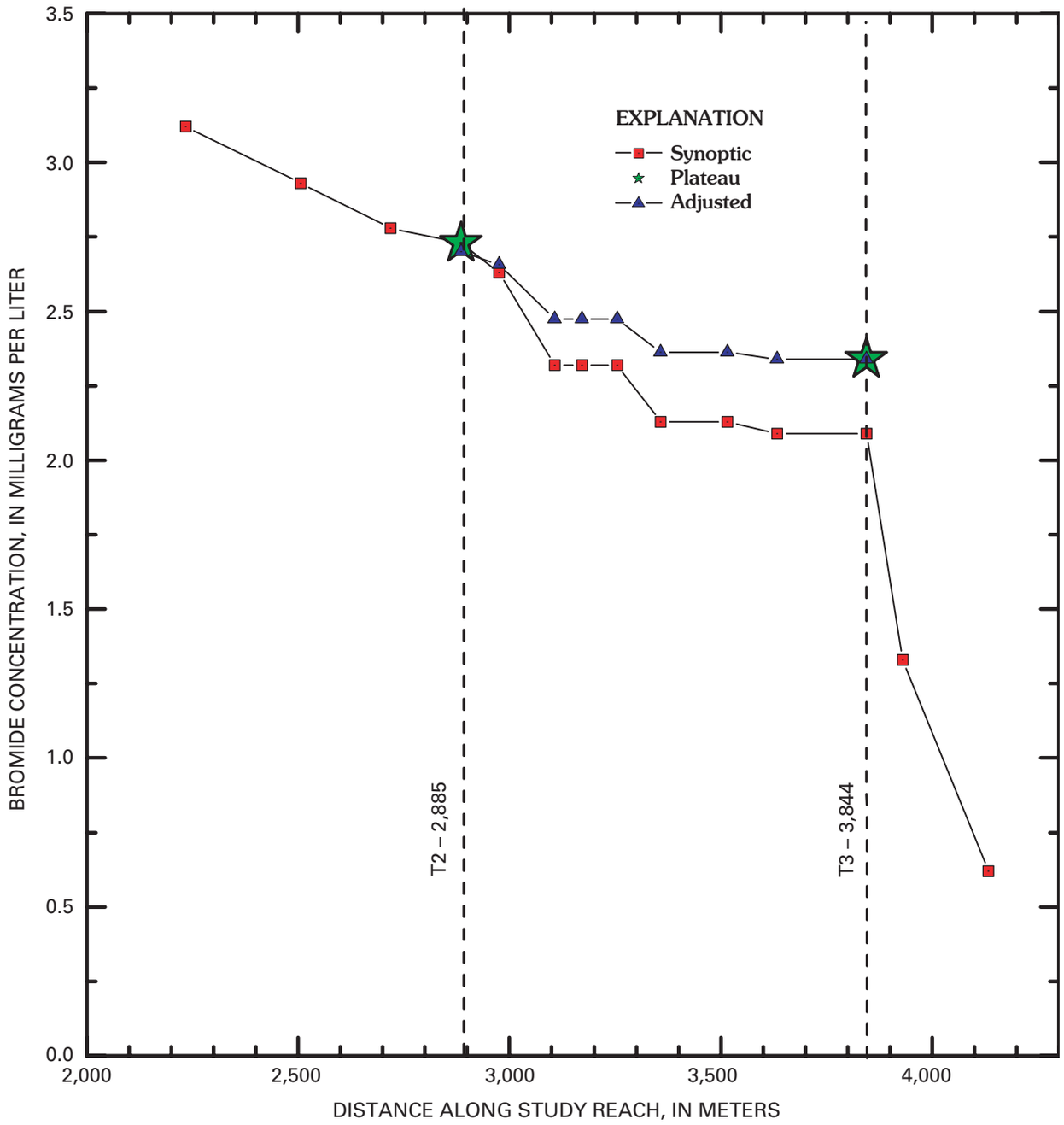

Figure 27. Variation of synoptic, plateau, and adjusted bromide concentrations with distance along study reach, upper Cement Creek, September 1999.

conductivity probably overestimates the actual hydraulic conductivity. Lower values of hydraulic conductivity would increase the calculated area of the hyporheic zone and the value of the ratio of the storage zone cross-sectional area to stream cross-sectional area. The ratio of the hyporheic, or storage zone to stream cross-sectional area is reported in many studies of stream transport. One such compilation showed the greatest value of this ratio to be 4.6 (Harvey and Wagner, 2000). Another compilation shows values ranging from 0.04 to 1.81 for cobble-bottom streams similar in character to upper Cement Creek (Broshears and others, 1993, table 4). Based on this comparison, it seems unreasonable to ascribe the differences between discharge measured by velocity meter and tracer dilution at T3 to flow in the hyporheic zone.

Therefore, we hypothesize that streamflow and tracer were lost near the top of the study reach. The large decrease in tracer concentration that occurred in the upper reaches of the stream (fig. 26*B*) seems too large to account for the increases

in streamflow observed in that reach. This stream reach contains glacial, colluvial, and alluvial deposits and some fracture zones (Burbank and Luedke, 1969; Yager and Bove, this volume; Blair and others, 2002) that could represent recharge zones for deeper circulating ground water. Therefore, flow was calculated using the discharge measured by velocity meter at T3 as the starting point. At sites upstream from T3, discharge was calculated by rearranging equation 4, and assuming the concentration of bromide in inflows was zero:

$$Q_U = Q_D \left(\frac{C_D}{C_U}\right) \quad (8)$$

The velocity-meter measurement and Parshall-flume measurement were used to complete the discharge profile at sites downstream from T3. Because tracer was lost, and the discharge measurements are being calculated to velocity-meter measurements, the discharge (flow in the hyporheic zone is unaccounted for) and the metal loads in this reach of Cement Creek are underestimated by an unknown amount. However, comparison of these data with flow measurements collected by the Colorado Division of Minerals and Geology (CDMG) under similar flow conditions shows that the adjusted discharge estimates are more similar to the CDMG values than are the initial discharge estimates (table 14; fig. 28). This favorable comparison lends credibility to the adjusted discharge values. In addition, certain trends in the loads of conservative constituents indicate that the error in the method used in this study is probably minimal.

Based on the adjusted discharge estimates (table 14; fig. 28), the largest contributor to flow is South Fork, which contributes 51 percent of the flow. The second largest contributor of flow is the Sunnyside mine effluent at the American tunnel, contributing 15.2 percent of the flow. The reaches containing the Queen Anne and Grand Mogul mines contribute slightly more than 6.4 percent of the flow. The two inflows from the Mogul mine account for 4.2 percent of the flow, and North Fork contributes 2.2 percent of the flow. Together these six distinct sources account for 79 percent of the flow. The remaining 21 percent of the flow originates in smaller tributaries, seeps, springs, and dispersed, subsurface flow that discharge to the stream.

Comparison of Conditions 1996 Versus 1999

In 1996 the CDMG conducted a study in Cement Creek to identify locations of waste rock and mine drainage within the Cement Creek basin (Jim Herron, Bruce Stover, and Paul Krabacher, Unpublished Cement Creek reclamation feasibility report, Upper Animas River Basin, Colorado Division of Minerals and Geology, 1998). As part of this investigation, stream samples and streamflow discharge measurements were collected from Cement Creek to enable calculation of load values during base flow in October 1996. In addition, during the USGS lower Cement Creek synoptic sampling experiment, conducted in September 1996, samples were collected along the downstream portions of upper Cement Creek. Comparison of the results of these two samplings with the 1999 results is instructive. Since 1996, some conditions have changed in upper Cement Creek. For instance, in early September 1996 a bulkhead was closed in the American tunnel that drains the Sunnyside mine workings (see Leib and others, this volume, Chapter E11). Closure of the bulkhead might force static water levels in the mountain to rise and cause re-plumbing and rerouting of the acid water intercepted in the American tunnel. The net result could be emergence of acidic, metal-rich water at higher elevations than before the placement of the bulkhead. In addition, in 1996, the treatment system for the American tunnel was collecting almost all of the water from upper Cement Creek just downstream from the confluence of North Fork. The collection and treatment of the upper Cement Creek water had stopped temporarily in 1999 during the mass-loading study. Both of these changes could produce poorer water quality in upper Cement Creek in 1999 relative to 1996.

The variation of discharge, pH, total copper, iron, manganese, and zinc concentration and load with distance are shown for the three data sets (USGS 1996 and 1999 studies; CDMG 1996 study) in figures 28 and 29–33. Discharge results (fig. 28) indicate that the CDMG data were collected at the lowest flow. In addition, at the North Fork, the CDMG noted, "***during August 1996, all the flow from North Fork was observed to infiltrate into the alluvial gravels prior to reaching Cement Creek," and "***the flow in Cement Creek was visibly reduced near the confluence with the North Fork" (Unpub. Cement Creek reclamation feasibility report, CDMG, 1998, p. 34). Therefore, water from North Fork and Cement Creek was recharging the ground-water system at the time of the CDMG sampling. In contrast, both USGS data sets indicate measurable surface flow from North Fork to Cement Creek at the time of sampling. The CDMG data show lower values of pH (fig. 29) upstream of the Mogul mine than the USGS data show for that area, but greater values downstream from the Mogul mine. The 1996 USGS data show greater pH values at all locations than are shown in the 1999 USGS data. Despite slightly different flow conditions, copper, iron, manganese, and zinc concentration and load data are remarkably similar between the USGS 1999 and CDMG 1996 data sets upstream from the Mogul mine (figs. 30–33). For the area downstream from the Mogul mine, the data sets do not show similar results; the 1999 USGS data generally have lower pH values and greater concentrations and loads than do either of the other two data sets.

The differences among the three data sets are partially the result of different hydrologic conditions. In particular, the different patterns between the 1996 CDMG and USGS data sets downstream from the North Fork confluence are attributed to the lack of surface flow in North Fork during the CDMG sampling. The different pH values reported for the 1999 USGS and 1996 CDMG data upstream from the Mogul mine also may be due to the lower flow that occurred during the CDMG sampling: at the lowest flow conditions perhaps only acid springs flow, whereas at slightly higher flow, there

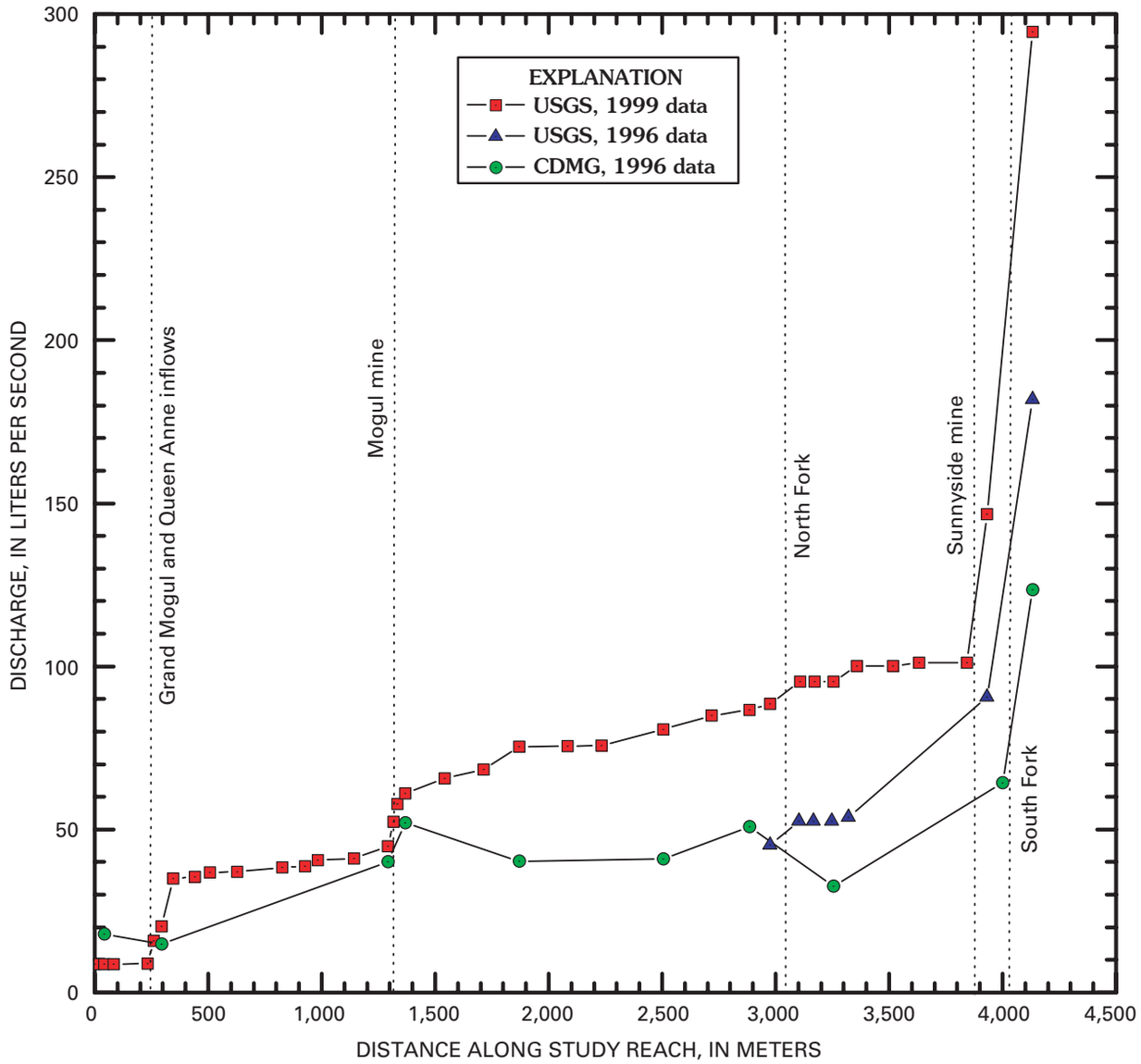

Figure 28. Variation of discharge measurements with distance along the study reach, upper Cement Creek, September 1996 and 1999.

is still some higher pH runoff or spring flow related to the latest storm events. In 1999, a major rainstorm had occurred a few days prior to the USGS synoptic sampling. Dilution from precipitation runoff would be expected to increase stream pH in the acidic conditions of Cement Creek.

Lower flow conditions in 1996 relative to 1999 cannot explain the higher values for copper, iron, manganese, and zinc concentrations and loads that occurred downstream from the Mogul mine in 1999 relative to 1996. Lower flow in 1996 should have caused more acid conditions similar to what occurred upstream from the Mogul mine. This was not the case. In addition, even considering the lower flow and lower pH in 1996 relative to 1999, copper, iron, manganese, and zinc concentrations and loads are remarkably similar between the two data sets upstream from the Mogul mine.

The differences in copper, iron, and zinc concentrations and loads downstream from the Mogul mine between 1996 and 1999 are caused by different chemistry and higher flow of the Mogul mine inflow between the 2 years. Flow and constituent concentrations are greater at the larger of the two Mogul mine inflows sampled by the USGS in 1999 than at the Mogul mine adit as represented by CDMG data in 1996 (table 14). As a result, metal loads are from 5 to more than 80 times greater in 1999 than in 1996. The differences between the 2 years do not seem to be related to higher flow alone, as the CDMG high-flow data for the Mogul mine adit (Unpub. Cement Creek reclamation feasibility report, CDMG, 1998) indicate a flow rate of 1.7 L/s, and more dilute chemistry than that represented in table 15. Changes that have occurred at the site of the Mogul inflow between 1996 and 1999 include collection and

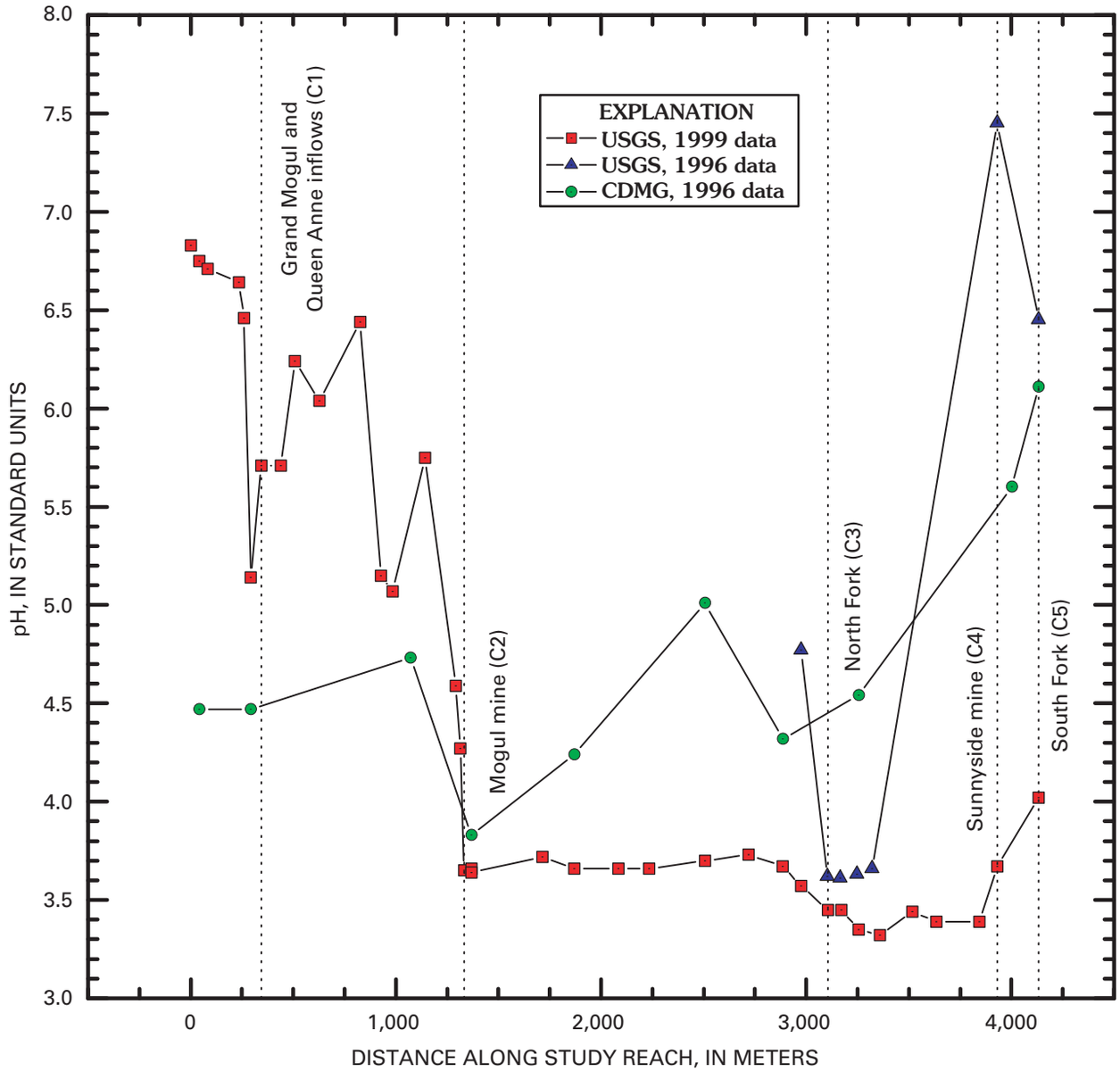

Figure 29. Relation of pH measured during three different studies, upper Cement Creek.

rerouting of flow from the Mogul mine around mine-waste deposits to help improve water quality (Jim Herron, CDMG, oral commun., 2001). This change cannot account for the large loading increases observed at the Mogul mine between 1996 and 1999. Rather, it seems that some fundamental change occurred in the flow rate and composition of flow exiting the Mogul mine between 1996 and 1999. Hydrologic changes resulting from placement of the bulkhead in the American tunnel could be responsible for the change, as maps of underground workings indicate an underground connection between the American tunnel and the Mogul mine (Burbank and Luedke, 1969, pl. 8). However, this direct connection requires a static water-level altitude of approximately 12,200 ft. Pressure behind the bulkheads in the American tunnel and Terry tunnel indicated water levels of approximately 11,600 ft in October 1999 (Larry Perino, Sunnyside Corporations, oral commun., 2001), which is above the altitude of the Mogul mine adit (approximately 11,300 ft).

The change in chemistry of the Mogul mine inflow from 1996 to 1999 indicates that a change in hydraulics (plumbing) involving the addition of water from east of Cement Creek has occurred. The Mogul mine drainage sampled by the USGS in 1999 and 2000 (table 15) is exceptionally rich in manganese (concentration greater than 25 mg/L). In 1999, the manganese load had increased more than 20 times relative to 1996. Studies of mine drainage in other parts of the Animas River watershed study area have indicated that drainage waters similarly elevated in manganese are typical of, and unique to, the Eureka vein systems that formed part of the ore mined at the Sunnyside mine (Bove and others, this volume). The

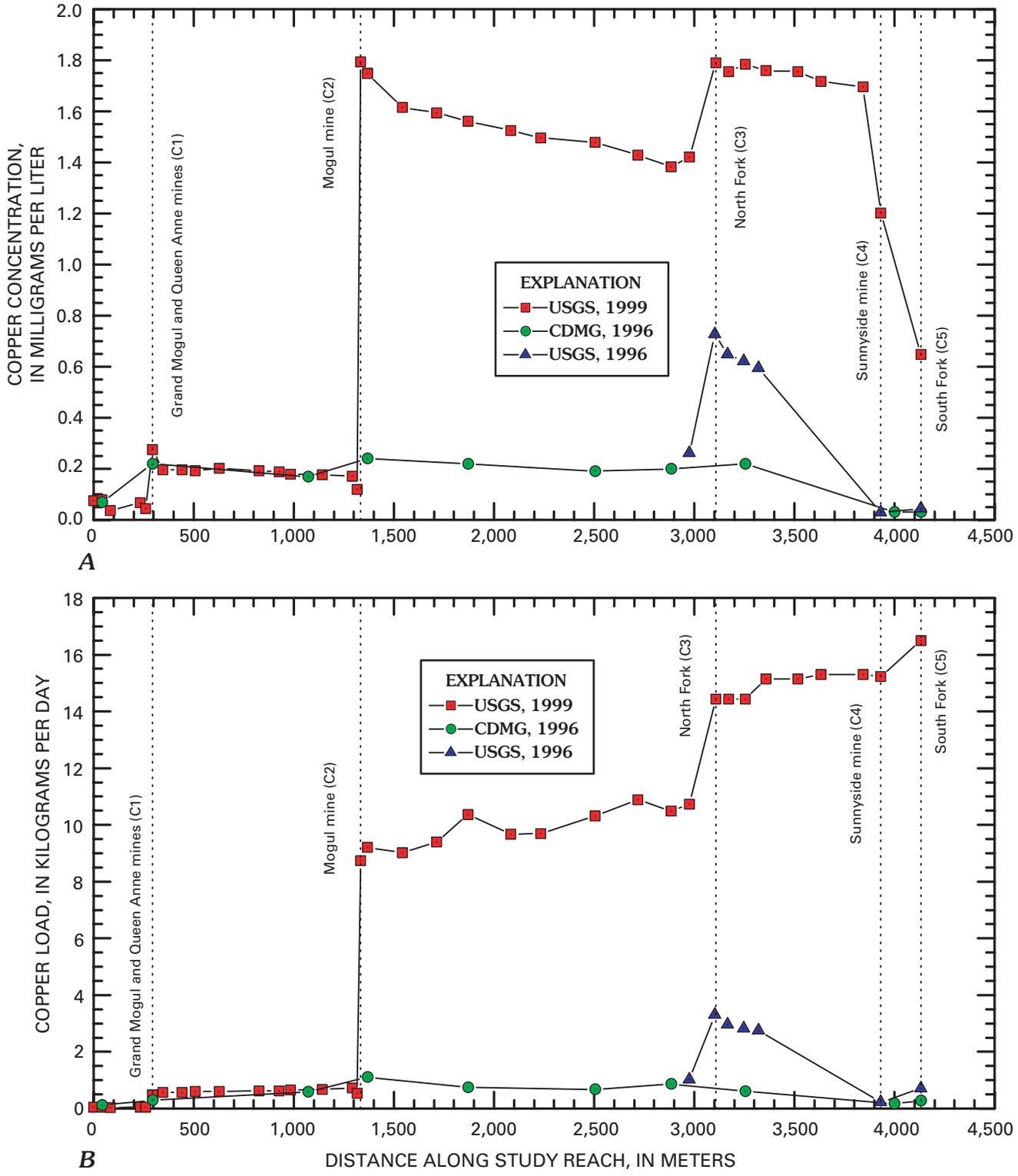

Figure 30. Relation of *A*, copper concentrations and *B*, corresponding copper loads measured during three different studies, upper Cement Creek.

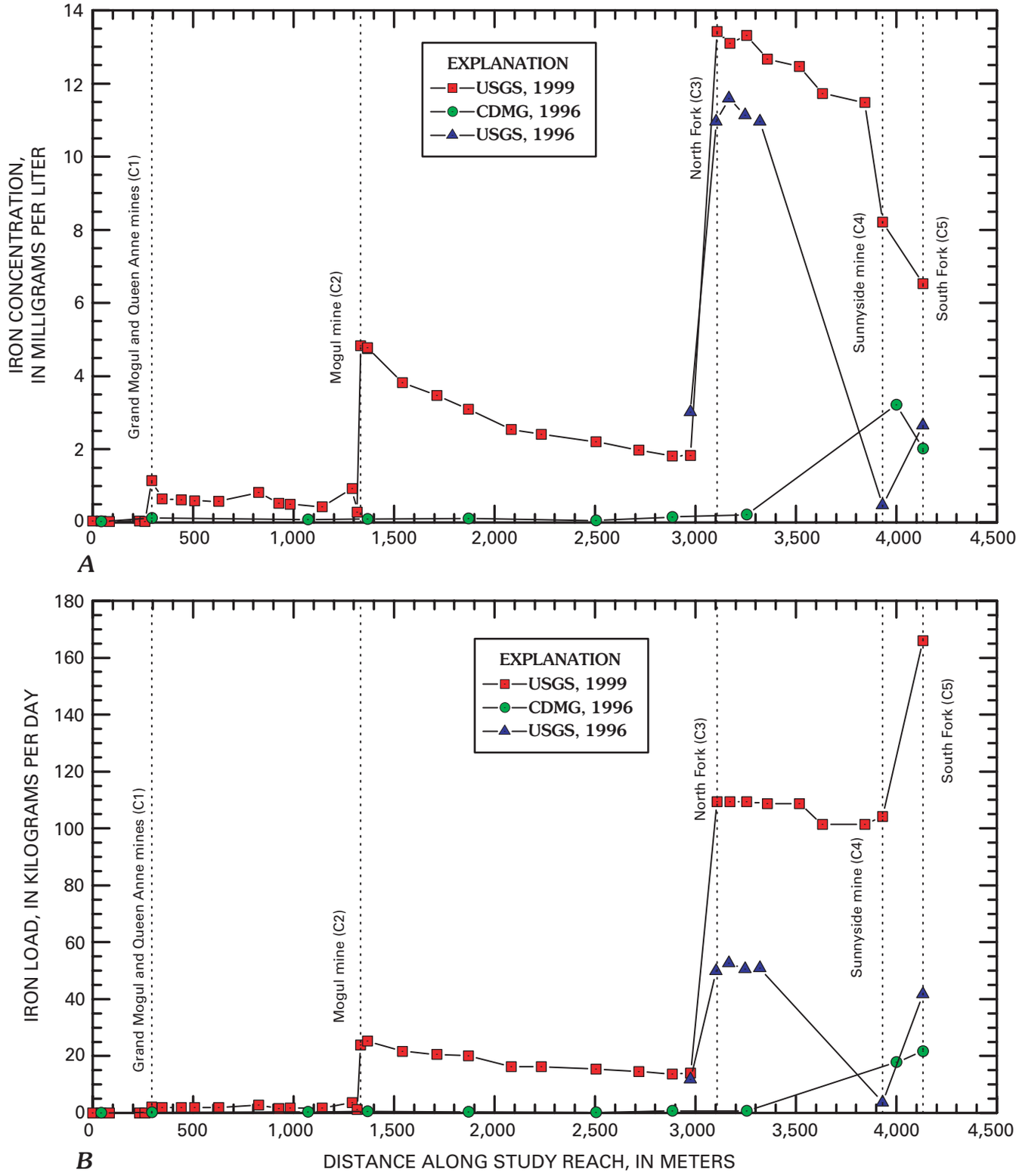

Figure 31. Relation of *A*, iron concentrations and *B*, corresponding iron loads measured during three different studies, upper Cement Creek.

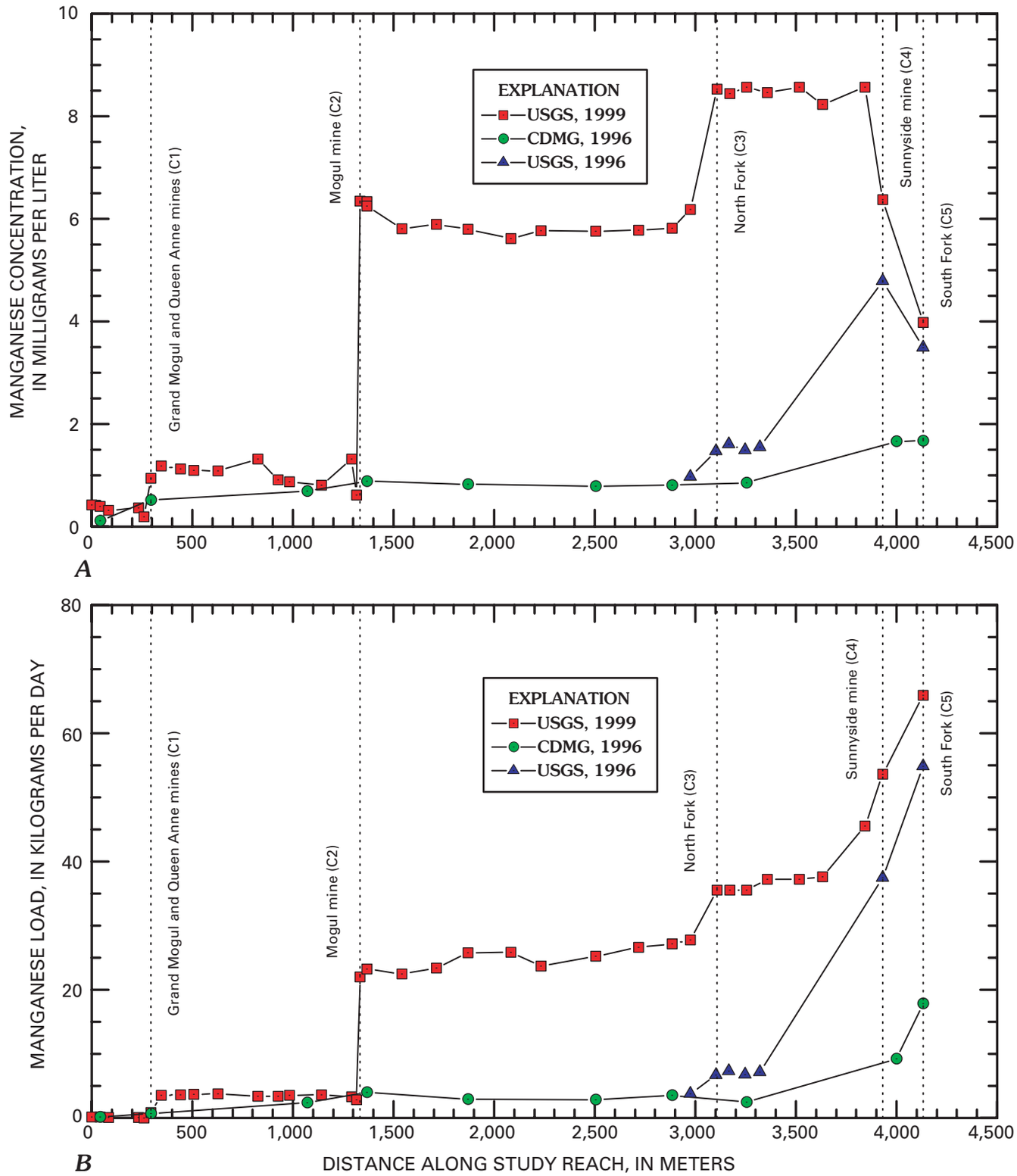

Figure 32. Relation of *A*, manganese concentrations and *B*, corresponding manganese loads measured during three different studies, upper Cement Creek.

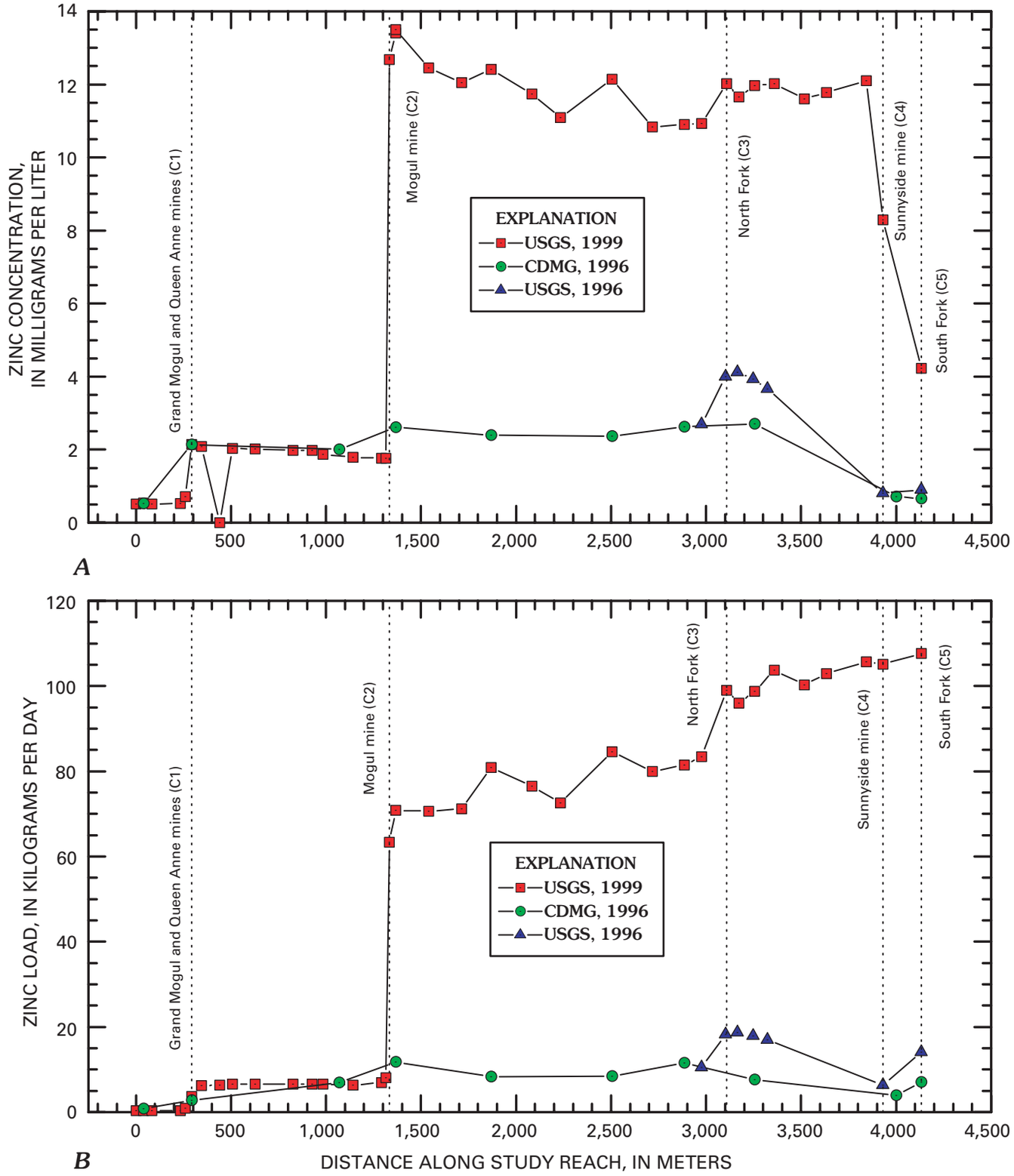

Figure 33. Relation of *A*, zinc concentrations and *B*, corresponding zinc loads measured during three different studies, upper Cement Creek.

Table 15. Relation of water quality and load for samples collected at the Mogul mine inflow by the Colorado Division of Minerals and Geology (CDMG) in 1996 and the U.S. Geological Survey (USGS) in 1999 and 2000, upper Cement Creek.

[Concentrations measured in total-recoverable sample except calcium, magnesium, sodium, sulfate, and silica, which are from dissolved sample; L/s, liters per second; Spec. cond., specific conductance; µS/cm, microsiemens per centimeter at 25°C; mg/L, milligrams per liter; kg/day, kilograms per day; NM, not measured; LDL, less than detection limit]

Constituent	CDMG[1] 1996	USGS 1[2] 1999	USGS 2[3] 1999	USGS 2000[4]	CDMG	USGS[5]	Load ratio USGS/CDMG
	Water-quality data				Load		
Discharge (L/s)	0.68	5.37	3.17	NM	NM	NM	NM
pH	2.89	2.85	3.89	3.11	NM	NM	NM
Spec. cond. (µS/cm)	1,098	1,869	318	1,084	NM	NM	NM
	Concentration (mg/L)				Load (kg/day)		
Calcium	83.53	169	34.5	179	4.91	87.9	18
Magnesium	4.2	11.7	3.3	11.6	.25	6.33	26
Sodium	3.32	3.4	1.5	4.6	.20	1.99	10
Sulfate	449	1,009	126	820	26.4	503	19
Aluminum	5.24	44.2	3.4	20.5	.29	23.0	78
Cadmium	.15	1.50	.054	.62	.01	.75	82
Copper	6.42	12.6	.5	4.6	.38	5.91	16
Iron	51.2	36.2	.3	25.4	2.84	16.3	6
Manganese	9.7	28.5	1.74	26.7	.57	12.3	22
Nickel	.015	.058	.007	LDL	.00	.03	22
Lead	.21	.211	.003	.137	.01	.10	9
Silica	9.5	44.5	17.2	40.4	.56	25.4	45
Zinc	28.1	82.2	4	53.8	1.73	38.1	22

[1]Colorado Division of Minerals and Geology, base-flow synoptic, Mogul mine sample (Unpub. Cement Creek reclamation feasibility report, CDMG, 1998).

[2]Sample from 1,318 m, 1999 USGS synoptic.

[3]Sample from 1,348 m, 1999 USGS synoptic.

[4]Sample from 1,318 m, 2000 USGS reconnaissance.

[5]Load is the sum of the loads for USGS 1 and USGS 2.

change in chemistry at the Mogul mine to values more typical of drainages occurring east of the Mogul and associated with the Sunnyside supports the idea that placing a plug in the American tunnel (that drained the Sunnyside mine) has altered the hydrology and chemistry of flow from the Mogul mine. An official of the Sunnyside mine (Larry Perino, Sunnyside Corporation, oral commun., 2001) has hypothesized that the increased water level resulting from the American tunnel bulkhead has caused water that formerly flowed to the Sunnyside mine and the American tunnel to now divert to the Mogul mine.

Another explanation of the changes observed between the 1996 and 1999 flow and water quality of the Mogul mine drainage is that the CDMG collected their sample at the outflow from the adit, whereas the USGS samples were collected where the flow from the adit joins Cement Creek. Conceivably, water is added to the mine effluent as it flows across the surface between the two locations (a distance of approximately 200 m). The CDMG data indicate a gain of approximately 12 L/s in Cement Creek between their monitoring stations located upstream and downstream from the Mogul mine inflow. They measured the Mogul mine inflow at 0.57 L/s. Therefore, possibly as much as 11.4 liters per second of flow is being added to the reach where the water from the Mogul adit flows before entering Cement Creek. In addition, the unsampled load at the Mogul mine, as calculated from the CDMG samples, did not account for approximately 0.1 kg/day of the copper load and 3 kg/day of the zinc load increases observed within the reach of Cement Creek that contains the Mogul mine inflow. The CDMG data showed a loss of iron in that reach. These small loads of zinc and copper are still much smaller than the differences noted between the 1996 CDMG and 1999 USGS data sets (35 kg/day zinc and 5.4 kg/day copper) at the stream sites just downstream from the Mogul mine. Therefore, in 1996, the 11.4 L of missing flow did not contain metals in sufficient concentrations to augment the loading in Cement Creek and account for the differences between the 1996 and 1999 data sets. If this substantial inflow between Mogul adit and the stream exists, then the chemistry of that inflow may have changed between 1996 and 1999.